Leptonic and Semi-Leptonic Decays of Heavy Mesons in Quenched Lattice QCD

Giuseppe Nicola Lacagnina

Doctor of Philosophy

The University of Edinburgh

2000

This thesis is dedicated to my sister Silvia.

Abstract

This thesis is the report of a lattice calculation of the matrix elements relevant to leptonic and semi-leptonic decays of heavy mesons. The simulations were run in quenched lattice QCD at two values of the coupling β, using a non-perturbatively improved action.

The theoretical formalism of Lattice QCD and Heavy Quark Effective Theory is introduced. Decay constants of B and D mesons are calculated. The form factors relevant to the $B \to D^* l \bar{\nu}_l$ decay are calculated and used to extract the slope parameter of the Isgur-Wise function and the parameter V_{cb} of the CKM matrix.

Declaration

This thesis, written entirely by me, is a presentation of the research work I did as a member of the UKQCD collaboration.

The calculations presented in this work were done using previously generated gauge configurations and lattice correlators. The analysis software was written by me on the basis of some existing routines written by members of the UKQCD collaboration.

The results presented in Chapter 5 appeared in:

Decay Constants of B and D Mesons from Non-perturbatively Improved Lattice QCD, K.C. Bowler *et al.*, hep-lat/0007020

Giuseppe Nicola Lacagnina

Acknowledgements

I have a very long list of people to thank for making my student life in Edinburgh pleasant and for helping me in my work.

In particular I wish to thank my supervisors, Prof. R.D. Kenway and Prof. K.C. Bowler, for their help and the interesting conversations I had with them about physics, and for their patience. My thanks also go to Dr. B. Pendleton and Dr. R. Ball, with whom I had many interesting conversations. I certainly cannot leave Dr. D. Richards out of this list, since he has been very helpful for all the time he was here (and afterwards, too). I also have to thank N. Fancey for having found some funding for me during the second and the third year of my Ph.D. , and Mrs. E. McKirdy for always being kind and helpful. I also have to acknowledge the invaluable help and friendship of Dr. Chris Maynard, Simon Albino, Dr Claudio Verdozzi and Dr. Balint Joo, who was also my flat mate. I also wish to thank Derek Hepburn, Varda Hood and James Gill.

Outside the department, I wish to thank Conrad Hughes, Serena and Jason Ayers, Alice Stigoe, Georgina Hewes and Anastassios Karpodinis.

I also wish to thank my family for support of all sorts and professor A. Zappalá for all his help.

Special thanks go to my Italian friends, for always supporting me from abroad and for sharing with me great holidays: Vincenzo and Sandro Costa, Franz Coppola, Dario Di Falco, Francesca D'Amico, Mariella and Alfio Scuderi, Alessandra D'Amico.

Notation

In this, work, the *natural units* have been used:

$$\hbar = c = 1$$

The signature choice for the Minkowski metric tensor was:

$$g_{\mu\nu} = g^{\mu\nu} = \mathrm{diag}(1, -1, -1, -1)$$

Four vectors are written with the notation:

$$x^{\mu} = (t, \vec{x})$$

while the scalar product of two of them is written as:

$$v_{\mu} w^{\mu} = v \cdot w = g_{\mu\nu} v^{\mu} w^{\nu} = v^{0} w^{0} - \vec{v} \cdot \vec{w}$$

where, as usual, Einstein's summation rule is assumed. The following notation is adopted:

$$\not{v} = \gamma^{\mu} v_{\mu}$$

the commutator of two gamma matrices will be written as:

$$\sigma_{\lambda\mu} = \frac{i}{2}[\gamma_{\lambda}, \gamma_{\mu}]$$

Contents

Chapter 1

Introduction

1.1 Foreword

At energy scales up to those accessible in modern particle accelerators, the Standard Model (SM) [1] is currently believed to be the most accurate theory which describes particles and interactions, with gravity as the only exception. This is not a major problem, since gravity is not expected to have any sizable effect at the energy scales that are described by the Standard Model.

The Standard Model has a number of unknown parameters which have to be extracted from experimental data. An accurate knowledge of these parameters is very important, since it puts severe validity limits on the Standard Model itself and helps in understanding where to look for hints of physics beyond it. One of the most interesting issues is for example that of CP violation, which is related to the observed baryon - anti-baryon asymmetry of the universe. Can the Standard Model account for all the observed CP violation? If not, what is the new physics? This problem is directly related to the nature of some of the unknown parameters of the SM: the elements of the CKM matrix [2, 3], i.e. the matrix that governs the mixing of quark flavours. There are currently several experimental facilities working on the measurement of these unknown parameters.

It is well known that QCD has many purely non-perturbative aspects, like con-

finement, and that it is not possible to study them within perturbation theory: QCD has an intrinsic energy scale below which the coupling becomes too big to be used as a perturbative series expansion parameter. A way to look at these aspects is to put the field theories on a lattice, i.e. on a finite grid in Euclidean space. In this formulation, field theories have a large but finite number of degrees of freedom, and therefore can be simulated on computers. Nonetheless, at the accessible scales, space-time is a continuum; this means that one needs to extrapolate all the quantities calculated on the lattice to the limit in which the lattice spacing vanishes. This is usually done by calculating the same quantity on a set of differently spaced lattices.

It is very important to have control over the uncertainties of a lattice calculation, since there are several sources of error. First of all, one gets errors due to the fact that the size of the lattice is finite; second, one gets errors proportional to powers of the lattice spacing, that vanish only in the continuum limit. Since the path integrals of the field theory are replaced with Monte Carlo averages, one also gets statistical errors, depending on the number of gauge field configurations one is averaging over. In order to produce a larger ensemble to average over, or to reduce the lattice spacing, or to make the lattice larger, one needs increasingly powerful computer resources, since the tasks become more and more computationally expensive.

Nonetheless, it is possible to take advantage of one of the features of lattice field theory to reduce the uncertainties in a more economic way. At a given non-zero lattice spacing, there is not a unique definition for the action; the only requirement is that all the candidates must agree in the continuum limit. Therefore, it is possible to implement a technique called improvement, which has the purpose of removing all the errors of a given power of the lattice spacing, leaving only the errors of higher powers of the lattice spacing. This is achieved by adding to the action and to the operators of the theory suitable terms that do not compromise the continuum limit, but are tuned to absorb all the errors of the chosen order.

Another source of systematic errors is the so-called quenched approximation, which consists in neglecting the quark-antiquark virtual loops. This is done to avoid the task of calculating the determinant of the fermionic matrix at each

Monte Carlo step, which is computationally very expensive.

Since lattice QCD provides a rigorous definition QCD, it is possible to calculate with it quantities such as masses and matrix elements from first principles. Lattice QCD becomes very important also in all those situations in which the non-perturbative effects become dominant.

The new experimental facilities (BaBar, Belle [4, 5, 6, 7]) which study heavy quark systems will provide crucial data for testing the Standard Model, and it is reasonable to assume that a great deal of information can be gained from the combination of experimental and lattice theoretical data. In fact, the differential decay rates of mesons, which are measured experimentally, depend on two unknown quantities: a hadronic matrix element, and a CKM matrix element. Since it is possible to calculate the hadronic matrix element on the lattice, one can combine experimental and lattice data to extract the CKM matrix element. The hadronic matrix elements are parametrised with a set of functions of the recoil energy known as form factors, that can be extracted on the lattice.

One of the most interesting areas of phenomenological particle physics is the study of the decays of B mesons. Lattice QCD can provide a good estimate of B meson decay matrix elements starting from first principles. For example, the decay constant f_B, which describes the leptonic decay of a B meson, is related to the issue of CP violation, and was calculated in this work. Another interesting possibility is the lattice analysis of the form factors for the $B \to D^* l\nu$ semi-leptonic decay. This decay is used in the extraction of $|V_{cb}|$, the modulus of the CKM matrix element governing the mixing of b and c quarks.

1.2 The Standard Model

The Standard Model is a fundamental theory of the elementary constituents of matter and their interactions, with gravity as the only exception. According to it, the building blocks of matter are quarks and leptons; in turn, these particles interact among themselves via the exchange of gauge bosons. These bosons mediate three of the four fundamental interactions: electro-magnetic, weak, and

strong. These bosons are the massless photon and gluons and the massive $W^{\pm}$ and Z particles. The underlying mathematical structure is the gauge group:

$$SU_{\mathrm{C}}(3) \otimes SU(2)_{\mathrm{L}} \otimes U(1)_{\mathrm{Y}} \ . \tag{1.1}$$

The labels "C", "L" and "Y" indicate colour, left-hand and hyper-charge. This symmetry is spontaneously broken into

$$SU_{\mathrm{C}}(3) \otimes U(1)_{\mathrm{Q}} \tag{1.2}$$

via the Higgs mechanism, through which the fermions and the weak interaction bosons acquire mass (Q is the electric charge). There is evidence of three generations of quarks and leptons. The scheme is the following:

$$\begin{pmatrix} \text{up} \\ \text{down} \end{pmatrix}, \begin{pmatrix} \text{charm} \\ \text{strange} \end{pmatrix}, \begin{pmatrix} \text{top} \\ \text{bottom} \end{pmatrix} \tag{1.3}$$

$$\begin{pmatrix} e \\ \nu_e \end{pmatrix}, \begin{pmatrix} \mu \\ \nu_\mu \end{pmatrix}, \begin{pmatrix} \tau \\ \nu_\tau \end{pmatrix} \tag{1.4}$$

Recent experiments suggest that the neutrinos are not massless as it was commonly believed [8, 9].

1.3 Quantum Chromodynamics (QCD)

QCD, the theory of strong interactions that describes the quarks and their bound states, the hadrons, is based on the colour symmetry $SU(3)$. This simply means that the QCD Lagrangian is constructed to be invariant under a local $SU(3)$ transformation:

$$\psi(x) \rightarrow G(x)\psi(x) \tag{1.5}$$

$$\bar{\psi} \rightarrow \bar{\psi}(x)G^{\dagger}(x) \ ,$$

where G is an element of $SU(3)$, the group of 3×3 matrices that satisfy:

$$G^{\dagger}G = \mathbf{1} \tag{1.6}$$

$$\det(G) = 1 \ . \tag{1.7}$$

According to the principle of causality, there cannot be any relation between the complex phases that multiply fields in separated points of space-time. Such a relation would require the propagation of signals at infinite speed.

$$G = G(x) = e^{i\theta_a(x)T^a} \ , \tag{1.8}$$

where $\theta_a(x)$ are arbitrary smooth functions of space-time points and the T matrices are the generators of $SU(3)$ that satisfy:

$$[T_a, T_b] = if_{abc}T^c \ . \tag{1.9}$$

The Dirac Lagrangian (used to describe quarks):

$$\mathcal{L} = \bar{\psi}(i\gamma^{\mu}\partial_{\mu} - m)\psi$$

is invariant under global $SU(3)$ transformations, but not under local ones. In order to have a Lagrangian that is invariant under a local $SU(3)$ transformation (or, in general, $SU(N)$), one must replace the common space-time derivatives with *covariant derivatives*, as is done in the general theory of relativity:

$$D_{\mu} = \partial_{\mu} - igA_{\mu} \ , \tag{1.10}$$

where

$$A_\mu(x) = A^a_\mu(x) T_a \ . \tag{1.11}$$

The fields A_μ, which are also $SU(3)$ matrices, will be identified (after quantisation) with the gluons (in the case of QED, they describe photons). It is interesting to notice that these fields do have a geometric interpretation. At each point in space time, the quarks (fermions) exist in three "colours":

$$\psi(x) = \begin{pmatrix} \psi_{\text{red}}(x) \\ \psi_{\text{green}}(x) \\ \psi_{\text{blue}}(x) \end{pmatrix} \ . \tag{1.12}$$

This means that there is a three-dimensional vector space attached to each point x. At each point in space-time, the basis of the vector space can be chosen differently: the colour quantum number is not an observable. Therefore, in order to subtract two fields at infinitesimally close points, i.e. to calculate derivatives, one must use parallel transport. If T_x is the three-dimensional colour vector space attached to the space-time point x, parallel transport is a function defined along a continuous and differentiable path P from x to y:

$$\Gamma_P(x, y) : T_x \to T_y \tag{1.13}$$

such that

$$\Gamma_P^{-1}(x, y)\psi(y), \ \psi(x)$$

are defined on the same basis and can be subtracted. The covariant differential can now be defined as follows, on a straight line connecting x and $x + dx$:

$$D\psi(x) \equiv \Gamma^{-1}(x, x + dx)\psi(x + dx) - \psi(x) \ . \tag{1.14}$$

By definition, Γ must satisfy:

$$\Gamma(x,x)\psi(x) = \psi(x) \ . \tag{1.15}$$

Therefore, for an infinitesimal displacement dx, the Γ function, known as the *comparator*, can be written as:

$$\Gamma(x,dx) = \mathbf{1} + igA_\mu(x)dx^\mu \tag{1.16}$$

in terms of a new set of fields $A_\mu(x)$. The covariant differential is now written as:

$$D\psi \equiv D_\mu\psi(x)\ dx^\mu \ . \tag{1.17}$$

it is easy to see that one recovers the definition given in (1.10). The gauge transformation $G(x)$ corresponds to a change of basis for the three-dimensional colour vector space at each x, and therefore Γ_P must transform according to:

$$\Gamma_P(x,y) \to G(x)\Gamma_P(x,y)G^\dagger(y) \ . \tag{1.18}$$

By considering again an infinitesimal displacement along a straight line, it is possible to show that, under $G(x)$, the gauge fields $A_\mu(x)$ transform according to:

$$A_\mu \to G^\dagger A_\mu G - (\partial_\mu G^\dagger)G \ . \tag{1.19}$$

Now, the most general gauge invariant object one can build using the $A_\mu(x)$ fields is the Wilson loop on a closed path P

$$W_P = \mathcal{P}\ \exp\left\{ig \oint_P A_\mu(x)\ dx^\mu\right\} \ , \tag{1.20}$$

where $\mathcal{P}$ denotes path ordering. If s is the parameter that specifies the position along the path P, the products of fields in the expansion of (1.20) are ordered

with s. From this result, it is possible to derive an $SU(3)$ invariant action for the gauge fields, the Yang-Mills gauge action:

$$S_{YM} = \int d^4x \frac{1}{4} F^2 \ , \tag{1.21}$$

where $F^2 = F^a_{\mu\nu} F^{\mu\nu}_a$ and:

$$F^{\mu\nu}_a = \partial^\mu A^\nu_a - \partial^\nu A^\mu_a - g f_a{}^{bc} A^\mu_b A^\nu_c \ . \tag{1.22}$$

This field strength tensor is very similar to the field tensor of electromagnetism, the main difference being the non linear gluon-gluon interaction term, which arises from the non-abelian nature of $SU(3)$.

1.4 The Weak Sector

Many of the less-known parameters of the Standard Model are related to the weak interactions. In particular the Cabibbo-Kobayashi-Maskawa matrix (CKM), that describes how the quarks couple to the W, is still under-determined. The current that describes the weak interaction of quarks can be written as:

$$J^\dagger_\mu = \frac{g_2}{2\sqrt{2}} (\bar{u}, \bar{c}, \bar{t}) \gamma_\mu (1 - \gamma_5) V_{\text{CKM}} \begin{pmatrix} d \\ s \\ b \end{pmatrix} \ . \tag{1.23}$$

The CKM matrix describes the mixing of quark flavours:

$$V_{\text{CKM}} = \begin{pmatrix} V_{ud} & V_{us} & V_{ub} \\ V_{cd} & V_{cs} & V_{cb} \\ V_{td} & V_{ts} & V_{tb} \end{pmatrix} \ . \tag{1.24}$$

In other words, the mass eigenstates do not coincide with the weak interaction eigenstates. This matrix has to be unitary, and it is defined up to a phase that

one can absorb in a re-definition of the quark fields. Thus, it is possible to write it using 4 independent parameters, following Wolfenstein [10]:

$$V_{\rm CKM} = \begin{pmatrix} 1-\lambda^2/2 & \lambda & A\lambda^3(\rho - i\eta) \\ -\lambda & 1-\lambda^2/2 & A\lambda^2 \\ A\lambda^3(1-\rho-i\eta) & -A\lambda^2 & 1 \end{pmatrix} + \mathcal{O}(\lambda^4) \ , \qquad (1.25)$$

where $\lambda = |V_{us}| \simeq 0.22$. It is interesting to note that a unitarity violation in the CKM matrix would be a signal of new quark-lepton generations. The CKM parameters are not predicted by the SM, and have to be measured or extracted by combining experimental input and computer simulations. Fortunately this goal, if not easy, is still achievable because of the extremely rich phenomenology of the weak decays. As a matter of fact, a precise knowledge of the elements of the CKM matrix is very important, since it would permit us to test several of the most interesting issues of the SM: CP violation, presence of new generations and, ultimately, new physics.

1.5 Weak decays of heavy-light mesons

This section is a brief introduction to the leptonic and semi-leptonic decays of heavy-light mesons, e.g. of mesons composed of a heavy quark Q and a light antiquark q [11, 12, 13]. More detailed discussions follow in Chapters 5 and 6.

Leptonic and semi-leptonic decays of mesons are realised through the interaction of a quark current and a W boson. At the lowest order, the diagram involved in leptonic decays is shown in Figure (1.1).

In the limit in which the momentum of the quark-antiquark pair satisfies:

$$k^2 \ll M_W^2 \qquad (1.26)$$

this process can be described using an *effective theory*, due to Fermi, in which the amplitude takes the form:

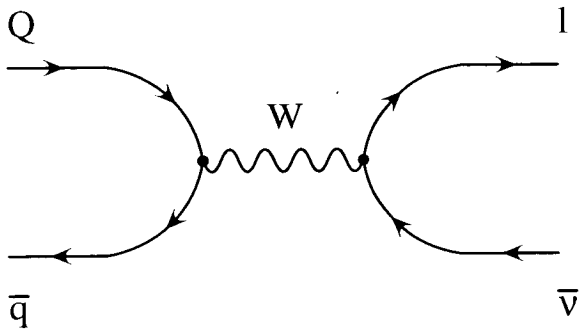

Figure 1.1: Leptonic decay of a meson

$$\mathcal{M} = \frac{G_F}{\sqrt{2}} V_{Qq} L_\mu^\dagger H^\mu \ , \tag{1.27}$$

where:

- G_F is Fermi's constant;
- V_{Qq} is the CKM angle describing the mixing of the quarks Q, q;
- $L_\mu = \bar{l}\gamma_\mu(1-\gamma^5)\nu_l$ is the leptonic current;
- $H^\mu = \langle M'|J^\mu|M\rangle$ is the hadronic matrix element: M and M' indicate the initial and final state mesons respectively.

Equation (1.27) implies that experimental input (cross sections, decay rates) can be used together with lattice calculations (H^μ) to extract elements of the CKM matrix.

The current $J^\mu(x)$ is defined by:

$$J^\mu(x) \equiv \bar{Q}(x)\gamma_\mu(1-\gamma^5)q(x) \tag{1.28}$$

The leptonic current is calculable in perturbation theory. The hadronic matrix element, though, contains the non-perturbative information about the decay process. It describes the confinement process that binds the quarks inside hadrons.

In other words, in order to extract physical information from leptonic and semi-leptonic decays, one must be able to disentangle the effects of the weak and the strong interactions. This is not a trivial task, but definitely an important one. Lattice methods are among the possible ways to evaluate hadronic matrix elements.

1.5.1 Leptonic decays

The purely leptonic decay of a meson M takes the general form:

$$M \to l\bar{\nu}_l \tag{1.29}$$

In this case, all the non-perturbative information is contained in a single quantity known as the *decay constant.* In particular, since there are no hadrons in the final state:

$$H^\mu = \langle 0|J^\mu|M\rangle \ , \tag{1.30}$$

where J^μ, defined above, is the difference of the vector and the axial currents:

$$\begin{aligned} V_\mu(x) &= \bar{Q}(x)\gamma_\mu q(x) \\ A_\mu(x) &= \bar{Q}(x)\gamma_\mu\gamma_5 q(x) \ . \end{aligned} \tag{1.31}$$

The corresponding hadronic matrix elements are parametrised according to:

$$\begin{aligned} \langle 0|A_\mu(0)|P(\vec{p})\rangle &= if_P p_\mu \\ \langle 0|V_\mu(0)|V(\epsilon)\rangle &= \epsilon_\mu \frac{M_V^2}{f_V} \end{aligned} \tag{1.32}$$

where $|P(\vec{p})\rangle$ is the state of a pseudoscalar meson with momentum $\vec{p}$, $|V(\epsilon)\rangle$ is the state of a vector meson with polarisation ϵ and M_V is the mass of the vector

meson. The pseudoscalar and vector decay constants, f_P and f_V, have different definitions for historical reasons: f_P has the dimensions of a mass, while f_V is a dimensionless number.

Other combinations vanish. To see this, it's sufficient to remember that the axial and the vector currents have opposite parity:

$$\begin{aligned}\langle 0|A_\mu|V\rangle = \langle 0|PP^\dagger A_\mu PP^\dagger|V\rangle = \\ = -\langle 0|A_\mu|V\rangle = 0\end{aligned} \tag{1.33}$$

where the invariance of the vacuum state under parity transformations was used.

1.5.2 Semi-leptonic decays

Semi-leptonic decays of mesons have hadrons in the final state:

$$M \to M' l \bar{\nu}_l \ . \tag{1.34}$$

The hadronic matrix element is more complex than in the purely leptonic case:

$$H^\mu = \langle M'(\vec{k})|J^\mu|M(\vec{p})\rangle \ , \tag{1.35}$$

where p and k are the initial and final state momenta respectively. Symmetry arguments (including Lorentz transformations) permit one to parametrise the matrix elements in terms of functions of the momentum transfer $q = k - p$. The form of these parametrisations depends on the quantum numbers of the initial and final states. In the case in which both M and M' are pseudoscalar mesons, the matrix elements are written as:

$$\langle M'(\vec{k})|V^\mu(0)|M(\vec{p})\rangle = F_+^V(q^2)(k+p)^\mu + F_-^V(q^2)(k-p)^\mu \tag{1.36}$$

Another interesting class of decays is that in which the initial hadron is a pseudoscalar and the final hadron is a vector meson. In this case, the parametrisation is, in terms of the momenta and the polarisation vector:

$$\begin{aligned} \langle M'(\vec{k},\epsilon)|V^\mu(0)|M(\vec{p})\rangle &= G_V(q^2)g^{\mu\lambda}\epsilon_{\lambda\nu\alpha\beta}\epsilon^{*\nu}k^\alpha p^\beta \\ \langle M'(\vec{k},\epsilon)|A^\mu(0)|M(\vec{p})\rangle &= G_{A_1}(q^2)\epsilon^{*\mu} + G_{A_2}(q^2)p^\mu + G_{A_3}(q^2)k^\mu \end{aligned} \tag{1.37}$$

the functions $F(q^2), G(q^2)$ are known as *form factors.*

1.6 Overview

This work is organised as follows. Chapters 2 and 3 describe the basic elements of lattice QCD, and the methods which are used to extract physical information. Improvement techniques and smearing methods are discussed. Chapter 4 is a brief introduction to Heavy Quark Effective Theory (HQET). Chapter 5 contains the results of a calculation of decay constants of B and D mesons. Chapter 6 contains an introduction to the calculation of the form factors of the $B \to D^* l\bar{\nu}_l$ decay, with results.

Chapter 2

Introduction to Lattice QCD

This chapter is meant to be a brief introduction to lattice QCD and to the lattice technology that was involved in this thesis' calculations. For a detailed exposition, see [14, 15].

2.1 Euclidean space

It is quite natural to define quantum field theory (QFT) in the Minkowski space-time of special relativity. Nonetheless, for several practical reasons, when studying field theories numerically, it is preferable to work in an Euclidean space-time, essentially $\Re^4$. Euclidean space is related to the Minkowski space-time by a Wick rotation, which replaces time with an imaginary valued variable:

$$x^0 = -ix^4, x^4 \in \Re \ . \tag{2.1}$$

It is possible to reformulate field theory in an Euclidean space-time, with due consideration to the conditions that make it possible to continue analytically any Green's function of the theory under study to the usual Minkowski space. Several of the quantities involved in any QFT take a different form in an Euclidean space-time. For instance the action, which is the starting point of any field theory, is

related to the Minkowski space version by:

$$S_E = -iS_M \ . \tag{2.2}$$

This will have an important effect in the evaluation of the theory's Green's functions, since it involves the transformation:

$$e^{iS_M} \rightarrow e^{-S_E} \ . \tag{2.3}$$

The first of these two exponentials is strongly oscillating and thus difficult to handle and to integrate, while the second is just an exponential decay. It will also be necessary to introduce Euclidean Dirac gamma matrices, which satisfy:

$$\{\gamma_\alpha^E, \gamma_\beta^E\} = \delta_{\alpha\beta} \ , \tag{2.4}$$

and are related to the usual Minkowski matrices by:

$$\gamma_j^E = -i\gamma_j^M \ , \tag{2.5}$$

$$\gamma_4^E = \gamma_0^M = -i\gamma_4^M \ .$$

2.2 The lattice

The lattice is a hypercubic grid in a four dimensional Euclidean space. For the purposes of this work, one can choose this grid to be equally spaced in all four directions. Thus, if the spacing is a, the lattice is:

$$\Lambda = \{x \in \Re^4 : x_\mu/a \in Z, \mu = 1...4\} \ . \tag{2.6}$$

Consequently, as long as the lattice extension is finite, the number of degrees of freedom of a field theory is going to be large but finite. In this work, the number of lattice sites, L, was the same in all spatial directions. The extension in the time direction is denoted by T.

Considering a generic function $f(x)$ defined on the Euclidean space, it is possible to write its Fourier transform:

$$\tilde{f}(p) = \int d^4x f(x) e^{-ipx} \tag{2.7}$$

This function is periodic with a period of $2\pi/a$, since

$$e^{2\pi i x_\mu / a} = 1 \tag{2.8}$$

This means that all the momentum integrations on the lattice will be restricted to the finite region known as the Brillouin Zone (BZ):

$$\mathcal{B} = \left\{ p : p_\mu \in \left(-\frac{\pi}{a}, \frac{\pi}{a} \right] \right\} . \tag{2.9}$$

Furthermore, lattice momenta are quantised. In order to see this, it is enough to consider any test function for which periodic boundary conditions hold:

$$f(0) = f(aL) . \tag{2.10}$$

In terms of a Fourier transform, this equation can be rewritten as:

$$\int \frac{dp}{2\pi} \tilde{f}(p) = \int \frac{dp}{2\pi} e^{-ipaL} \tilde{f}(p) . \tag{2.11}$$

For an arbitrary choice of f, this equation is satisfied if and only if:

$$p = \frac{2\pi}{aL} n , \tag{2.12}$$

where n is an integer. In general, throughout this work, all spatial components of momenta will be specified in units of $2\pi/(aL)$. On the lattice, Dirac's delta function (spatial) will take the form:

$$\delta^{(3)}(\vec{p}-\vec{k}) = \frac{1}{L^3}\sum_{\vec{x}} e^{i(\vec{p}-\vec{k})\cdot\vec{x}} \ . \tag{2.13}$$

2.3 Quantum field theory on a lattice

The starting point of any field theory is the Lagrangian density functional. Assuming a classical Lagrangian which depends on some field $\phi(x)$ and its first derivatives, it is possible to write the action:

$$S_E = \int d^4x_E \mathcal{L}(\phi, \partial_\mu \phi) \ . \tag{2.14}$$

Classical field equations are then derived by imposing:

$$\delta S_E = 0 \ , \tag{2.15}$$

and assuming that the field deformations vanish on the boundary of space-time. Now, it is possible to relate quantum field theory to a classical, statistical field theory, using the language of path integrals. In this approach to quantum field theory, one starts by evaluating the Euclidean generating functional:

$$\mathcal{Z}_E = \int \mathcal{D}\phi \ e^{-S_E[\phi]} \ . \tag{2.16}$$

This generating functional looks very similar to the partition function of a system in statistical mechanics. In fact, it is possible to draw an analogy between Euclidean field theory and statistical mechanics. If now $\hat{O}$ is a generic quantum field operator, it is possible to relate its vacuum expectation value to a path integral of classical fields:

$$\langle \hat{O}[\hat{\phi}] \rangle = \frac{1}{\mathcal{Z}_E} \int \mathcal{D}\phi \; O[\phi] \; e^{-S_E} \tag{2.17}$$

which is analogous to the ensemble average of statistical mechanics. This formula can be used to evaluate the Green's functions, which are used to extract the physical information of the theory under study:

$$\mathcal{G}_E(x_1^E, ..., x_n^E) \equiv \langle 0|T[\hat{\phi}(x_1^E)...\hat{\phi}(x_n^E)]|0\rangle \; . \tag{2.18}$$

The symbol T stands for time ordering. From now on, the "E" label will be omitted.

2.3.1 Boundary conditions

Due to the finite extension of the lattice, it is necessary to impose boundary conditions on the fields. For the data set used in this work, the following conditions have been chosen:

- **fermions**: periodic in the spatial directions, antiperiodic in time;
- **gauge bosons**: periodic in all four directions.

2.3.2 Reflection positivity

One obviously wants to be able to continue the Green functions analytically to Minkowski space. This means they will have to satisfy the Osterwalder-Schrader reflection positivity condition. In order to write it down, a few definitions are needed. First of all, the time inversion operator is defined, by specifying how it acts on four-vectors and on fields:

$$\theta : (t, \vec{x}) \rightarrow (-t, \vec{x}) \; , \tag{2.19}$$

$$\Theta\phi(x) = \bar{\phi}(\theta x) \tag{2.20}$$

where $\bar{\phi}$ is the complex conjugate of ϕ. Quantum mechanics requires this operator to be anti-linear:

$$\Theta(\lambda_1\phi_1 + \lambda_2\phi_2) = \bar{\lambda}_1\Theta(\phi_1) + \bar{\lambda}_2\Theta(\phi_2) \ , \tag{2.21}$$

and to satisfy:

$$\Theta(\phi_1\phi_2) = (\Theta\phi_1)(\Theta\phi_2) \ . \tag{2.22}$$

One can now consider a series of functions $f_j(x_1, ..., x_j)$ which are square integrable and have support only at positive or zero values of $x_k^4, (k = 1...j)$. It is possible to define a functional F:

$$F = \sum_j \int d^4x_1...d^4x_j f_j(x_1, ...x_j)\phi(x_1)...\phi(x_j) \tag{2.23}$$

Now, the reflection positivity condition would be, for F:

$$\langle(\Theta F)F\rangle \geq 0 \ . \tag{2.24}$$

2.3.3 Gauge fields on a lattice

In order to put QCD on a lattice, it is necessary to build a lattice definition of the comparator (see Chapter 1). Staring at a point x, one can consider the nearest site along a specific direction μ. The comparator will be:

$$\Gamma(x, x + dx) = e^{iagA_\lambda(x)dx^\lambda} \equiv U_\mu(x) \ , \tag{2.25}$$

where the displacement dx has a non-vanishing component in the μ direction only. This is also known as the *link variable.*

The next step consists in considering what is the smallest closed loop on a lattice: the unit square, which is called a *plaquette.* Therefore, the smallest Wilson loop on a lattice will be an ordered product of four link variables. It is important to notice that:

$$U_\mu^\dagger(x) = U_{-\mu}(x + \hat{\mu}) \tag{2.26}$$

where $\hat{\mu}$ is the unit vector in the μ direction. The link variable is an $SU(3)$ matrix. It is now possible to write the Wilson loop on a plaquette, the *plaquette variable*:

$$U_{\mu\nu}(x) \equiv U_\mu(x)U_\nu(x + \hat{\mu})U_\mu^\dagger(x + \hat{\nu})U_\nu^\dagger(x) \tag{2.27}$$

where summation over indices is not involved. One of the possible lattice actions for pure gauge $SU(3)$ is the one proposed by Wilson [16]:

$$S_W^{\text{gauge}} = \beta \sum_x \sum_{\mu<\nu} \left[1 - \frac{1}{N_C} \Re\text{Tr}\, U_{\mu\nu}(x)\right] , \tag{2.28}$$

where, if N_C is the number of colours ($N_C = 3$) and g is the $SU(N_C)$ coupling:

$$\beta = \frac{2N_C}{g^2} . \tag{2.29}$$

As the lattice spacing gets small ($a^2 \ll 1$), it is possible to show that:

$$S_W^{\text{gauge}} = S_{YM} + \mathcal{O}(a^2) . \tag{2.30}$$

2.3.4 Fermion fields on a lattice

Consider a continuum action for fermions in an Euclidean space-time:

$$S_f = \int d^4x \bar{\psi}(x)(\gamma^\mu \partial_\mu + m)\psi(x) \ . \tag{2.31}$$

On the lattice, integral and differential operators must be replaced by:

$$a^4 \sum_x \tag{2.32}$$

$$\tilde{\partial}_\mu \psi_\alpha(x) = \frac{1}{2a}[\psi_\alpha(x+\hat{\mu}) - \psi_\alpha(x-\hat{\mu})] \ , \tag{2.33}$$

where the Greek index on the field ψ refers to the spin degrees of freedom. Putting all these elements together, it is possible to write a lattice action for fermions:

$$S_f^{\text{latt.}} = \sum_{x,y} \bar{\psi}_\alpha(x) \mathcal{M}_{\alpha\beta}(x,y) \psi_\beta(y) \ , \tag{2.34}$$

where the matrix $\mathcal{M}$ has the form:

$$\mathcal{M}_{\alpha\beta}(x,y) = \frac{1}{2} \sum_\mu \gamma^\mu_{\alpha\beta} (\delta_{x,y+\hat{\mu}} - \delta_{x,y-\hat{\mu}}) + m\delta_{x,y}\delta_{\alpha\beta} \tag{2.35}$$

Now, it is possible to show that:

$$\langle \psi_\alpha(x) \bar{\psi}_\beta(y) \rangle = \mathcal{M}^{-1}_{\alpha\beta}(x,y) \tag{2.36}$$

This means that the calculation of this two-point Green's function amounts to the inversion of a matrix. Writing explicitly

$$\sum_z \left[\mathcal{M}_{\alpha\gamma}(x,z) \mathcal{M}^{-1}_{\gamma\beta}(z,y) \right] = \delta_{\alpha\beta} \delta^{(4)}(x,y) \ , \tag{2.37}$$

and recalling the lattice version of Dirac's delta function, while writing $\mathcal{M}$ as inverse Fourier transform of $\widetilde{\mathcal{M}}(p)$, it is possible to show that:

$$\mathcal{M}^{-1}_{\alpha\beta}(x,y) = \lim_{a\to 0}\int_{-\pi/a}^{\pi/a}\frac{d^4p}{(2\pi)^4}\frac{(-i\gamma_\lambda\pi_F^\lambda + m)_{\alpha\beta}}{\pi_F^2 + m^2}e^{ip(x-y)} \tag{2.38}$$

with the definition:

$$\pi_F^\mu = \frac{1}{a}\sin(ap^\mu)\ . \tag{2.39}$$

This formulation leads to the well-known problem of lattice fermion doubling. It is possible to see this effect by evaluating the same matrix element in the case of scalar fields, which turns out to be quite different:

$$\mathcal{G}(x,y) = \lim_{a\to 0}\int_{-\pi/a}^{\pi/a}\frac{d^4p}{(2\pi)^4}\frac{e^{ip(x-y)}}{\pi_B^2 + m^2} \tag{2.40}$$

where

$$\pi_B^\mu = \frac{2}{a}\sin\left(\frac{a}{2}p^\mu\right)\ . \tag{2.41}$$

This means that, inside the BZ, the components of π_F have twice the number of zeros of π_B, spoiling the continuum limit. In d space-time dimensions, one gets 2^d fermionic species, of which $2^d - 1$ are lattice artefacts.

2.3.5 Wilson fermions

A possible solution to the doubling problem, due to Wilson, consists in giving to the additional fermionic species, masses proportional to the inverse lattice spacing, to make them decouple from the low energy regime. This is achieved by adding to the action a term which vanishes in the continuum limit, at the price of breaking explicitly the chiral symmetry of the original action:

$$\Delta S_{\mathrm{W}} = -a^5 \frac{r}{2} \sum_x \sum_\mu \bar{\psi}(x)\gamma_\mu \frac{[\psi(x+\mu) - 2\psi(x) + \psi(x-\mu)]}{a^2} , \tag{2.42}$$

which is the discrete version of:

$$-a\frac{r}{2} \int d^4x \bar{\psi}(x)\partial^2\psi(x) . \tag{2.43}$$

As a matter of fact, a "no-go" theorem by Nielsen and Ninomiya [17] proves that for any fermionic action that is hermitian, local and invariant under translations, the doubling problem cannot be solved without breaking the chiral symmetry of the massless case.

Adding the Wilson term to the naive fermionic action the result is, once the fields are redefined to be dimensionless:

$$S_{\mathrm{WF}} = \sum_x \left(\sum_\mu \bar{\psi}(x) \left[(\gamma_\mu - r)\psi(x+\mu) - (\gamma_\mu + r)\psi(x-\mu) \right] + \frac{1}{\kappa}\bar{\psi}(x)\psi(x) \right) \tag{2.44}$$

where κ is the *hopping parameter*:

$$\kappa = \frac{1}{2m + 8r} . \tag{2.45}$$

It is common practice to set $r = 1$.

The chiral symmetry breaking term dominates the discretisation errors of the fermionic action. In other words, the Wilson action corresponds to an additive mass renormalisation [18].

This extra mass renormalisation is obtained by defining the bare quark mass the following way:

$$m_q = \frac{1}{2a}\left(\frac{1}{\kappa} - \frac{1}{\kappa_{\mathrm{crit}}}\right) . \tag{2.46}$$

with the introduction of the "critical" hopping parameter κ_{crit}, at which the quark mass vanishes. In the simple case of a free theory:

$$\kappa_{\text{crit}} = \frac{1}{8} \,. \tag{2.47}$$

In the more general case of an interacting theory, the value of this parameter is not know a priori and has to be extracted from simulations.

2.4 Lattice quark masses

There are restrictions on the range of quark masses that can be simulated on a lattice. First of all, if m_Q is the mass of a quark in some physical units, this quantity cannot be greater then the inverse lattice spacing. In fact, $m_Q > a^{-1}$ implies that the Compton wave-length of the quark is shorter than the lattice spacing. In this case, the lattice is too coarse to resolve the structure of the heavy quark. In other words, it is like the quark "fell" through the lattice.

On the other hand, the inversion of the fermion matrix, which gives the information on the propagation of quarks, becomes computationally more expensive as the simulated quark mass gets lighter. Furthermore, if the quark is too light, its Compton wave-length becomes comparable to the total extent of the lattice, giving rise to finite-size effects.

Due to this restrictions, the quark masses that were simulated in this work were chosen in the following way:

- "heavy quarks": masses around the charm quark mass;
- "light quarks": masses around the strange quark mass;

Therefore, all physical quantities that depend on quark masses, were extracted on the lattice at these values of the quark masses and then extrapolated to the physical values of the masses.

2.5 Full QCD action

In order to write an action for lattice QCD, it is necessary to modify Wilson's fermionic action to preserve gauge invariance. In general, in a theory with quarks and gluons, it's possible to build two kinds of gauge invariant objects:

- closed loops of gauge links;
- strings of gauge links with a fermion at one end and an antifermion at the other.

Setting $r = 1$, the fermionic action in presence of gauge fields becomes:

$$S_{\mathrm{WF}} = \sum_x \left(\sum_\mu \bar{\psi}(x) \left[U_\mu(x)(\gamma_\mu - 1)\psi(x+\mu) + \right.\right.$$
$$\left.\left. -U_\mu^\dagger(x-\mu)(\gamma_\mu + 1)\psi(x-\mu) \right] + \frac{1}{\kappa}\bar{\psi}(x)\psi(x) \right) \tag{2.48}$$

and the Wilson lattice QCD action is:

$$S_{\mathrm{LQCD}} = S_{\mathrm{WF}} + S_W^{\mathrm{gauge}} \,. \tag{2.49}$$

2.6 Improvement

For a more complete discussion, see [19, 18, 20, 21]. It is possible to see the lattice spacing a as an inverse momentum cutoff, and therefore the continuum limit as the removal of this cutoff, which is necessary in order to get physical quantities. Furthermore, at a given non-zero lattice spacing, it must be possible to treat lattice QCD as an effective continuum theory with a^{-1} as a momentum cutoff. The Lagrangian can be written as an expansion in a, with operators of growing mass dimension:

$$\mathcal{L} = \mathcal{L}_0 + a\mathcal{L}_1 + a^2\mathcal{L}_2 + \dots , \tag{2.50}$$

$$[\mathcal{L}_k] = [m]^{4+k} . \tag{2.51}$$

Any suitable action for lattice QCD must have the correct continuum limit, i.e. the standard continuum action of QCD. However, it is always possible to add to the action operators that vanish in the continuum limit. In other words, if the continuum limit is seen as the removal of a cutoff, one can, at fixed lattice spacing, add operators that are irrelevant in the sense defined by Wilson.

The improvement programme consists in modifying the action and the operators of lattice QCD by adding irrelevant terms that have the purpose of cancelling the discretisation errors of a given order in the lattice spacing. In the case of $\mathcal{O}(a)$ improvement, used in this work, the improvement operators are introduced with a set of coefficients that are tuned to guarantee that the discretisation errors in lattice calculations appear at $\mathcal{O}(a^2)$ rather than $\mathcal{O}(a)$. It is important to stress that improvement does not guarantee that, at a fixed value of a, the discretisation effects get smaller. The main purpose of the improvement programme is to give better control of the discretisation errors in order to make continuum extrapolations easier.

Each of the terms of the expansion in equation (2.50) can be written as a linear combination of certain operators which have the right mass dimension and share the symmetries of the lattice action. Considering the $\mathcal{L}_1$ term, it is possible to show that it can be written as a linear combination of five operators:

$$\begin{aligned}
\mathcal{O}_1 &= \bar{\psi} i\sigma^{\lambda\mu} F_{\lambda\mu}\psi \\
\mathcal{O}_2 &= \bar{\psi} D^\mu D_\mu \psi + \bar{\psi}\, \overleftarrow{D^\mu}\overleftarrow{D_\mu}\, \psi \\
\mathcal{O}_3 &= m\mathrm{Tr}\,(F^2) \\
\mathcal{O}_4 &= m[\bar{\psi}\gamma^\mu D_\mu \psi - \bar{\psi}\, \overleftarrow{D_\mu}\, \gamma^\mu \psi] \\
\mathcal{O}_5 &= m^2 \bar{\psi}\psi .
\end{aligned} \tag{2.52}$$

If only on-shell quantities are considered, it is possible to apply the field equations in order to reduce the number of independent operators. Once this is done, the $\mathcal{O}(a)$ improvement term for the action has the form:

$$\Delta S_{(a)} = a^5 \sum_x \left[c_1 \mathcal{O}_1(x) + c_3 \mathcal{O}_3(x) + c_5 \mathcal{O}_5(x) \right] . \tag{2.53}$$

Now, the $\mathcal{O}_3$ and $\mathcal{O}_5$ operators correspond to a renormalisation of the bare mass and coupling, and can be dropped. This means that the bare quark mass and the bare coupling will have to be improved:

$$\tilde{m}_q = m_q(1 + b_{\rm m} a m_q) , \tag{2.54}$$

$$\tilde{g}_0^2 = g_0^2(1 + b_{\rm g} a m_q) . \tag{2.55}$$

Thus, action improvement reduces to the following, as proposed by Sheikholeslami and Wohlert [22]:

$$\Delta S_{\rm SW} = a^5 c_{\rm SW} \sum_x \bar{\psi}(x) \frac{i}{2} \sigma_{\mu\nu} \hat{F}_{\mu\nu}(x) \psi(x) , \tag{2.56}$$

where $c_{\rm SW}$ is a parameter that has to be tuned and $\hat{F}_{\mu\nu}(x)$ is a lattice definition of the field strength tensor. A possible choice, used in this work, is:

$$\hat{F}_{\mu\nu}(x) = \frac{1}{8a^2} \left[Q_{\mu\nu}(x) - Q_{\nu\mu}(x) \right] , \tag{2.57}$$

where $Q_{\mu\nu}(x)$ is the sum of the four plaquettes around the point x and lying on the plane spanned by the $\hat{\mu}, \hat{\nu}$ unit vectors.

In order to carry out a full $\mathcal{O}(a)$ improvement, it is necessary to improve a set of lattice operators:

$$V_\mu(x) = \bar{\psi}(x) \gamma_\mu \psi(x)$$

$$\begin{aligned} A_\mu(x) &= \bar{\psi}(x)\gamma_\mu\gamma_5\psi(x) \\ T_{\mu\nu}(x) &= \bar{\psi}(x)i\sigma_{\mu\nu}\psi(x) \\ S(x) &= \bar{\psi}(x)\psi(x) \\ P(x) &= \bar{\psi}(x)\gamma_5\psi(x)\ . \end{aligned} \tag{2.58}$$

Improvement of the above operators is carried out as follows [23, 24]:

$$\begin{aligned} V^{\mathrm{I}}_\mu(x) &= V_\mu(x) + ac_{\mathrm{V}}\tilde{\partial}_\nu T_{\mu\nu}(x) \\ A^{\mathrm{I}}_\mu(x) &= A_\mu(x) + ac_{\mathrm{A}}\tilde{\partial}_\mu P(x) \\ T^{\mathrm{I}}_{\mu\nu}(x) &= T_{\mu\nu}(x) + ac_{\mathrm{T}}\tilde{\partial}_{[\mu}V_{\nu]} \\ P^{\mathrm{I}}(x) &= P(x) \\ S^{\mathrm{I}}(x) &= S(x)\ . \end{aligned} \tag{2.59}$$

All the improvement coefficients have to be tuned in order to cancel all $\mathcal{O}(a)$ lattice artifacts. For some of these parameters non-perturbative evaluations are available. In other cases, they can be evaluated using lattice perturbation theory or Boosted Perturbation Theory(BPT), which is an improvement of lattice perturbation theory proposed by Lepage and Mackenzie [25]. BPT starts from the consideration that the bare lattice coupling constant is a bad expansion parameter for lattice perturbation theory: the authors propose a "renormalised" coupling:

$$\tilde{g}^2 = \frac{g^2}{\langle \frac{1}{3}\mathrm{Tr}\ (U_{\mathrm{P}})\rangle} \tag{2.60}$$

dividing g^2 by the average over gauge configurations of the plaquette operator.

In addition, as mentioned above, there is an additional mass and coupling renormalisation to take into account. The generic current renormalisation scheme is the following:

$$X_{\mathrm{I,R}} = Z_{\mathrm{X}}(1 + b_{\mathrm{X}}am_{\mathrm{q}})X_{\mathrm{I}} \equiv Z^{\mathrm{eff}}_{\mathrm{X}}X_{\mathrm{I}}\ , \tag{2.61}$$

where Z_X is the unimproved renormalisation constant, calculated in a mass independent renormalisation scheme.

Once the improvement programme is completely carried out, it is possible to write an action for lattice QCD which has $\mathcal{O}(a^2)$ discretisation errors:

$$S_{\mathrm{LQCD}} = S_{\mathrm{WF}} + S_W^{\mathrm{gauge}} + \Delta S_{\mathrm{SW}} \ . \tag{2.62}$$

2.7 Path integral measure

In order to extract information from lattice simulations of QCD, one needs in general to be able to evaluate expectation values of the following form:

$$\langle F[\bar{\psi}, \psi, A] \rangle = \frac{1}{\mathcal{Z}} \int \mathcal{D}A \mathcal{D}\bar{\psi} \mathcal{D}\psi F[\bar{\psi}, \psi, A] e^{-S_{LQCD}} \ , \tag{2.63}$$

where $F[\bar{\psi}, \psi, A]$ is a functional of the fields (fermions and gauge bosons). It is then necessary to define properly the integral measures for this path integral. The fermionic measure is:

$$\mathcal{D}\bar{\psi}\mathcal{D}\psi = \prod_x d\bar{\psi}(x) \ d\psi(x) \tag{2.64}$$

and it satisfies the Grassmann algebra. It is possible to integrate out the fermionic degrees of freedom. If $\mathcal{M}$ is the fermionic matrix:

$$S_f = \int d^4x d^4y \ \bar{\psi}(x) \mathcal{M}(x, y; A) \psi(y) \tag{2.65}$$

it is possible to show that:

$$\int \mathcal{D}\bar{\psi}\mathcal{D}\psi e^{-S_f} = \det(\mathcal{M}(\mathcal{A})) \ . \tag{2.66}$$

Once this is done, one needs to integrate only the gauge fields. It is also possible to re-absorb the fermionic determinant in a redefinition of the action:

$$e^{-S_g[A]} \det(\mathcal{M}(A)) = e^{-S_g[A]+\log(\det(\mathcal{M}(A)))} . \tag{2.67}$$

If now

$$\lambda_1, \lambda_2, ...$$

are the eigenvalues of the fermionic matrix:

$$\log(\det((\mathcal{M}(A)))) = \log\left(\prod_j \lambda_j\right) = \mathrm{Tr}\ (\log \mathcal{M}(A)) . \tag{2.68}$$

Therefore, any expectation value will be a path integral over gauge fields only, with the effective action:

$$S_{\text{effective}}[A] = S_g[A] - \mathrm{Tr}\ (\log \mathcal{M}(A)) \tag{2.69}$$

For a continuum gauge theory, the gauge fields have an infinite range:

$$A^a_\mu(x) \in (-\infty, \infty) \tag{2.70}$$

A gauge fixing term is needed, in order to guarantee the convergence of the functional integrals. Nonetheless, there is no need of gauge fixing terms on a lattice [16]. In fact, if the lattice has a finite size, the total volume of integrations is finite. Furthermore, if the lattice is infinite in size, the factor $1/\mathcal{Z}$ will remove the divergences (similarly, in perturbation theory, it removes the "vacuum bubbles").

A possible choice is the gauge invariant Haar measure:

$$\mathcal{D}A = \prod_{x,\mu} dU_\mu(x) . \tag{2.71}$$

The Haar measure over a gauge group G has the following properties:

$$\int_G \mathcal{D}A = 1 \tag{2.72}$$

$$\int_G \mathcal{D}A f[U] = \int_G \mathcal{D}A f[UU'] = \int_G \mathcal{D}A f[U'U] \, . \tag{2.73}$$

The last equation holds for any $U' \in G$.

2.8 The Quenched approximation

So far, it has been shown that, once the fermion fields are integrated out, it is possible to express expectation values of operators as:

$$\langle F \rangle = \frac{1}{\mathcal{Z}} \int \mathcal{D}A \; F \; \det(\mathcal{M}(A)) \; e^{-S_{\text{gauge}}} \tag{2.74}$$

where the generating functional $\mathcal{Z}$ is equal to:

$$\mathcal{Z} = \int \mathcal{D}A \; \det(\mathcal{M}(A)) \; e^{-S_{\text{gauge}}} \tag{2.75}$$

The calculation of the determinant of the fermionic matrix is a computationally expensive task, mainly because of the size of the matrix itself. Lattice calculations can be greatly simplified by making the approximation:

$$\det(\mathcal{M}(A)) = \text{const.} \tag{2.76}$$

This assumption, known as the *quenched approximation*, corresponds to neglecting the virtual quark-antiquark loops. In fact, some phenomenological and theoretical considerations suggest that the quark loops might often give a small contribution to observables [26, 27, 28, 29].

In the quenched approximation, the fermionic determinant can be taken out of the integrals and simplifies between the numerator and the denumerator of (2.74). The expectation values take the much simpler form:

$$\langle F \rangle = \frac{1}{\mathcal{Z}} \int \mathcal{D}A \; F \; e^{-S_{\text{gauge}}} \tag{2.77}$$

It is important to say that the quenched approximation is a limitation for any lattice calculation which uses it, mainly because it introduces a systematic error whose size cannot be reliably evaluated.

2.9 Monte Carlo numerical integration

All the calculations presented in this work have been done in the quenched approximation. In general, the integral in equation (2.77) can be evaluated as a numerical average over a set of gauge configurations, with the Monte Carlo technique:

$$\langle F \rangle \simeq \frac{1}{N_{\text{C}}} \sum_{j=1}^{N_{\text{C}}} \{ F e^{-S[A_{(j)}]} \}_{\{A\}_j} \tag{2.78}$$

The sample of gauge configurations has to be generated with some algorithm. The simplest choice would be to pick gauge field configurations at random. This method would not be at all efficient. In fact, one would pick with equal probability configurations that give a sizeable contribution to the path integral and configurations that give a vanishingly small contribution. A more efficient method consists in generating gauge configurations with a probability distribution:

$$d\mu = \frac{1}{\mathcal{Z}} e^{-S[A]} \mathcal{D}A \tag{2.79}$$

In order to generate gauge configurations with the probability distribution given by (2.79), an algorithm is used that produces the configurations as a sequence. A possible choice is the Metropolis algorithm [30], which works as follows. Given

a gauge field configuration $\{A\}$, a new configuration $\{A'\}$ is randomly generated: the new configuration is accepted with a probability:

$$\mathcal{P}_{AA'} = \min\left(1, e^{S-S'}\right) \tag{2.80}$$

where S and S' are the values of the action as calculated on the configurations $\{A\}$ and $\{A'\}$ respectively. This means that:

- if $S' < S$, the new configuration is accepted;
- if $S' > S$, the new configurations is accepted with a probability of $\exp(S - S')$.

Gauge field configurations produced by adjacent Metropolis steps are not statistically independent. It is therefore useful only to keep gauge configurations that are separated by a given number of algorithmic steps.

Chapter 3

Lattice correlation functions

3.1 Quark propagator

One of the basic ingredients of a lattice QCD simulation is the quark propagator:

$$S(x,y) = \langle 0|T[\psi(x)\bar{\psi}(y)]|0\rangle \ . \tag{3.1}$$

The quark propagator is the amplitude of the process in which a quark is created at the space-time point labelled by y and travels to the point x, where it is annihilated. This object is not invariant under local $SU(3)$ gauge transformations. As it will be shown, complicated field operators can be expressed in terms of integrals of gauge invariant products of quark propagators that are evaluated on specific gauge field configurations:

$$S(x,y;A) = \mathcal{M}^{-1}(x,y;A) \ . \tag{3.2}$$

The fermionic matrix $\mathcal{M}$ must be inverted to build the quark propagators. One of the two points (x,y) is usually taken to be the origin of the lattice in order to make the computation cheaper. Since the fermionic matrix is quite large, its inversion is indeed a computationally intense calculation and requires a considerable amount of computer power. The calculation of $S(x,0;A)$, the point-to-all propagator,

is cheaper because it involves the inversion of a single row (or column) of the fermionic matrix.

3.2 Meson fields

Starting from quark fields, it is possible to build operators that describe some of their bound states: mesons. The most general definition one can think of is:

$$\Omega_M(z) = \int d^4x d^4y \; \bar{\psi}_\alpha(x)\Gamma^{\alpha\beta}(x,y;z)\psi'_\beta(y) \; . \tag{3.3}$$

where colour indices have been summed over, and Greek letters are spin indices. Up to factors, Γ is the product of the gauge links along some path, making $\Omega_M(z)$ a gauge invariant object. The matrix Γ is a function of (x,y,z) for the simple reason that there is not a unique way to build a bound state of quarks, like the meson. One can only build a state with the same quantum numbers as the desired meson, by the action of a creation operator $\Omega_M^\dagger$:

$$|M\rangle = \Omega_M^\dagger|0\rangle \; . \tag{3.4}$$

As it will be shown, it is possible and desirable to choose Γ such that the overlap of the meson state with the vacuum is optimised.

3.3 Lattice completeness relation

Considering a field theory that admits bound states, like QCD, one finds that its spectrum will be composed by one-particle and multi particle states [31]. It is possible to write the identity operator as a sum over particle states:

$$\mathbf{I} = \frac{1}{L^3}\sum_{\lambda,n}\frac{1}{2E_n(\lambda)}|\lambda,\vec{p_n}\rangle\langle\lambda,\vec{p_n}| \; , \tag{3.5}$$

where the sum over λ indicates the sum over single and multi particle states. Here and in the following, energies are expressed in lattice units.

3.4 Two point functions

It is interesting to consider the process in which a meson is created at a given point in space time y (source), and travels to another point x where it is annihilated (sink). For simplicity, one can put $y = 0$. The matrix element relevant to this process is the two-point correlation function:

$$\langle 0|T[\Omega_M(x)\Omega_M^\dagger(0)]|0\rangle \equiv \langle \Omega_M(x)\Omega_M^\dagger(0)\rangle \ . \tag{3.6}$$

What one wants to do is to rewrite it in terms of single quark propagators. In order to achieve this goal, the fermion fields must be integrated out. In the quenched approximation, this expectation value becomes:

$$\langle \Omega_M(x)\Omega_M^\dagger(0)\rangle = \frac{1}{\mathcal{Z}} \int \mathcal{D}A\mathcal{D}\psi\mathcal{D}\bar{\psi} \mathrm{Tr}\ [\Omega_M(x;A)\Omega_M^\dagger(0;A)]e^{-S_g - S_f} \ . \tag{3.7}$$

The meson operators can be explicitly written:

$$\begin{aligned} \Omega_M(x) &= \bar{\psi}_a(x)\Gamma\psi_b(x) \\ \Omega_M^\dagger(0) &= -\bar{\psi}_b(0)\tilde{\Gamma}\psi_a(0) \ , \end{aligned} \tag{3.8}$$

where

$$\tilde{\Gamma} = \gamma_4\Gamma^\dagger\gamma_4 \tag{3.9}$$

and a, b are colour indices. Once the fermion fields are integrated out:

$$\langle \Omega_M(x)\Omega_M^\dagger(0)\rangle =$$

$$\frac{1}{\mathcal{Z}}\int \mathcal{D}A \, \det(\mathcal{M}(A))\mathrm{Tr}\,[\gamma_5\Gamma S_a(x,0;A)\tilde{\Gamma}\gamma_5 S_b^\dagger(x,0;A)]e^{-S_g} \, . \tag{3.10}$$

The identity:

$$S_a(x,y;A) = \gamma_5 S_a^\dagger(y,x;A)\gamma_5 \tag{3.11}$$

has also been used.

It is now possible to replace the path integral with a Monte Carlo average over gauge configurations, and define the meson two point function:

$$C_2(\vec{p},t) \simeq \frac{1}{N_C}\sum_{k=1}^{N_C}\left(\sum_{\vec{x}} e^{-i\vec{p}\cdot\vec{x}}\mathrm{Tr}\,[\gamma_5\Gamma S_a(x,0;A)\tilde{\Gamma}\gamma_5 S_b^\dagger(x,0;A)]\right)_{\{A\}_k} \, . \tag{3.12}$$

From now the explicit average over the gauge configurations will be dropped. It is possible to derive a very useful expression for the meson two-point function. Using the lattice completeness relation:

$$C_2(\vec{p},t) = \sum_{\lambda,n,\vec{x}} \frac{e^{-i\vec{p}\cdot\vec{x}}}{2E_n(\lambda)L^3}\langle 0|\Omega_M(x)|\lambda,\vec{p}_n\rangle\langle\lambda,\vec{p}_n|\Omega_M^\dagger(0)|0\rangle = \tag{3.13}$$

$$= \sum_{\lambda,n,\vec{x}} \frac{e^{-i\vec{p}\cdot\vec{x}}}{2E_n(\lambda)L^3}e^{-iE_n(\lambda)t}e^{i\vec{p}_n\cdot\vec{x}}|\langle 0|\Omega_M(0)|\lambda,\vec{p}_n\rangle|^2 \, .$$

Recalling the definition of lattice Dirac's delta function, one gets:

$$C_2(\vec{p},t) = \sum_{\lambda} \frac{e^{-E(\vec{p},\lambda)t}}{2E(\vec{p},\lambda)}|\langle 0|\Omega_M(0)|\lambda,\vec{p}\rangle|^2 \, .$$

Considering this exponential decay behaviour, it is reasonable to assume that at there is a time t^* after which the contribution of the excited states is negligible:

$$C_2(\vec{p},t)|_{t\gg t^*} \simeq \frac{e^{-E(\vec{p})t}}{2E(\vec{p})}|\langle 0|\Omega_M(0)|\vec{p}\rangle|^2 \ . \tag{3.14}$$

In other words, only the ground state is taken into account. It is common to define the overlap factor:

$$Z_A(p^2) = \langle 0|\Omega_A(0)|\vec{p}\rangle \ . \tag{3.15}$$

The index A is used to label the quantum numbers of the meson under study (pseudoscalar, vector, etc.). Taking the lattice boundary conditions into account, two-point functions can, at $t \gg t^*$, be modeled by:

$$C_2(\vec{p},t) = \frac{1}{2}A\left[e^{-Et} + be^{-E(T-t)}\right] \ , \tag{3.16}$$

where $b = 1$ if the meson propagator does not change sign under time reversal and $b = -1$ if it does. Thus,

$$C_2(\vec{p},t) = \begin{cases} Ae^{-ET/2}\cosh\left[E\left(\frac{T}{2}-t\right)\right] & (b=1) \\ Ae^{-ET/2}\sinh\left[E\left(\frac{T}{2}-t\right)\right] & (b=-1) \end{cases} \tag{3.17}$$

and

$$A = \frac{Z_A^2}{2E} \ . \tag{3.18}$$

By fitting the two-point functions against time, it is then possible to extract energies and overlap factors of any meson state.

3.4.1 Effective mass

It is obviously important to have a method for estimating the time t^* after which the contribution of the excited states is negligible. It is common to define

$$aM_{\text{eff}}(t) = \log\left[\frac{C_2(t)}{C_2(t+1)}\right] . \tag{3.19}$$

This quantity is called the "*effective mass*": as t reaches t^*, and the approximation in (3.14) holds, $M_{\text{eff}}(t)$ becomes a plateau, up to corrections which are of the order of the statistical errors. By plotting $M_{\text{eff}}(t)$ it is then possible to estimate t^*. This method is used to find out what is the time range on the lattice for which equation (3.14) can be used to extract masses and overlap amplitudes.

3.5 Three-point functions

It is common to deal with processes in which a meson is created at a source, interacts with a current at a given point in space-time which might change its quark composition, and is finally annihilated at a sink (see Figure 3.5).

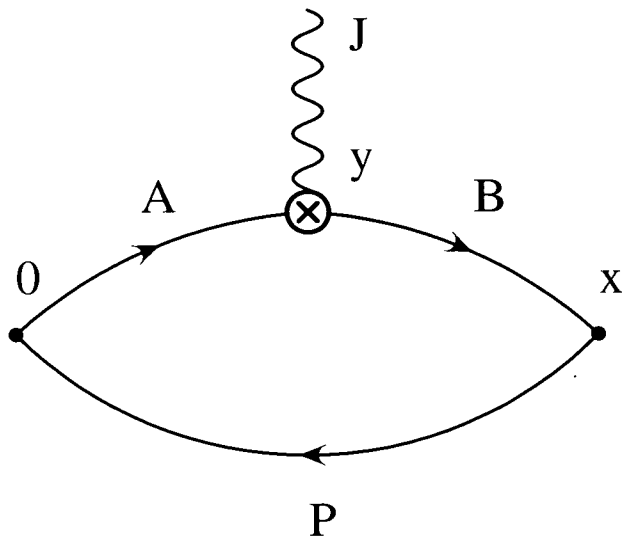

Figure 3.1: The three-point function

The amplitude for this process is given by the three-point function:

$$C^{\mu}_{3,\text{AB}}(\vec{p},\vec{q};t_x,t_y) = \sum_{\vec{x},\vec{y}} e^{-i(\vec{p}\cdot\vec{x}+\vec{q}\cdot\vec{y})}\langle 0|T[\Omega_{\text{B}}(x)J^{\mu}(y)\Omega^{\dagger}_{\text{A}}(0)|0\rangle . \tag{3.20}$$

The source has been taken to be the origin of the lattice. In the diagram, the line labelled with a "P" indicates the light quark, which is called *passive*, since it does not take an active role in the decay. The quark line with the label "B" involves what is called an *all-to-all propagator*, since the points x and y are both arbitrary. All-to-all propagators are computationally very expensive. It is possible to circumvent this problem by defining the *extended propagator*:

$$S_E(\vec{y},0;\vec{p},t_x) \equiv \sum_{\vec{x}} e^{i\vec{p}\cdot\vec{x}} S_P(0,x;A)\gamma^5 S_B(x,y;A) \ . \tag{3.21}$$

The operators appearing in the three-point function can be written in terms of quarks fields:

$$\begin{aligned} \Omega_{\rm B}(x) &= \bar{\psi}_{\rm P}(x)\Gamma_{\rm B}\psi_{\rm B}(x) \ , \\ J^\mu(y) &= \bar{\psi}_{\rm B}(y)\Gamma^\mu\psi_{\rm A}(y) \ , \\ \Omega^\dagger_{\rm A}(0) &= -\bar{\psi}_{\rm A}(0)\Gamma_{\rm A}\psi_{\rm P}(0) \ . \end{aligned} \tag{3.22}$$

Assuming $\Gamma_{\rm B} = \gamma_5$ (pseudoscalar state), and applying Wick's theorem, one can show that:

$$C^\mu_{3,{\rm AB}}(\vec{p},\vec{q};t_x,t_y) = -\sum_{\vec{y}} e^{-i\vec{q}\cdot\vec{y}} \ {\rm Tr}\ \left(\gamma_5 S^\dagger_{\rm E}(\vec{y},0;\vec{p},t_x;A)\Gamma^\mu S_{\rm A}(y,0;A)\Gamma_{\rm A}\right) \ . \tag{3.23}$$

In this work, t_x and t_y have been chosen to satisfy:

$$t_x < t_y < 0 \ . \tag{3.24}$$

This corresponds to a particular choice of time ordering. In particular, t_x has been fixed to be the time-slice 28, at both the two values of β that were simulated in this work, for which $T = 48$. This choice leads to a simplification of the expression of the three-point function. Recalling that:

$$\Omega_M(x) = e^{ik\cdot x}\Omega_M(0)e^{-ik\cdot x} \tag{3.25}$$

and applying the completeness relation twice, one can show that, once Wick rotation to Euclidean space is performed:

$$C^{\mu}_{3,\mathrm{AB}}(\vec{p},\vec{q};t_x,t_y) = \sum_{\lambda,\lambda'} \frac{\langle 0|\Omega_{\mathrm{B}}(0)|\lambda,\vec{p}\rangle}{2E(\lambda,\vec{p})} \frac{\langle \lambda',\vec{p}+\vec{q}|\Omega^{\dagger}_{\mathrm{A}}(0)|0\rangle}{2E(\lambda',\vec{p}+\vec{q})} \times \tag{3.26}$$

$$\times \langle \lambda,\vec{p}|J^{\mu}(0)|\lambda',\vec{p}+\vec{q}\rangle e^{-E(\lambda,\vec{p})t_x} e^{-(E(\lambda',\vec{p}+\vec{q})-E(\lambda,\vec{p}))t_y} \ ,$$

where the sum over λ and λ' refers to single and multi particle states. If both t_y and $(t_x - t_y)$ are taken in the asymptotic region, the contribution of the excited states can be treated as negligible. In this case:

$$C^{\mu}_{3,\mathrm{AB}}(\vec{p},\vec{q};t_x,t_y) = \frac{Z_{\mathrm{B}}(\vec{p})}{2E_{\mathrm{B}}(\vec{p})} \frac{Z_{\mathrm{A}}(\vec{p}+\vec{q})}{2E_{\mathrm{A}}(\vec{p}+\vec{q})} \times \tag{3.27}$$

$$\times \langle \mathrm{B},\vec{p}|J^{\mu}(0)|\mathrm{A},\vec{p}+\vec{q}\rangle e^{-E_{\mathrm{B}}(\vec{p})t_x} e^{-(E_{\mathrm{A}}(\vec{p}+\vec{q})-E_{\mathrm{B}}(\vec{p}))t_y}$$

$|A,\vec{p}+\vec{q}\rangle$ and $|B,\vec{p}\rangle$ are both meson ground states.

3.6 Smearing

According to (3.3), a meson field is built by interpolating quark fields. The basic requirement is to create a state with the quantum numbers of the desired particle. There are infinite ways to do so, and this fact is expressed by the freedom in the choice of the function Γ. Nonetheless, it has been shown that, in lattice calculations, one is often interested in the asymptotic behaviour of correlators, i.e. at the times at which the contributions of excited states have decayed away. Since correlation functions on the lattice are fitted at asymptotic times to extract

quantities of interest, it is desirable to try to build the correlators such that they get to the "asymptotic region" as soon as possible in time. This can be achieved by maximising the overlap of the state one is studying with the ground state wave function, by properly choosing Γ. This technique is known as "smearing" [32].

3.6.1 Fuzzing

At a naive level, it is possible to picture a meson as a system composed of a quark and an antiquark connected by a colour flux tube. The Fuzzing technique [33] consists in smearing each link variable by replacing it with a sum of two parts: the link variable itself, multiplied by a numerical factor, plus all the three-link variable strings that can close the first link into a plaquette variable. However, the group $SU(3)$ is not closed under the addition of its elements, and it is necessary to project back the fuzzed gauge operators onto $SU(3)$. This is possible, using the method developed by Cabibbo and Marinari [34]. The definition of the fuzzed link variable is, then:

$$U_\mu^f(x) = \mathcal{P}_{CM}\left[C_f U_\mu(x) + \sum_{\lambda\neq\mu} U_\lambda(x)U_\mu(x+\lambda)U_\lambda^\dagger(x+\mu)\right] . \tag{3.28}$$

$\mathcal{P}_{CM}$ is the operator that projects the fuzzed link variable back onto $SU(3)$. The fuzzing operation can be iterated several times. For the data used in this work, fuzzing was iterated five times and $C_f = 2$. The definition of a quark propagator that is fuzzed at the sink is:

$$S_F(\vec{x},t;0;R;A) = \sum_{i=1}^{6} \psi(\vec{x}+\vec{R}_i,t)\Lambda_i(\vec{x},t;\vec{R}_i;A)\bar{\psi}(\vec{0},0) \tag{3.29}$$

where

$$\Lambda_i(\vec{x},t;\vec{R}_i;A) = \prod_{k=0}^{N-1} U_k^f(x+ki) \tag{3.30}$$

is a product of fuzzed link variables and $N = R/a$. The smearing sum is done over a fixed number of sites N, while the sum over the i index is a sum on all the spatial directions (positive and negative) coming out of the point $\vec{x}$ on the lattice.

The R parameter, the fuzzing radius, is tuned in order to minimise the contamination of meson correlators coming from the first excited state.

3.6.2 Boyling

For the data used in this work, when dealing with heavy quarks, the smearing technique known as Boyling [35] was adopted. This method is based on the fact that heavy quarks can be described by non-relativistic wave functions. Furthermore, a meson can be seen as a system of two particles interacting via a non-relativistic potential, like for an hydrogen atom:

$$H = H_0 + V(r) \; . \tag{3.31}$$

The potential $V(r)$ is spherically symmetric. Therefore, the wave-functions that are solutions of the Schrödinger equation can be factorised in terms of radial wave functions and spherical harmonics:

$$\psi_{nlm}(r, \theta\, \phi) = R_{nl}(r) Y_{lm}(\theta, \phi) \; . \tag{3.32}$$

If spherically symmetric functions $S_n(r)$ only are considered, it is possible to build, on a lattice, non-local interpolation functions of the form:

$$S_n(\vec{x}, 0) \equiv \sum_{r=0}^{N} r^2 S_n(r) \sum_{j=1}^{6} \delta^{(3)}(\vec{x} - \vec{r_j}) \; . \tag{3.33}$$

Meson operators can be constructed:

$$\Omega_n(x) = \int d^3y \bar{\psi}(y) S_n(y, x) \psi(x) \; . \tag{3.34}$$

If ψ_n is the wave function of the physical state that is simulated, one wants to choose the smearing function in order to optimise the overlap:

$$C_{mn} = \int d^3x \; \psi_m^*(\vec{x}) S_n(\vec{x}, 0)$$

$$= \sum_{r=0}^{N} r^2 \psi_m^*(r) S_n(r) = \langle \psi_m | S_n \rangle \; . \tag{3.35}$$

If $S_n(r)$ is a good approximation of $\psi_m(r)$, the orthogonality property of wave functions guarantees that:

$$C_{mn} = \delta_{mn} + \eta_{mn} \tag{3.36}$$

where η_{mn} is a negligible perturbation.

It is necessary to define a smearing of the quark fields that takes gauge invariance into account. This can be done by introducing an appropriate product of fuzzed link variables:

$$\psi_{\text{boyled}}(\vec{x}, t) = \sum_{r=0}^{N} \left(r + \frac{1}{2} \right) S_n(\vec{x}, t) \sum_{i=1}^{6} \prod_{j=0}^{r-1} U_j^f(x + n e_{(j)}) \psi(\vec{x} + \vec{r}_j, t) \tag{3.37}$$

where $e_{(j)}$ is the unit vector pointing in the j direction.

It is possible to choose $S_n(r)$ to be a solution of the radial part of the Schrödinger equation for the hydrogen atom, expressed in terms of Laguerre polynomials:

$$S_n(\tilde{r}) = e^{-\tilde{r}} L_n(\tilde{r}) \tag{3.38}$$

where $\tilde{r}$ is a dimensionless parameter:

$$\tilde{r} = \frac{1}{n+1} \frac{r}{r_B} \tag{3.39}$$

and r_B is Bohr's radius. Laguerre polynomials have the general form:

$$L_n(x) = \frac{e^x}{n!}\frac{d^n}{dx^n}(x^n e^{-x}) \tag{3.40}$$

with

$$L_0(x) = e^{-x} \ . \tag{3.41}$$

Needless to say, Laguerre polynomials are real-valued. Assuming that both the physical state under study and the simulated state are described by hydrogenic wave functions with Bohr radii r_ψ and r_S, one can calculate the overlap between the first excited state of the simulated state and the ground state of the physical state:

$$C_{10} = \int_0^\infty r^2 \psi_0(r) S_1(r) dr \ . \tag{3.42}$$

Now:

$$\psi_0(\tilde{r}_\psi) = e^{-\tilde{r}_\psi} \ ,$$

$$S_1(\tilde{r}_S) = \left(1 - \frac{r}{2r_S}\right) e^{-\tilde{r}_S} \ . \tag{3.43}$$

Using these formulas, one can show, after some algebra:

$$C_{10} = \frac{4}{3}\frac{r_*^3}{r_S}\delta_R + \mathcal{O}(\delta_R^2) \tag{3.44}$$

where

$$r_* = \frac{2r_S r_\psi}{2r_S + r_\psi} \tag{3.45}$$

and

$$\delta_R = r_S - r_\psi \tag{3.46}$$

is assumed to be small ($\delta_R^2 \ll \delta_R$). The overlap is proportional to the difference in Bohr radii. The Bohr radius is tuned in order to minimise the overlap with the first excited state. According to Equation (3.44), C_{10} has the same sign as δ_R; if the trial radii r' and r'' correspond to values of C_{10} that are opposite in sign there must be, by continuity, a value of r, $r' \leq r \leq r''$ for which $C_{10} = 0$. However, this exact result is often not achievable because of the non-hydrogenic nature of the physical wave-function.

3.6.3 Smearing labelling convention

Meson correlation functions are labelled by their smearing according to the following scheme:

$$C_{AA',BB'}(\vec{p},t) = \sum_{\vec{x}} e^{i\vec{p}\cdot\vec{x}} \langle \Omega_{AA'}(\vec{x},t)\Omega^\dagger_{BB'}(0)\rangle \tag{3.47}$$

where A, A', B, B' can be:

- "L": local, i.e. not smeared;
- "F": fuzzed;
- "B": Boyled.

If only two labels are given, $A' = A, B' = B$ is assumed.

3.7 Statistical analysis

In lattice field theory, path integrals are replaced by averages over previously generated gauge field configurations. In particular, one has often to deal with

statistically correlated data, like propagators that are evaluated on different time slices. If there are N_G gauge configurations, and the same correlator is evaluated on each of them, it is possible to write a gauge ensemble average:

$$\langle C(t) \rangle = \frac{1}{N_G} \sum_{j=1}^{N_G} C_j(t) \ , \tag{3.48}$$

where the standard deviation is simply given by:

$$\sigma_c(t) = \left[\frac{1}{N_G - 1} \sum_{j=1}^{N_G} [C_j(t) - \langle C(t) \rangle]^2 \right]^{1/2} \ . \tag{3.49}$$

Having to deal with statistically correlated data, it is necessary to introduce a covariance matrix:

$$\sigma_c(t,t') = \frac{1}{N_G(N_G-1)} \sum_{k=1}^{N_G} [C_k(t) - \langle C(t) \rangle][C_k(t') - \langle C(t') \rangle] \tag{3.50}$$

where

$$\sigma_c(t,t) = \frac{1}{N_G} \sigma_c^2(t) \ , \tag{3.51}$$

while, for uncorrelated data, off-diagonal terms of the covariance matrix should be zero. It is sensible to introduce a re-scaled matrix that takes values between -1 and 1, the correlation matrix:

$$\rho_c(t,t') = \frac{\sigma_c(t,t')}{\sqrt{\sigma_c(t,t)}\sqrt{\sigma_c(t',t')}} \tag{3.52}$$

3.8 Fitting the correlators

What happens in practice is that some Green's function $C_i(t)$, is fitted to a model function with a given number of parameters p:

$$C(t) = F(t; \theta_1, ..., \theta_p) \ . \tag{3.53}$$

The fit will be carried out by minimising χ^2, which for correlated data is:

$$\chi^2(\theta) = \sum_{t,t'} [F(t;\theta) - \langle C(t) \rangle] \rho_c^{-1}(t,t') [F(t';\theta) - \langle C(t') \rangle] \ . \tag{3.54}$$

The data that are fitted are usually correlated. In order to understand why lattice data are often correlated, it is necessary to go one step back. Lattice quantities are averaged over gauge configurations which are generated with an algorithm. Generation of gauge field configurations for which a field has a drastic variation from one site to one of the nearest neighbours is very unlikely. For this reason, if a quantity $Q_i(t)$, calculated on the i-th configuration is such that:

$$Q_i(t) > \langle Q(t) \rangle \tag{3.55}$$

where $\langle Q(t) \rangle$ is the average over all the configurations, the probability of having:

$$Q_i(t+1) \ll \langle Q(t) \rangle \tag{3.56}$$

is usually very small. This means that the error bars of some Green's function at different time-slices are usually correlated.

If the fit is done over N_t time-slices, the number of degrees of freedom is:

$$\Delta = N_t - p \ . \tag{3.57}$$

And if the reduced χ^2 is defined,

$$\tilde{\chi}^2 \equiv \frac{\chi^2}{\Delta} \tag{3.58}$$

it is possible to judge the goodness of a fit. For a good fit,

$$\tilde{\chi}^2 \simeq 1 \ .$$

The other statistical indicator of the goodness of a fit is:

$$Q = \frac{\Gamma(\Delta/2, \chi^2/2)}{\Gamma(\Delta/2)} \ . \tag{3.59}$$

where $\Gamma(n, x)$ is the incomplete Euler gamma function. For a good fit, $Q \simeq 1/2$.

3.8.1 Bootstrap resampling

In principle, in order to estimate the statistical errors of the parameters of a fit, one should repeat the whole calculation on different sets of gauge configurations. At present, this is still very impractical, and it is necessary to use a statistical technique to "simulate" the process of repeating the simulation. In this work, the "bootstrap" method has been used. From N_C configurations, one makes N_B ensembles of N_C configurations, taken randomly from the original set of N_C configurations, allowing repetitions. The quantities of interest are calculated in each of these samples, and the distributions of their values are built. From these distributions it is possible to define the statistical error to correspond to the 68% level of confidence.

Chapter 4

Heavy Quark Effective Theory

4.1 Basic ideas

This work is focused on mesons containing a heavy and a light quark, which can be studied by applying the Heavy Quark Effective Theory, HQET. A complete review of the subject can be found in [36]. It is possible to consider HQET as a complementary theory to chiral symmetry (which works in the limit of vanishing quark masses). To begin with, it is necessary to give a meaning to the expression "heavy quark". It is possible to do so by looking at the one-loop form of the strong coupling:

$$\alpha_s(Q^2) = \frac{12\pi}{(33 - 2n_f)\ln\left(\frac{Q^2}{\Lambda^2_{QCD}}\right)} . \tag{4.1}$$

Here n_f is the number of flavours and $\Lambda_{QCD} \simeq 0.2\ GeV$ is the physical scale that separates the regions of small and large coupling. It is then natural to define a quark as:

- **heavy** if $m_q \gg \Lambda_{QCD}$ (c,b,t)
- **light** if $m_q \ll \Lambda_{QCD}$ (u,d,s) .

For heavy-light mesons, the typical momenta exchanged between heavy and light constituents are of the order of Λ_{QCD}. The heavy quark is surrounded by the light valence quark and by a confined cloud of strongly interacting soft gluons and quark-antiquark pairs, known as "*brown muck*" [37, 38]. Now, one can define a "hadronic length scale":

$$R_{had} = \frac{1}{\Lambda_{QCD}} \simeq 1\text{fm} .$$

If m_Q is the mass of the heavy quark, it is easy to see that:

$$\lambda_Q = \frac{1}{m_Q} \ll R_{had} . \tag{4.2}$$

This means that the Compton wavelength of the heavy quark is much shorter than the average wavelength associated with the brown muck. Henceforth, the brown muck "does not see" the degrees of freedom of the heavy constituent, i.e. it is "blind" to flavour and spin of the heavy quark. In other words, the brown muck sees the heavy quark as a heavy scalar particle. If the mass of the heavy quark is large enough, then, an additional spin-flavour symmetry is acquired. On the other hand, the brown muck is a strongly non-perturbative object, and its presence makes the study of heavy-light systems much more difficult.

The presence of a heavy quark symmetry has interesting consequences on the weak decay processes. In particular, in the limit of infinite quark mass, it is possible to express the form factors for the semi-leptonic decays of heavy mesons in terms of an universal function of the velocity exchange $\xi(v \cdot v')$, known as the Isgur-Wise function [37, 38]. In general, HQET hadronic matrix elements can be parametrised using form factors which describe the light degrees of freedom and are otherwise universal, in the sense that they are independent of the heavy degrees of freedom.

At this point, it becomes necessary to be able to produce reasonable estimates of the corrections to the heavy quark symmetry limit. There are two kinds of corrections that have to be taken into account: power corrections in the heavy

quark masses, and radiative corrections coming from the exchange of hard gluons, that can resolve the quantum numbers of the heavy quark.

4.2 HQET formalism

This paragraph is a brief introduction to the formalism of HQET (see also [39, 40, 41, 42, 43, 44, 45, 46, 47, 48]). Consider a meson that is composed of a heavy quark of mass m_Q and a light quark. The heavy quark will carry the largest fraction of the total momentum:

$$P_Q^\mu = m_Q v^\mu + k^\mu \ . \tag{4.3}$$

k is a residual momentum, which is typically of $\mathcal{O}(\Lambda_{QCD})$; v is the velocity of the heavy quark that, in the limit $m_Q \to \infty$, is unchanged by soft processes [43] (velocity changes are $\delta v \simeq \Lambda_{QCD}/m_Q$). It is also interesting to notice that the heavy quark is almost on-shell.

The standard Lagrangian for a heavy quark is:

$$\mathcal{L}_Q = \bar{Q}(x)(i\not{D} - m_Q)Q(x) \tag{4.4}$$

It is possible to rewrite this Lagrangian as a series in $1/m_Q$. The first step consists in introducing a set of two projection operators:

$$\mathcal{P}_\pm \equiv \frac{1}{2}(1 \pm \not{v}) \tag{4.5}$$

By means of these operators, one can define two fields:

$$\begin{aligned} h_v(x) &= e^{im_Q v\cdot x}\mathcal{P}_+ Q(x) \\ H_v(x) &= e^{im_Q v\cdot x}\mathcal{P}_- Q(x) \end{aligned} \tag{4.6}$$

The physical interpretation of h_v and H_v is evident in the rest frame, where they correspond to the upper and lower components of Q. It is possible to verify that:

$$\begin{aligned} \not{v} h_v &= h_v \\ \not{v} H_v &= -H_v \ . \end{aligned} \tag{4.7}$$

The heavy quark Lagrangian is now rewritten as:

$$\mathcal{L}_{hH} = \bar{h}_v iv \cdot D h_v - \bar{H}_v (iv \cdot D + 2m_Q) H_v + \bar{h}_v i \not{D}_\perp H_v + \bar{H}_v i \not{D}_\perp h_v \ , \tag{4.8}$$

where D is the standard covariant derivative of QCD. The differential operator $D_\perp$ is defined by:

$$D_\perp^\mu = D^\mu - v^\mu (v \cdot D) \tag{4.9}$$

and satisfies:

$$v \cdot D_\perp = 0 \ . \tag{4.10}$$

Now, inspection of equation (4.8) shows that h_v is a massless degree of freedom, while H_v corresponds to a degree of freedom of mass $2m_Q$. At a classical level, it is possible to apply the equations of motion to eliminate the heavy degrees of freedom H_v (being interested in energy scales at which heavy antiquarks cannot be produced):

$$(iv \cdot D + 2m_Q) H_v = i \not{D}_\perp h_v \tag{4.11}$$

This equation can be solved formally:

$$H_v = \frac{1}{2m_Q} \left(1 + \frac{iv \cdot D}{2m_Q} \right)^{-1} i \not{D}_\perp h_v \tag{4.12}$$

giving a Lagrangian:

$$\mathcal{L}_h = \bar{h}_v iv \cdot D h_v + \frac{1}{2m_Q} \bar{h}_v i \not{D}_\perp \left(1 + \frac{iv \cdot D}{2m_Q}\right)^{-1} i \not{D}_\perp h_v \ . \tag{4.13}$$

Now, as long as m_Q is large but finite, this Lagrangian leads to virtual processes in which a heavy quark travels for a short distance given by:

$$\delta x \simeq 1/m_Q \ . \tag{4.14}$$

This makes the Lagrangian non-local. Nonetheless, it is possible to rewrite it in terms of an infinite series of local terms. One can show that the condition $k^2 \ll m_Q^2$ makes a geometric expansion possible:

$$H_v = \frac{1}{2m_Q} \sum_{k=0}^{\infty} \left(\frac{-iv \cdot D}{2m_Q}\right)^k i \not{D}_\perp h_v \ . \tag{4.15}$$

This result can be put back in the Lagrangian, which reads:

$$\mathcal{L}_h = \bar{h}_v iv \cdot D h_v + \frac{1}{2m_Q} \bar{h}_v i \not{D}_\perp \sum_{k=0}^{\infty} \left(\frac{-iv \cdot D}{2m_Q}\right)^k i \not{D}_\perp h_v \ . \tag{4.16}$$

This Lagrangian can be written more explicitly as a series in $1/m_Q$

$$\mathcal{L}_h = \sum_{n=0}^{\infty} \frac{1}{m_Q^n} \mathcal{L}_n \ , \tag{4.17}$$

where the first term, corresponding to the limit $m_Q \to \infty$ (dependence on m_Q has been analytically removed), is:

$$\mathcal{L}_0 = \bar{h}_v iv \cdot D h_v \tag{4.18}$$

and the $1/m_Q$ term, $\mathcal{L}_1$, has the form:

$$\mathcal{L}_1 = \frac{1}{2m_Q}\left[\bar{h}_v(iD)^2 h_v + \frac{g_s}{s} Z(\mu)\bar{h}_v \sigma_{\alpha\beta} G^{\alpha\beta} h_v\right] . \tag{4.19}$$

Z is, in the leading logarithmic approximation, the renormalisation factor of the colour magnetic moment operator:

$$Z(\mu) = \left[\frac{\alpha_s(m_Q)}{\alpha_s(\mu)}\right]^{9/(33-2n_f)} . \tag{4.20}$$

It is quite interesting to evaluate the propagator of a heavy quark:

$$\mathcal{G}(P_Q) = i\frac{\not{P}_Q + m_Q}{P^2 - m_Q^2} . \tag{4.21}$$

Applying equation (4.3), one can show that:

$$\mathcal{G}(P_Q) = i\frac{1}{v\cdot k}\mathcal{P}_+ + \mathcal{O}\left(\frac{k}{m_Q}\right) . \tag{4.22}$$

It is also possible to show that:

$$\mathcal{P}_+\gamma_\mu\mathcal{P}_+ = \mathcal{P}_+ v_\mu \mathcal{P}_+ . \tag{4.23}$$

This identity has the effect of reducing the vertex of a heavy quark and a gluon to:

$$-igv_\mu T^a . \tag{4.24}$$

These two modified Feynman rules confirm the statement that the heavy quark is "seen" by the light degrees of freedom as a spinless scalar field.

In the $m_Q \to \infty$ limit, the soft gluons of the brown muck can't resolve the flavour or the spin of the heavy quark. This corresponds to a $SU(2N_{\mathrm{h}})$ symmetry, where N_{h} is the number of heavy quark flavours.

A more formal derivation of the HQET Lagrangian, in the framework of path integrals, can be found in [49].

4.2.1 Mass independent meson state normalisation

In the framework of HQET, it is common to express mesonic states in terms of the velocity rather than the momentum. This modified normalisation is related to the common, relativistic one by:

$$|M(v)\rangle \equiv \frac{1}{\sqrt{m_M}}|M(p)\rangle \tag{4.25}$$

such that:

$$\langle M(v')|M(v)\rangle = \frac{2E}{m_M}(2\pi)^3\delta^{(3)}(\vec{p}' - \vec{p}) \tag{4.26}$$

4.3 Expansion of quark currents

Assume $J(m_Q, m_{Q'})$ is a current of the full heavy quark QCD Lagrangian (4.4):

$$J = \bar{Q}'\Gamma Q \tag{4.27}$$

with $\Gamma = \{\gamma_\mu, \gamma_\mu\gamma_5\}$. These operators admit an expansion in terms of the currents of HQET [50]:

$$\begin{aligned} J(m_Q, m_{Q'}) \;\simeq\; & \sum_{i=1}^{3} C_i(\bar{m}/\mu)\hat{J}_i(\mu) + \\ & + \sum_{m,n=1}^{\infty} \frac{1}{m_Q^m}\frac{1}{m_{Q'}^n}\sum_k C_k^{(mn)}(\bar{m}/\mu)\hat{J}_k^{(mn)}(\mu)\ , \end{aligned} \tag{4.28}$$

where

$$\bar{m} = \frac{2m_Q m_{Q'}}{m_Q + m_{Q'}} \tag{4.29}$$

and μ is a subtraction scale. The operators of the first term of the expansion can be written as:

$$\hat{J}_i = \bar{h}_Q \Gamma_i h_{Q'} \tag{4.30}$$

where $\Gamma_i = \{\gamma_\mu(\gamma_5), -v_\mu(\gamma_5), -v'_\mu(\gamma_5)\}$ (v and v' are the velocities of the two heavy quarks, Q and Q'). The second term of (4.28) is a sum over all the operators $\hat{J}_k^{(mn)}$ of higher mass dimension. The equality in (4.28) is not strictly correct: in fact, what should be compared is the expectation value of both sides. The expectation value of left hand side should be taken between states of the full theory, while that of the right hand side should be taken between states of the effective theory. Once this is done, one can show that:

$$\langle J(m_Q, m_{Q'})\rangle = \sum_{i=1}^{3} C_i(\bar{m}/\mu)\langle \hat{J}_i(\mu)\rangle + \mathcal{O}\left(\frac{\Lambda_{QCD}}{m_Q}\right) \tag{4.31}$$

The unphysical dependence of the expectation value of J upon the subtraction scale μ is removed by the means of Renormalization Group Equation:

$$\sum_{j=1}^{3}\left(\delta_{ij}\mu\frac{d}{d\mu} - \gamma_{ij}\right) C_j(\bar{m}/\mu) = 0 \tag{4.32}$$

where γ is the anomalous dimension matrix for the operators $\hat{J}_i$. The coefficients $C_i(\bar{m}/\mu)$ are used to extract a set of μ-independent coefficients that are the building blocks in the calculation of the radiative corrections to the Heavy Quark Symmetry.

4.4 Weak decay form factors

The weak decay of a heavy-light meson is triggered by the interaction with an external current that can change the velocity and the flavour of the heavy quark. In particular, the matrix elements that describe the weak decays of a heavy-light pseudoscalar meson into a heavy-light meson are parametrised in terms of a set of form factors:

$$\langle \mathrm{PS}'(v')|h'_{v'}\gamma_\mu h_v|\mathrm{PS}(v)\rangle = h_+(\omega)(v+v')_\mu + h_-(\omega)(v-v')_\mu \quad (4.33)$$

$$\langle \mathrm{V}(v',\eta)|h'_{v'}\gamma^\mu h_v|\mathrm{PS}(v)\rangle = ih_V(\omega)\epsilon^{\mu\nu\alpha\beta}\eta^*_\nu v'_\alpha v_\beta \quad (4.34)$$

$$\langle \mathrm{V}(v',\eta)|h'_{v'}\gamma^\mu\gamma_5 h_v|\mathrm{PS}(v)\rangle = h_{A_1}(\omega)(\omega+1)\eta^{*\mu} - \left[h_{A_2}(\omega)v^\mu + h_{A_3}(\omega)v'^\mu\right](\eta^*\cdot v) \quad (4.35)$$

where

$$\omega = v\cdot v' \ . \quad (4.36)$$

v and v' are the velocities of the colour source the light degrees of freedom interact with before and after the insertion of the external current. The ω variable is related to the momentum transfer q and the masses of the initial and final meson by:

$$\omega = \frac{m_M^2 + m_{M'}^2 - q^2}{2m_M m_{M'}} \quad (4.37)$$

and satisfies:

$$\omega \in \left[1, \frac{m_M^2 + m_{M'}^2}{2m_M m_{M'}}\right] \ . \quad (4.38)$$

All these form factors become related to each other in the infinite quark mass limit. In fact, as the heavy quark gets infinitely heavy, the theory acquires an additional flavour symmetry, and the interactions between the brown muck and

the heavy quark are described by a universal function $\xi(\omega)$, known as the Isgur-Wise function.

Following [50], it is possible to show that:

$$h_j(\omega) = [\alpha_j + \beta_j(\omega; m_Q, m_{Q'}) + \gamma_j + ...]\,\xi_{\rm ren}(\omega) \ , \tag{4.39}$$

where

$$\begin{aligned} \alpha_+ = \alpha_V = \alpha_{A_1} = \alpha_{A_3} = 1 \\ \alpha_- = \alpha_{A_2} = 0 \end{aligned} \tag{4.40}$$

and $\xi_{\rm ren}$ is the renormalisation group invariant Isgur-Wise function [50].

The β and γ functions are corrections to the heavy quark symmetry. These corrections are of two kinds: radiative QCD corrections (perturbative) and power corrections in the heavy quark masses (non-perturbative), here considered up to $\mathcal{O}(1/m_Q)$. The expressions for the radiative corrections have been derived in [50] as:

$$\beta_i = \beta_i(\omega, m_Q, m_{Q'}, z)$$

where $z = m_{Q'}/m_Q$ is assumed to satisfy:

$$z \leq 1 \ . \tag{4.41}$$

The estimates of the radiative corrections used in this work are accurate up to

$$\alpha_s^2 (z \ln z)^n \tag{4.42}$$

corrections, with $n = 0, 1, 2$. The power corrections are non-perturbative in nature, and describe the breaking of the heavy quark symmetry. They can be

calculated within Lattice QCD, or using QCD sum rules [51]. However, Luke's theorem [52] guarantees that, at zero recoil, there are no, to order $1/m_Q$, power corrections to h_{A_1} and h_+:

$$\gamma_{A_1}(\omega)|_{\omega=1} = \gamma_+(\omega)|_{\omega=1} = \mathcal{O}\left(\frac{1}{m_Q^2}\right) . \tag{4.43}$$

4.5 The Isgur-Wise function

The Isgur-Wise function is a fundamental quantity, and its knowledge is of paramount importance in the study of the non-perturbative aspects of the Standard Model. An important aspect of the Isgur-Wise function is its universality in the heavy quark limit: any weak decay of heavy mesons into heavy mesons can be described with this function, which does not depend on the masses of the mesons.

The Isgur-Wise function is real valued; furthermore, current conservation predicts that, at zero recoil ($\omega = 1$):

$$\xi(1) = 1 . \tag{4.44}$$

At small recoil ($\omega \simeq 1$), $\xi(\omega)$ is modeled as a linear function of $\omega - 1$:

$$\xi(\omega) = 1 - \rho^2(\omega - 1) + \mathcal{O}((\omega - 1)^2) , \tag{4.45}$$

where ρ^2 is the so called slope parameter:

$$\rho^2 = -\left(\frac{d\xi(\omega)}{d\omega}\right)_{\omega=1} . \tag{4.46}$$

Several models have been proposed for $\xi(\omega)$, that all agree up to $\mathcal{O}((\omega - 1)^2)$ terms. They are [53, 54, 36]:

$$\begin{aligned}
\xi_{\mathrm{BSW}}(\omega) &= \left(\frac{2}{\omega+1}\right)\exp\left[-(2\rho^2-1)\frac{\omega-1}{\omega+1}\right] \\
\xi_{\mathrm{ISGW}}(\omega) &= \exp\left[-\rho^2(\omega-1)\right] \\
\xi_{\mathrm{POLE}}(\omega) &= \left(\frac{2}{\omega+1}\right)^{2\rho^2} .
\end{aligned} \tag{4.47}$$

Theoretical constraints on the possible values of ρ^2 have been derived by Bjorken [55, 56] and Voloshin [57]:

$$\frac{1}{4} \leq \rho^2 \leq \frac{1}{4} + \frac{m_M - m_Q}{2E_m} . \tag{4.48}$$

In this equation, m_M and m_Q are meson and heavy quark mass respectively. The energy E_m is the energy of the first excited state of the meson.

Chapter 5

Quenched heavy-light decay constants

5.1 Introduction

Within the phenomenology of the weak interaction, the study of the decays of B and D mesons plays a crucial role. In particular, in order to extract the CP violating phase of the CKM matrix, it is necessary to know the decay constant f_B. More specifically, one needs to know the combination $f_B\sqrt{B_B}$, where B_B is a phenomenological parameter that describes the $B^0 - \bar{B}^0$ mixing, and is expected to be close to one. The decay constants of the D mesons are useful to the studies of non-leptonic decays of B mesons into charmed mesons [58, 59].

This chapter presents the results of a calculation of the decay constants of B and D mesons, at two values of β, within the quenched approximation. The action that was used in this work has been introduced in Chapter 2.

In the infinite quark mass limit, in which the Heavy Quark Symmetry (HQS) is perfectly realised, the vector and the pseudoscalar decay constants become related. Therefore, in dealing with heavy quark systems, it is possible to use HQS to justify the form used to extrapolate the decay constants to the B scale.

Table 5.1: Summary of results

$$f_B = 218 \pm 5^{+5}_{-41} \text{ MeV} \qquad f_{B^*} = 22.6 \pm 0.7^{+4.4}_{-3.6}$$

$$f_D = 220 \pm 3^{+2}_{-24} \text{ MeV} \qquad f_{D^*} = 7.5 \pm 0.1^{+1.3}_{-0.8}$$

$$f_{B_S} = 242 \pm 4^{+13}_{-48} \text{ MeV} \qquad f_{B_s^*} = 20.9 \pm 0.4^{+3.3}_{-4.2}$$

$$f_{D_S} = 241 \pm 2^{+7}_{-30} \text{ MeV} \qquad f_{D_s^*} = 7.3 \pm 0.1^{+0.9}_{-0.4}$$

$$f_{B_s}/f_B = 1.11 \pm 0.01^{+0.05}_{-0.03} \qquad f_{B_s^*}/f_{B^*} = 0.92 \pm 0.01^{+0.04}_{-0.03}$$

$$f_{D_s}/f_D = 1.09 \pm 0.01^{+0.05}_{-0.02} \qquad f_{D_s^*}/f_{D^*} = 0.98 \pm 0.01^{+0.02}_{-0.04}$$

Table 5.2: Some simulation parameters

	$\beta = 6.2$	$\beta = 6.0$
Volume	$24^3 \times 48$	$16^3 \times 48$
N_{config}	216	305
N_{boot}	1000	1000

The results for the decay constants are given in Table 5.1.

The first error quoted is statistical, the second is systematic (discussed later on). For the central values, the lattice spacing has been fixed by using the Sommer [60, 61] scale r_0.

5.2 Simulation parameters

The calculation of the decay constants has been performed at two values of β, 6.0 and 6.2. Some important simulation parameters are listed in table 5.2.

The N_{boot} parameter is the number of bootstrap resamplings. The values of the hopping parameters corresponding to heavy and light simulated quarks are shown

Table 5.3: Hopping parameters used in this work

	$\beta = 6.2$	$\beta = 6.0$
heavy	0.12000	0.11230
	0.12330	0.11730
	0.12660	0.12230
	0.12990	0.12730
light	0.13460	0.13344
	0.13510	0.13417
	0.13530	0.13455

in Table 5.3.

The four heavy quarks have physical masses around the charm scale, while the light quark masses are close to the strange quark mass. This means the extraction of the decay constant of the D meson will involve just an interpolation, while a long extrapolation is needed to extract f_B. This is a source of systematic uncertainty, and has been studied carefully.

5.2.1 Improvement coefficients

It is now necessary to list the improvement coefficients as they were used in this work. Although all the coefficients have been calculated in one-loop perturbation theory, it is desirable to use non-perturbative determinations whenever available, in order to remove all the $\mathcal{O}(a)$ discretisation errors. In fact, the perturbative calculations are affected by discretisation errors of $\mathcal{O}(\alpha_s a)$. The ALPHA collaboration have provided non-perturbative determinations of $c_{SW}, c_A, b_V, Z_V, Z_A$. The b_m parameter has been extracted using non-perturbative methods only at $\beta = 6.2$ [62], while a perturbative estimate exists at $\beta = 6.0$, that has been used in this work. A summary of the chosen determinations of the coefficients is given in Table 5.4.

The determination of c_V is quite difficult and, at the time of this work, a definitive

Table 5.4: The improvement coefficients that were used in this work

Coeff.	$\beta = 6.2$	$\beta = 6.0$	Ref.
c_{SW}	1.614	1.769	NP [24]
c_{A}	−0.0371	−0.0828	NP [23]
c_{V}	−0.0258	−0.0275	BPT [63]
Z_{A}	0.8067(79)	0.7906(94)	NP [24]
Z_{V}	0.7922(10)	0.7809(6)	NP [24]
b_{A}	1.47(12)	1.44(13)	NP [64, 65]
b_{V}	1.404(7)	1.477(7)	NP [24]
b_{m}	−0.652	−0.662	BPT [63]

non-perturbative estimation was not available. The ALPHA determination of this quantity differs from the perturbative result by an order of magnitude, and has a quite large uncertainty, like the determination by Battacharya *et al.*. For this reasons, the value used in this work is the one calculated in boosted perturbation theory.

The values of the decay constants that are extracted using the different determinations of c_{A} and c_{V} are inconsistent with each other. A better determination of the improvement coefficients is quite important: some of the current determinations are inconsistent with each other by one sigma or more. Therefore, the different determinations of the coefficients have not been taken into account when estimating the systematic errors. However, as more precise determinations become available, should they be substantially different, the results of this work would change in a significant manner.

5.3 Pseudoscalar decay constant

At zero momentum, pseudoscalar decay constants are defined as follows, in terms of the improved and renormalised axial current:

$$Z_{\rm A}^{\rm eff}\langle 0|A_4^{\rm I}(0)|P\rangle = M_{\rm P} f_{\rm P} \ . \tag{5.1}$$

Thus, it is necessary to evaluate on the lattice the masses of the meson states and the matrix element, via fits to the proper two-point functions. Masses and matrix elements are extracted from:

$$C_{\rm AB}^{\rm PP}(t,\vec{p}) = \sum_{\vec{x}} e^{-i\vec{p}\cdot\vec{x}}\langle P_{\rm A}(t,\vec{x}) P_{\rm B}^{\dagger}(0)\rangle \ , \tag{5.2}$$

where $P_{\rm A}^{\dagger}$ is the interpolating operator of a meson pseudoscalar state, with smearing A. Asymptotically,

$$C_{\rm FF}^{\rm PP}(t,\vec{p}) \simeq \frac{e^{-E_{\rm P}(\vec{p})(T/2)}}{E_{\rm P}(\vec{p})}(Z_{\rm P}^{\rm F})^2 \cosh\left[E_{\rm P}(\vec{p})\left(\frac{T}{2}-t\right)\right] \ , \tag{5.3}$$

where

$$E_{\rm P}(\vec{p}) = \sqrt{\vec{p}^2 + M_{\rm P}^2} \tag{5.4}$$

and

$$Z_{\rm P}^{\rm F} = \langle 0|P_{\rm F}(0)|P\rangle \ . \tag{5.5}$$

From the zero momentum correlator it is then possible to extract the masses and the fuzzed overlap amplitude $Z_{\rm P}^{\rm F}$. Similarly, defining

$$C_{\rm LF}^{\rm AP}(t,\vec{p}) \equiv \sum_{\vec{x}} e^{-i\vec{p}\cdot\vec{x}}\langle 0|A_{\rm L}^4(0) P_{\rm F}^{\dagger}(\vec{x},t)|0\rangle \tag{5.6}$$

by inserting a complete set of pseudoscalar states, one can show that

$$C_{\rm LF}^{\rm AP}(t,\vec{p}) \simeq e^{-E_{\rm P}(\vec{p})(T/2)}\frac{1}{2} Z_{\rm P}^{\rm F} f_{\rm P} \sinh\left[E_{\rm P}(\vec{p})\left(\frac{T}{2}-t\right)\right] \ . \tag{5.7}$$

From these two equations, follows a relation for the ratio of the correlators, at zero momentum:

$$R \equiv \frac{C_{\mathrm{LF}}^{\mathrm{AP}}(t)}{C_{\mathrm{FF}}^{\mathrm{PP}}(t)} \simeq \frac{f_{\mathrm{P}}}{E_{\mathrm{P}} Z_{\mathrm{P}}^{F}} \tanh\left[M_{\mathrm{P}}\left(\frac{T}{2}-t\right)\right] . \tag{5.8}$$

Therefore, f_{P} can be extracted by a two stage fit:

1. the fuzzed-fuzzed $C_{\mathrm{FF}}^{\mathrm{PP}}(t)$ correlator is fitted and M_{P} and $Z_{\mathrm{P}}^{\mathrm{F}}$ are extracted;
2. keeping M_{P} and $Z_{\mathrm{P}}^{\mathrm{F}}$ from the first fit, the ratio in equation (5.8) is fitted, and f_{P} is evaluated from the value of the plateau of the tanh function.

5.4 Vector decay constant

For historical reasons, the vector decay constant has a different definition:

$$Z_{\mathrm{V}}^{\mathrm{eff}} \langle 0|V_{\mu}^{\mathrm{I}}(0)|V\rangle = \epsilon_{\mu} \frac{M_{\mathrm{V}}^{2}}{f_{\mathrm{V}}} \tag{5.9}$$

where ϵ is the polarisation 4-vector. According to this definition, f_{V} is a dimensionless quantity. In this work, the three spatial components of the vector correlator have been averaged:

$$C_{\mathrm{AB}}^{\mathrm{VV}}(t,\vec{p}) = \sum_{j=1}^{3} \sum_{\vec{x}} e^{-i\vec{p}\cdot\vec{x}} \langle 0|V_{\mathrm{A}}^{j}(t,\vec{x}) V_{\mathrm{B}}^{j\dagger}(0)|0\rangle \tag{5.10}$$

In particular, asymptotically:

$$C_{\mathrm{FF}}^{\mathrm{VV}}(t,\vec{p}) \simeq -\frac{3}{2} \frac{e^{-E_{\mathrm{V}}(\vec{p})(T/2)}}{E_{\mathrm{V}}(\vec{p})} (Z_{\mathrm{V}}^{F})^{2} \cosh\left[E_{\mathrm{V}}(\vec{p})\left(\frac{T}{2}-t\right)\right] \tag{5.11}$$

At zero momentum it is possible to show that:

Table 5.5: Mass fit ranges

β	PS	V
6.0	$10-22$	$10-21$
6.2	$12-22$	$12-22$

$$\frac{C_{\rm LF}^{VV}(t)}{C_{\rm FF}^{VV}(t)} \simeq \frac{1}{(Z_V^{\rm F})^2}\frac{M_V^2}{f_{\rm V}} \tag{5.12}$$

This means that, once the vector meson mass and the overlap factor have been extracted from a fit of $C_{\rm FF}^{\rm VV}(t)$, these parameters can be passed to a fit of the ratio $C_{\rm LF}^{VV}(t)/C_{\rm FF}^{VV}(t)$ to obtain $f_{\rm V}$.

5.5 Fit ranges

The fit ranges for the masses were chosen on the basis of a study of the effective mass plots, and are summarised in the Table (5.5). Table (5.6) shows the ranges for the fit:

$$R(t) = R_0 \ \tanh\left[M_{\rm P}\left(\frac{T}{2}-t\right)\right] \tag{5.13}$$

these ranges have been chosen according to the following criteria:

- existence of a plateau;
- stability of the value of the decay constant;
- reasonable values of χ^2, Q.

Tabulated values of the masses and the decay constants at each heavy-light combination can be found in the appendices.

Table 5.6: Decay constant fit ranges

β	PS	V
6.0	14 – 21	15 – 23
6.2	14 – 21	16 – 23

5.6 Quark masses

The values of the improved, RG invariant quark masses, defined by:

$$m_Q^{\rm phys} = Z_{\rm m} m_q (1 + b_{\rm m} a m_q) \tag{5.14}$$

are shown in tables 5.7 and 5.8. The scale was set using r_0.

Table 5.7: Improved, renormalised heavy quark massses, in physical units. Bare quark masses are also shown. The scale is set using r_0.

$\beta = 6.2$			$\beta = 6.0$		
κ	am_Q	$m_Q^{\rm phys}$ (GeV)	κ	am_Q	$m_Q^{\rm phys}$ (GeV)
0.1200	0.485	1.75(4)	0.1123	0.756	1.40(4)
0.1233	0.374	1.49(4)	0.1173	0.566	1.32(2)
0.1266	0.268	1.16(3)	0.1223	0.392	1.08(3)
0.1299	0.168	0.79(2)	0.1273	0.231	0.73(2)

Table 5.8: Improved, renormalised light quark massses, in physical units. Bare quark masses are also shown. The scale is set using r_0.

$\beta = 6.2$			$\beta = 6.0$		
κ	am_Q	$m_Q^{\rm phys}$ (MeV)	κ	am_Q	$m_Q^{\rm phys}$ (MeV)
0.1346	0.033	171(2)	0.13344	0.050	180(1)
0.1351	0.019	101(2)	0.13417	0.030	109(2)
0.1353	0.014	73(2)	0.13455	0.019	71(2)

5.7 Extrapolation in the light quark mass

Meson masses and decay constants are calculated at several unphysical values of the heavy and the light quark masses, and therefore have to be extrapolated to the physical values. In the case of a heavy-light meson, the simplest ansatz for the dependence of the mass and the decay constant on the light quark mass is linear:

$$aX = \alpha_X + \beta_X a\tilde{m}_q \ . \tag{5.15}$$

Masses and decay constants are extrapolated in the light hopping parameter to both $\kappa_{\rm s}$ and $\kappa_{\rm n}$, corresponding to strange and normal quark mass respectively. The normal quark mass is defined by:

$$m_n = \frac{1}{2}(m_u + m_d) \ . \tag{5.16}$$

The following table summarises the value of these parameters:

	$\beta = 6.2$	$\beta = 6.0$
$\kappa_{\rm crit}$	0.13581^{+2}_{-1}	0.13525^{+2}_{-1}
$\kappa_{\rm n}$	0.13578^{+2}_{-1}	0.13520^{+2}_{-1}
$\kappa_{\rm s}$	0.13495^{+2}_{-2}	0.13476^{+3}_{-5}

Not surprisingly, the values of $\kappa_{\rm crit}$ and $\kappa_{\rm n}$ are very similar. Physical light quark masses are determined as follows [66]. According to the PCAC relation, the pseudoscalar mesons satisfy:

$$M_{\rm P}^2 = B(m_1 + m_2) \tag{5.17}$$

The B parameter is extracted from lattice fits. Once a quantity is chosen to set the scale one has, in lattice units:

$$m_n = \frac{(m_\pi^{\text{latt.}})^2}{2B} \tag{5.18}$$

$$m_s = \frac{(m_K^{\text{latt.}})^2}{B} - m_n \tag{5.19}$$

The Kaon mass, m_K, is taken to be:

$$m_K^2 \equiv \frac{1}{2}(m_{K^\pm}^2 + m_{K^0}^2) \tag{5.20}$$

which gives $m_K = 495.7(\text{MeV})$. One can also use vector mesons, using the following equation:

$$M_{\text{V}} = A + C(m_1 + m_2) \tag{5.21}$$

that gives:

$$m_n = \frac{m_\rho^{\text{latt.}} - A}{2C} \tag{5.22}$$

$$m_s = \frac{m_{K^*}^{\text{latt.}} - A}{C} - m_n \tag{5.23}$$

The mass of the K^* meson is taken to be:

$$m_{K^*} \equiv \frac{1}{2}(m_{K^{*\pm}} + m_{K^{*0}}) \tag{5.24}$$

which is 893.9 (MeV). It has to be said that these two methods of extracting the strange quark mass are often not consistent: this uncertainty has been taken into account as a systematic error.

Choosing r_0 to set the scale, and applying (5.14), the strange quark mass is fixed around 120 MeV, whilst the normal quark mass is around 5 MeV.

Figure (5.1) shows an example of chiral extrapolation of the pseudoscalar decay constant and mass. Extrapolated values of meson masses and decay constants can be found in the appendices.

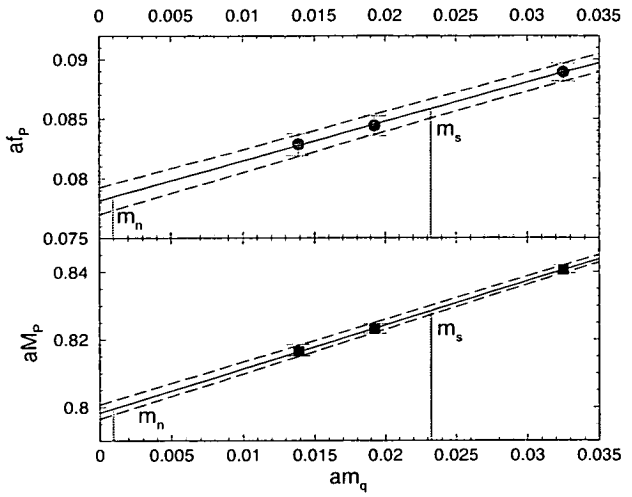

Figure 5.1: The chiral extrapolation of the pseudoscalar decay constant and mass against light quark mass, at $\beta = 6.2$, with $\kappa_H = 0.1200$

5.8 Heavy Quark Symmetry

As already mentioned in the beginning of this chapter, heavy quark symmetry predicts a scaling behaviour for the decay constants [67]. In the case of pseudoscalar mesons, it is possible to study the scaling by looking at the following function:

$$\Phi(M_{\rm P}) \equiv f_{\rm P}\sqrt{M_{\rm P}}\;\Theta(M_{\rm B}, M_{\rm P})\;, \tag{5.25}$$

where $M_{\rm B}$ is the mass of the B meson and the function $\Theta(M_{\rm P})$ accounts for the logarithmic corrections to leading order:

$$\Theta(M_{\rm B}, M_{\rm P}) = \left[\frac{\alpha_s(M_{\rm P})}{\alpha_s(M_{\rm B})}\right]^{-2/\beta_0}\;. \tag{5.26}$$

β_0 is the one-loop determination of the QCD beta function:

$$\beta_0 = 11 - \frac{2}{3}n_f \tag{5.27}$$

In the quenched approximation, $n_f = 0$, and $\beta_0 = 11$. The QCD fundamental scale was chosen to be $\Lambda_{QCD} = \Lambda^{(4)}_{\overline{\rm MS}} = 295$ MeV [68].

In the infinite quark mass limit, Φ is a constant. However, at large but not infinite values of the meson masses, scaling violations are expected. In order to extract these scaling violations, the Φ function is fitted to:

$$\Phi_{\rm P}(M_{\rm P}) = \gamma_{\rm P}\left(1 + \frac{\delta_{\rm P}}{M_{\rm P}} + \frac{\eta_{\rm P}}{M_{\rm P}^2}\right) \tag{5.28}$$

Experimental determinations of the masses of the D and B mesons are then used to extract the values of the corresponding decay constants. In the case of vector decay constants, a similar extrapolation is performed:

$$\Phi_{\rm V}(M_{\rm V}) \equiv \Theta(M_{\rm B}, M_{\rm V})\frac{M_{\rm V}}{f_{\rm V}}\sqrt{M_{\rm V}} = \gamma_{\rm V}\left(1 + \frac{\delta_{\rm V}}{M_{\rm V}} + \frac{\eta_{\rm V}}{M_{\rm V}^2}\right) \tag{5.29}$$

Figure (5.2) shows a fit of the Φ_P function at $\beta = 6.2$. The vertical lines indicate the inverse physical masses of the D and the B mesons, in lattice units, with two different choices of the quantity used to set the scale. In order to study the stability of the extrapolation, alternative fits have been done using only the heaviest three masses, and are shown in the figure. This issue has been considered in the evaluation of the systematic errors.

In the heavy quark limit, the pseudoscalar and vector decay constants are related by a HQS relation [69]:

$$U(M) \equiv \frac{f_{\rm V} f_{\rm P}}{M} = \left(1 + \frac{8}{3}\frac{\alpha_s(M)}{4\pi} + \mathcal{O}(1/M)\right) \tag{5.30}$$

where M is the spin-averaged mass:

$$M \equiv \frac{M_{\rm P} + 3M_{\rm V}}{4} \tag{5.31}$$

It is possible to redefine the U function to eliminate the radiative corrections:

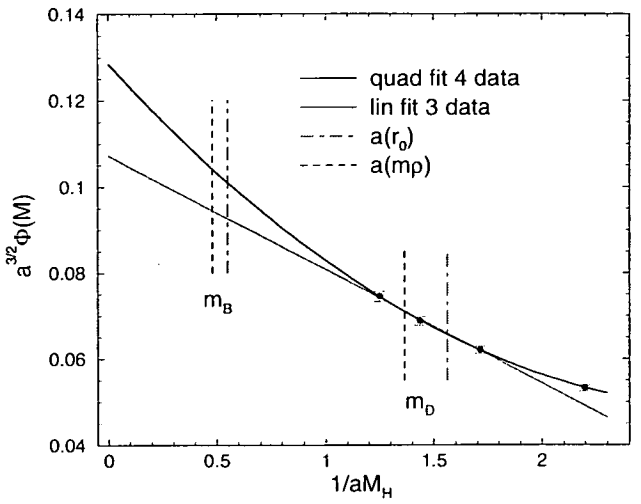

Figure 5.2: The extrapolation of the pseudoscalar decay constant in heavy meson mass at $\beta = 6.2$.

$$\tilde{U}(M) \equiv U(M)\left(1 + \frac{8}{3}\frac{\alpha_s(M)}{4\pi}\right)^{-1} \tag{5.32}$$

This function is calculated at each value of the extrapolated heavy meson mass, and then fitted to the following functional form:

$$\tilde{U}(M) = \omega_0 + \frac{\omega_1}{M} + \frac{\omega_2}{M^2} \tag{5.33}$$

HQS predicts that $\omega_0 = 1$; nonetheless ω_0 is left as a free parameter of the fit in order to verify the applicability of HQS. In a similar way, it is possible to fit simultaneously Φ_P and Φ_V, imposing $\gamma_P = \gamma_V$. This relation is modified by higher order QCD corrections:

$$\gamma_P = \gamma_V\left(1 + \frac{8}{3}\frac{\alpha_s(M)}{4\pi}\right) \tag{5.34}$$

As was mentioned before, the extraction of the decay constants at the scale of the b quark involves long extrapolations, and it is necessary to estimate the systematic uncertainty arising from the alternative procedures that can be used:

1. Φ functions are fitted linearly against $1/M$ with the three heaviest masses;
2. Φ functions are fitted quadratically against $1/M$ using the four available heavy masses

The uncertainty coming from the choice of the method used for the extrapolations were found to be significantly smaller than the error coming from different determinations of the lattice spacing.

Extrapolations of the $\tilde{U}(M)$ function show good agreement with the HQS predictions at $\beta = 6.2$, but not at $\beta = 6.0$ (see Figure (5.3)). This might be due to the presence of larger discretisation errors at $\beta = 6.0$ that spoil the scaling behaviour. At $\beta = 6.2$, the imposition of the constraint $\omega_0 = 1$ does not make a sizable difference in the fit, while at $\beta = 6.0$ constrained and unconstrained fits are incompatible. Furthermore, linear and quadratic fits of $\tilde{U}(M)$ are in good agreement only at $\beta = 6.2$.

β	$\tilde{U}(\infty)$
6.0	0.62^{+5}_{-5}
6.2	1.01^{+4}_{-4}

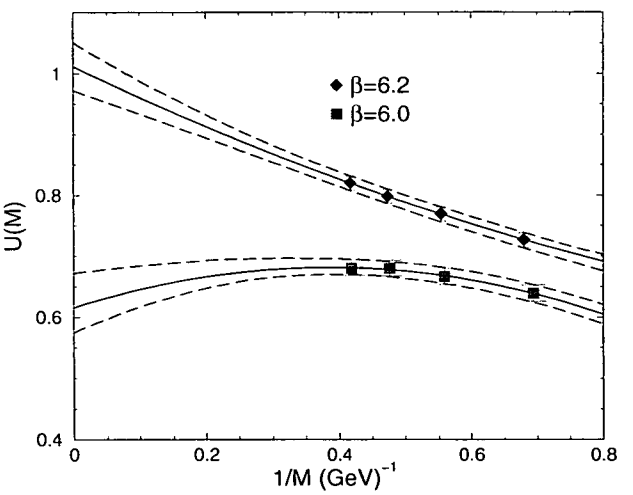

Figure 5.3: The HQS radiatively corrected U function, at $\beta = 6.0$ and $\beta = 6.2$

A similar effect is seen when imposing the constraint

$$\gamma_P = \gamma_V \tag{5.35}$$

Figure (5.4) illustrates this point.

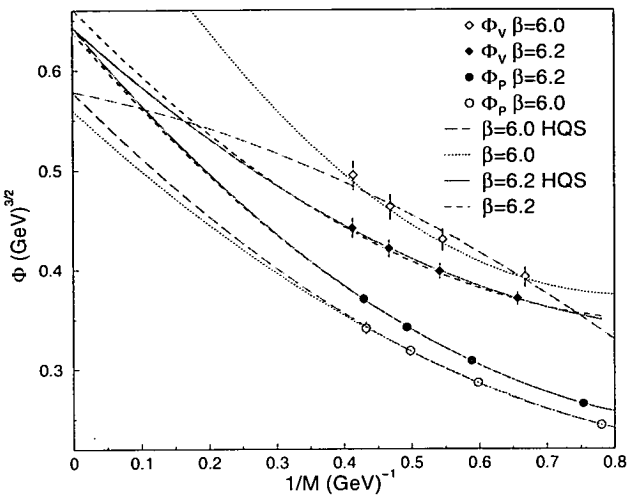

Figure 5.4: The extrapolation of the decay constants to the infinite quark mass limit, with and without the HQS constraint. The solid (long dashed) lines show the extrapolation with the constraint at $\beta = 6.2$ ($\beta = 6.0$). The dashed (dotted) lines show the extrapolation without the constraint at $\beta = 6.2$ ($\beta = 6.0$).

5.9 The decay constants

Results for the decay constants at physical meson masses are shown in Table 5.9. The extrapolation in the heavy meson mass for the pseudoscalar decay constant at $\beta = 6.2$ is shown in Figure (5.2). The difference between a quadratic fit to all four points and a linear fit to the heaviest three can be seen. This has no effect for the D meson, but is one of the main uncertainties in the B meson decay constant. The dot-dashed and dashed lines show the meson masses (B and D) with the scale set by r_0, and m_ρ respectively. Although this effect appears small in the figure, once the explicit scale dependence of $\Phi_P(M_P)$ is considered, it is responsible for the largest systematic uncertainty in this calculation.

Table 5.9: The decay constants at both β values with the scale set by r_0 or m_ρ and a quadratic (Q) or linear (L) fit for the extrapolation in inverse heavy meson mass. The quadratic fit uses all four heavy masses, while the linear fit uses the heaviest three.

		$\beta = 6.2$				$\beta = 6.0$			
		f_P(MeV)		f_V		f_P(MeV)		f_V	
		Q	L	Q	L	Q	L	Q	L
r_0	B	218(5)	200(4)	22.6(7)	23.8(7)	196(6)	183(4)	18.9(8)	20.4(8)
	D	220(3)	221(3)	7.5(1)	7.4(1)	206(3)	207(3)	6.7(2)	6.8(2)
	B_s	242(4)	222(3)	20.9(4)	22.0(4)	213(4)	198(3)	18.1(5)	19.5(4)
	D_s	241(2)	242(2)	7.3(1)	7.3(1)	221(2)	222(2)	6.9(1)	6.8(1)
m_ρ	B	186(4)	169(3)	26.4(8)	28.5(8)	170(5)	158(4)	21(1)	24(1)
	D	197(3)	198(3)	8.5(2)	8.6(2)	187(3)	187(3)	7.5(2)	7.5(1)
	B_s	212(3)	193(2)	23.5(4)	25.4(4)	189(3)	175(2)	19.8(5)	22.2(4)
	D_s	221(2)	222(2)	8.1(1)	8.1(1)	204(2)	204(2)	7.5(1)	7.4(1)

5.10 The KLM norm

The action and the operators used in this work have been improved to remove all $\mathcal{O}(a)$ discretisation errors. Nonetheless, it is possible to estimate higher order discretisation effects of the form $\mathcal{O}((am)^n)$ using the KLM norm [70]. This normalisation of the quark field is based on the comparison between a free lattice quark propagator and its continuum counterpart, and corresponds to:

$$\psi \to \sqrt{1 + am_q}\,\psi \tag{5.36}$$

This means that, applying the KLM norm, the axial current is multiplied by:

$$\sqrt{1 + am_1}\sqrt{1 + am_2} \tag{5.37}$$

At this point, one must be very careful. In fact, the KLM norm can't be used in this form when working with an $\mathcal{O}(a)$ improved action: the $\mathcal{O}(am)$ errors are

already accounted for. The KLM normalisation of the axial current has to be modified by dividing off the $\mathcal{O}(am)$ corrections. In fact,

$$\sqrt{1+am_1}\sqrt{1+am_2} = 1 + \frac{1}{2}(am_1 + am_2) + \mathcal{O}((am)^2) \tag{5.38}$$

The factor multiplying the axial current is, then

$$\frac{\sqrt{1+am_1}\sqrt{1+am_2}}{1+(am_1+am_2)/2} \tag{5.39}$$

Application of the KLM norm does not make the decay constants of the D and the B mesons dramatically different. At $\beta = 6.2$, where the quark masses are in lattice units less than one half, the KLM normalisation of the axial current is close to one. The fact that masses are larger at $\beta = 6.0$ makes the KLM factor larger: f_D and f_B get larger by 2% and 8% respectively.

5.11 Flavour-breaking ratios

The flavour breaking ratios of the decay constants have been calculated and are presented in Table (5.10). This calculation has been performed in two different ways. The first method consisted in calculating the decay constants, extrapolating them in both the light and heavy quark mass and finally in taking their ratios. The second method consisted in making ratios of decay constants that were extrapolated only in the light quark mass; this ratios were fitted to quadratic functions of inverse meson mass (extrapolated in the light quark mass) and then extrapolated to the D and B scales. The two methods gave answers that were in excellent agreement with each other.

5.12 Analysis of systematic errors

The extraction of the decay constants is affected by several sources of systematic uncertainty, araising from the different possible procedures that can be used. The

Table 5.10: Flavour breaking ratios

$$f_{B_s}/f_B = 1.11 \pm 0.01^{+0.05}_{-0.03} \qquad f_{B_s^*}/f_{B^*} = 0.92 \pm 0.01^{+0.04}_{-0.03}$$

$$f_{D_s}/f_D = 1.09 \pm 0.01^{+0.05}_{-0.02} \qquad f_{D_s^*}/f_{D^*} = 0.98 \pm 0.01^{+0.02}_{-0.04}$$

systematic errors that are estimated are

- choice of scale fixing quantity;
- different value of β;
- heavy meson extrapolation (linear vs. quadratic);
- uncertainty in strange quark mass;
- different determinations of b_A (only applies to the pseudoscalar case).

The simulations were run at only two different values of β, and therefore no continuum limit extrapolations can be attempted. The values at $\beta = 6.2$ are taken as central values, the reason being that the agreement of the data with the HQS constraints seems to suggest that the dataset at $\beta = 6.2$ is closer to the continuum limit. The difference in the results is treated as a systematic error. The simulations also show that $\mathcal{O}(a^2)$ errors are probably not small at $\beta = 6.0$, where the data are in poor agreement with the constraints imposed by HQS.

It is evident that different determinations of the improvement coefficients induce systematic errors in the extraction of any physical quantity. These errors have not been estimated, the only exception being the uncertainty arising from the different determinations of b_A.

In particular, an extraction of the decay constants has been done following Becirevic *et al.* [71], using the determination of b_A from boosted perturbation theory, fixing the scale with m_{K^*} ($a^{-1} = 2.75$GeV), applying the KLM norm and choosing a linear heavy extrapolation. The result for f_B, 172(3)MeV, is consistent with Becirevic *et al.* (179(12)MeV). Preliminary UKQCD determinations of the decay

Table 5.11: Percentage systematic uncertainties. Central values correspond to the following procedures: using r_0 to set the scale at $\beta = 6.2$, a quadratic heavy quark extrapolation, the central value of b_A, using m_K^2 to set the strange quark mass.

Pseudoscalar	f_B	f_D	f_{B_s}	f_{D_s}	$\frac{f_{B_s}}{f_B}$	$\frac{f_{D_s}}{f_D}$
scale set by m_ρ	15	10	12	8	3	3
$\beta = 6.0$	10	6	12	8	2	2
heavy meson extrapolation	8	–	8	–	–	–
coeff. b_A	5	2	5	2	–	–
strange quark mass	–	–	2	2	2	2
Vector	f_{B^*}	f_{D^*}	$f_{B_s^*}$	$f_{D_s^*}$	$\frac{f_{B_s^*}}{f_{B^*}}$	$\frac{f_{D_s^*}}{f_{D^*}}$
scale set by m_ρ	18	17	14	12	3	3
$\beta = 6.0$	17	9	14	6	4	2
heavy meson extrapolation	7	–	7	–	–	–
strange quark mass	–	–	3	1	2	2

constants followed this procedure, omitting the KLM normalisation and using m_ρ to set the scale [72, 73].

No attempt was made to estimate the systematic error due to the quenched approximation. The systematic errors have been added in quadrature, and their percentage values are presented in Table 5.11.

5.13 Conclusions

The decay constants and their ratios determined in this work are found to be consistent with analogous determinations of other lattice collaborations [74, 75]. However, a central value of the pseudoscalar decay constant has been found that is larger than the world average of quenched lattice determinations by about 20%. One of the reasons for this discrepancy has been identified in the systematic error induced by the choice of the quantity that was used to set the scale.

Comparison with some of the first estimates of $N_f = 2$ unquenched simulations [76, 77] shows that full QCD decay constants could be larger than their quenched determinations by about 15%.

By the time this work was completed, a new determination of the improvement coefficients has been released by Bhattacharya *et al.* [78]. Using these new values, and setting the scale with f_π, the analysis presented in this chapter has been repeated. The results are to be considered preliminary.

The largest differences have been observed at $\beta = 6.0$. First of all, the values of the decay constants were found to be closer to the $\beta = 6.2$ determinations: scaling violations were below the 3% level. Furthermore, the HQS constraints were satisfied. These preliminary calculations confirm the importance of the availability of precise determinations of the improvement coefficients.

At $\beta = 6.2$, considering statistical errors only, preliminary results are:

- $f_D = 208(4)$ MeV, $f_B = 197(6)$ MeV; $f_{D_s} = 231(4)$ MeV, $f_{B_s} = 223(6)$ MeV;
- $f_{D^*} = 8.5(3)$, $f_{B^*} = 27(1)$; $f_{D_s^*} = 8.2(2)$, $f_{B_s^*} = 25(1)$

At present, these new results are being analysed and should be presented in a publication.

Chapter 6

The $\mathrm{B} \to \mathrm{D}^* l \bar{\nu}_l$ decay

This chapter contains the results of a lattice study of the semi-leptonic decay $\mathrm{B} \to \mathrm{D}^* l \bar{\nu}$.

6.1 Definitions

The quantum matrix elements describing the decay $\mathrm{B} \to \mathrm{D}^* l \bar{\nu}$ can be expressed in term of four form factors:

$$\begin{aligned} \langle \mathrm{D}^*(v',\eta)|V^\mu|\mathrm{B}(v)\rangle &= i h_V(\omega)\epsilon^{\mu\nu\alpha\beta}\eta^*_\nu v'_\alpha v_\beta \\ \langle \mathrm{D}^*(v',\eta)|A^\mu|\mathrm{B}(v)\rangle &= h_{A_1}(\omega)(\omega+1)\eta^{*\mu} - \left[h_{A_2}(\omega)v^\mu + h_{A_3}(\omega)v'^\mu\right](\eta^*\cdot v) \end{aligned} \tag{6.1}$$

where $\omega = v' \cdot v$ and η is the polarisation vector of the D^* meson. Velocities and momenta are related by:

$$\begin{aligned} v' &= \frac{k}{M_{\mathrm{V}}} \\ v &= \frac{p}{M_{\mathrm{PS}}} \,. \end{aligned} \tag{6.2}$$

The matrix elements are extracted from the three-point function:

$$C_J^{\mu\nu}(\vec{p},\vec{q};t_x,t_y) = \sum_{\vec{x},\vec{y}} e^{-i(\vec{p}\cdot\vec{x}+\vec{q}\cdot\vec{y})}\langle 0|\Omega_{\rm V}(x)J^{\mu}(y)\Omega^{\dagger}_{\rm PS}(0)|0\rangle \tag{6.3}$$

where $q = k - p$. Following the results in Chapter 3, this function can be written, at asymptotic times, as:

$$C_J^{\mu\nu}(\vec{p},\vec{q};t_x,t_y) = \frac{Z_{\rm PS}(\vec{p})}{2E_{\rm PS}(\vec{p})}\frac{Z_{\rm V}(\vec{k})}{2E_{\rm V}(\vec{k})}J^{\mu\nu}(\vec{p},\vec{q})e^{-E_{\rm V}t_y}e^{-E_{\rm PS}(t_x-t_y)} \tag{6.4}$$

where the tensor $J^{\mu\nu}$ is equal to

$$J^{\mu\nu}(\vec{p},\vec{q}) = \sum_r \eta_r^{\nu *}\langle {\rm V}(\vec{k},\eta)|J^{\mu}|PS(\vec{p})\rangle \ . \tag{6.5}$$

The current J can either be the vector or the axial current. In terms of form factors, one gets

$$J^{\mu\nu} = V^{\mu\nu} = \frac{ih_V(\omega)}{\sqrt{M_{\rm PS}M_{\rm V}}}\epsilon^{\mu\nu\alpha\beta}k_\alpha p_\beta \tag{6.6}$$

for the vector current, and:

$$J^{\mu\nu} = A^{\mu\nu} = \left(-g^{\mu\nu} + \frac{k^\mu k^\nu}{M_{\rm V}^2}\right)(\omega+1)\sqrt{M_{\rm PS}M_{\rm V}}h_{A_1}(\omega) + \tag{6.7}$$

$$-\left(\frac{p\cdot k}{M_{\rm V}^2}k^\nu - p^\nu\right)\left[\frac{1}{M_{\rm PS}}\sqrt{\frac{M_{\rm V}}{M_{\rm PS}}}h_{A_2}(\omega)p^\mu + \frac{1}{M_{\rm V}}\sqrt{\frac{M_{\rm V}}{M_{\rm PS}}}h_{A_3}(\omega)k^\mu\right]$$

for the axial current. The relation

$$\sum_r \eta_r^\mu(k)\eta_r^{\nu *}(k) = \left(-g^{\mu\nu} + \frac{k^\mu k^\nu}{M_{\rm V}}\right) \tag{6.8}$$

has been applied.

6.2 Extraction of the form factors

The matrix element $J^{\mu\nu}$ contains the non-perturbative information about the $B \rightarrow D^* l\bar{\nu}_l$ decay. The form factors $h_i(\omega)$ can be extracted from the matrix element via equations (6.6), (6.7). The three-point function $C_J^{\mu\nu}$ can be written as

$$C_J^{\mu\nu}(\vec{p},\vec{q};t_x,t_y) = F J^{\mu\nu} e^{-\Delta E\ t_y} \tag{6.9}$$

where

$$F = \frac{Z_{\rm PS}}{2E_{\rm PS}} \frac{Z_{\rm V}}{2E_{\rm V}} e^{-E_{\rm PS} t_x} \tag{6.10}$$

and

$$\Delta E = E_{\rm V} - E_{\rm PS}\ . \tag{6.11}$$

These factors are calculated using the parameters of the fits of the two-point functions. Recall that in this work $t_x = 28$.

Every matrix element is a function of the masses of three quarks: the light passive and the two heavy quarks involved in the interaction with the external current (the active and the extended). On the lattice, matrix elements are calculated on a set of different unphysical mass combinations.

Now, several momentum combinations (initial, final) are considered: each of these is regarded as a "channel". For a given channel, as the form factors are functions of $q^2 = (p-k)^2$ (or ω), all the matrix elements for the same value of q^2, that are formally equal, can be averaged. Vector and axial matrix elements are considered separately. For each channel, once the averaging of equal operators is done, one is left with a set of different matrix elements that can be fitted simultaneously to extract the form factors:

$$y_i(\omega;t) = \sum_j F_{ij} h_j(\omega) e^{-\Delta E t} \tag{6.12}$$

where F_{ij} is a matrix of simple kinematic factors. The i index runs over all the different averages of matrix element components that are available in each channel, while the j index labels the different form factors: just one value in the vector case, three values in the axial case.

For each kinematic channel, there is a set of equations for the matrix elements. All the distinct correlators are fitted simultaneously to a single exponential decay. In particular, the energy difference ΔE and the factors F_{ij} are constructed using the parameters of previous fits of two-point functions and kept frozen during the fit. The values of the form factors at a specific value of ω (or q^2) are the output of the fit.

The matrix element $J^{\mu\nu}$ could have been extracted by taking ratios of two and three-point functions. In fact, the ratio:

$$R^{\mu\nu} = \frac{C^{\mu\nu}(\vec{p},\vec{q};t_x,t_y)}{C^2_{\mathrm{PS}}(\vec{p},t_x-t_y)C^2_{\mathrm{V}}(\vec{k},t_y)} \tag{6.13}$$

becomes a constant in time as soon as the contamination of the excited states is suppressed. Nonetheless, the plateaus thus obtained were shorter than the plateaus of the matrix elements that were reconstructed using equation (6.9). A possible explanation is the following: the contamination of the excited states is sizeably smaller in the three-point functions than in the two-point functions, and the signal given by $R^{\mu\nu}$ is spoiled by the lack of cancellation between numerator and denominator in (6.13).

Tables with the values of the form factors can be found in the appendices.

6.3 Kinematic channels

A summary of the combinations of initial and final momenta that were considered in this work is given in Tables 6.1 and 6.2. Quoted momenta are expressed in lattice units of $12/(a\pi)$.

In the extraction of the form factors, the following kinematic channels have been used:

- channel 0: $\vec{p} = \vec{0} \to \vec{k} = \vec{0}$;
- channel 1: $|\vec{p}| = 0 \to |\vec{k}| = 1$;
- channel 2: $|\vec{p}| = 1 \to |\vec{k}| = 0$;
- channel 3: $|\vec{p}| = 1 \to |\vec{k}| = 1,\ \vec{p}\cdot\vec{k} = 1$;
- channel 4: $|\vec{p}| = 1 \to |\vec{k}| = 1,\ \vec{p}\cdot\vec{k} = 0$;
- channel 5: $|\vec{p}| = 1 \to |\vec{k}| = 1,\ \vec{p}\cdot\vec{k} = -1$.

The channels with $|\vec{k}| \geq \sqrt{2}$ have been discarded for having a very poor signal to noise ratio. Furthermore, these channels would have not been used in the main calculations of this chapter, because they correspond to values of ω (> 1.2) for which the approximations on the power corrections to the form factors don't hold.

Table 6.1: Three-point function momenta with $\vec{p} = 0$

chan	$\vec{q}$	chan	$\vec{q}$	chan	$\vec{q}$	$\lvert\vec{q}\rvert$
1	(0, 0, 0)					0
2	(-1, 0, 0)	3	(0,-1, 0)	4	(0, 0,-1)	$\sqrt{1}$
5	(-1,-1, 0)	6	(-1, 0,-1)	7	(0,-1,-1)	
8	(-1, 1, 0)	9	(1, 0,-1)	10	(0,-1, 1)	$\sqrt{2}$
11	(-1,-1,-1)	12	(1,-1,-1)	13	(1,-1, 1)	
14	(-1,-1, 1)					$\sqrt{3}$
15	(-2, 0, 0)	16	(0,-2, 0)	17	(0, 0,-2)	$\sqrt{4}$

Table 6.2: Three-point function momenta with $\vec{p} = (1, 0, 0)$

chan	$\vec{q}$	$\vec{k}$	chan	$\vec{q}$	$\vec{k}$	$\lvert\vec{q}\rvert$	$\lvert\vec{k}\rvert$
1	(-1, 0, 0)	(0, 0, 0)				$\sqrt{1}$	0
2	(0, 0, 0)	(1, 0, 0)				0	$\sqrt{1}$
3	(-2, 0, 0)	(-1, 0, 0)				$\sqrt{4}$	$\sqrt{1}$
4	(-1, 1, 0)	(0, 1, 0)	5	(-1,-1, 0)	(0,-1, 0)		
6	(-1, 0, 1)	(0, 0, 1)	7	(-1, 0,-1)	(0, 0,-1)	$\sqrt{2}$	$\sqrt{1}$
8	(0, 1, 0)	(1, 1, 0)	9	(0, 0, 1)	(1, 0, 1)		
10	(0,-1, 0)	(1,-1, 0)	11	(0, 0,-1)	(1, 0,-1)	$\sqrt{1}$	$\sqrt{2}$
12	(-1, 1, 1)	(0, 1, 1)	13	(-1, 1,-1)	(0, 1,-1)		
14	(-1,-1, 1)	(0,-1, 1)	15	(-1,-1,-1)	(0,-1,-1)	$\sqrt{3}$	$\sqrt{2}$
16	(0, 1, 1)	(1, 1, 1)	17	(0,-1, 1)	(1,-1, 1)		
18	(0, 1,-1)	(1, 1,-1)	19	(0,-1,-1)	(1,-1,-1)	$\sqrt{2}$	$\sqrt{3}$
20	(1, 0, 0)	(2, 0, 0)				$\sqrt{1}$	$\sqrt{4}$

6.4 Front vs. back side of the lattice

Since the extension time-slice, t_x, was not chosen to be the mid-point of the lattice, correlators on the front and the back side of the lattice were different objects and could not be averaged. Therefore, a careful study of each fit has been performed on both sides of the lattice, checking:

- goodness and stability of signals;
- size of statistical errors

The most important consequence of the fact that the extension time-slice is not the mid-point of the time axis is that the time separation $\Delta t = |t_y - t_x|$ between operators in three-point functions is shorter on the back side on the lattice than on the front side.

In general, as Δt grows:

- the contamination of the excited states is exponentially suppressed;

- the signal-to-noise ratio of correlators gets worse.

Furthermore, since the lattice is periodic in time, three-point functions are contaminated by contributions of other time-orderings propagating in the opposite time direction. The signals corresponding to different time orderings are usually exponentially suppressed as they propagate around the lattice. When the lattice is not symmetric, signals of different time orderings are more likely to be suppressed on the shorter side, having to propagate for a longer interval.

By making the lattice asymmetric in time, one cannot improve the signal of the correlation functions by averaging the signals around the mid-point. However, an asymmetric lattice can be used to test whether contaminations of different time ordered correlators are sizeable or not.

6.5 Simulated quark masses

The form factors have been calculated for different values of the hopping parameters of the three quarks involved in the decay. The available values of the mass of the active quark were four at $\beta = 6.0$ and two at $\beta = 6.2$ [1]. There were four values of the extended quark mass and two values of the light passive quark mass at both values of β. A summary is given in Table 6.3.

6.6 Axial current renormalisation

The matrix elements of the PS $\to$ V decay can be used to extract the axial current renormalisation constant, Z_A^{eff}. In fact, at zero recoil, since $\gamma_{A_1}(1) = 0$ (Luke's theorem) and $\xi(1) = 1$:

$$Z_A^{\text{eff}} h_{A_1}^{\text{L}}(1) = 1 + \beta_{A_1}(1) + \mathcal{O}\left(\frac{1}{m_Q^2}\right) \tag{6.14}$$

[1] At $\beta = 6.2$, only two active heavy quark masses were simulated, because of disk space constraints that occurred in the data production phase.

Table 6.3: Summary of the hopping parameters

	$\beta = 6.2$	$\beta = 6.0$
active (A)	0.12000	0.11230
	0.12660	0.11730
	–	0.12230
	–	0.12730
extended (E)	0.12000	0.11230
	0.12330	0.11730
	0.12660	0.12230
	0.12990	0.12730
passive (P)	0.13460	0.13344
	0.13510	0.13417

where $h^{\rm L}_{A_1}$ is the lattice determination of h_{A_1} and $Z_A^{\rm eff}$ is defined in Chapter 2. The form factor at zero recoil is extracted from the channel:

$$\vec{p} = \vec{k} = \vec{0}\ (\omega = 1)$$

For this channel, one has:

$$R_0 = \frac{1}{3}\sum_{i=1}^{3} A_{ii} = 2\sqrt{M_{\rm PS} M_{\rm V}}\, h_{A_1}(1) \tag{6.15}$$

Not all the mass combinations can be used to extract $Z_A^{\rm eff}$. In fact, the determinations of the radiative corrections are reliable only as long as the mass of the heavy quark of the vector meson is smaller or equal to the mass of the heavy quark of the pseudoscalar meson. The number of mass combinations that satisfy this constraint is ten at $\beta = 6.0$, and four $\beta = 6.2$.

$h^{\rm L}_{A_1}(1)$ has been extracted from fits on both sides of the lattice. The fits on the back side of the lattice have been preferred in the end, since their determinations of the form factor were compatible with the front side determinations but had sizeably smaller statistical errors, as one can see in Figure (6.1). The values of

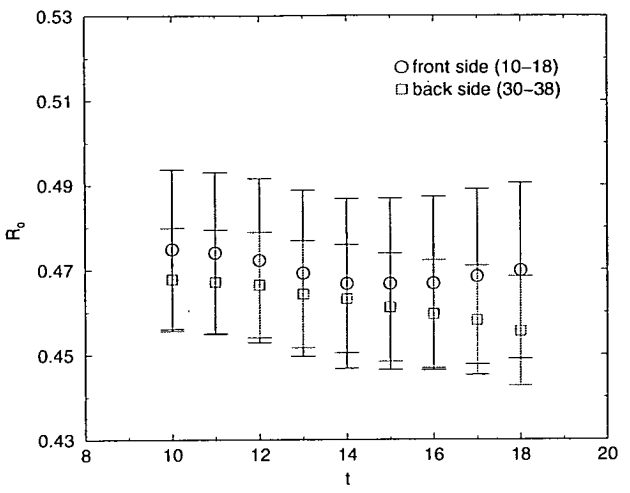

Figure 6.1: R_0, at $\beta = 6.2$, with $\kappa_A = \kappa_E = 0.1200$ and $\kappa_p = 0.1346$

R_0 on the back side of the lattice have been superimposed on the values on the front side with the replacement $t \rightarrow T - t$.

Results at both values of β are shown in Figures (6.2) and (6.3), in comparison with a determination of Z_A^{eff} done using Z_A as determined by the ALPHA collaboration [24]:

$$Z_A^{\text{ALPHA}} = \frac{1 - 0.8496 g_0^2 + 0.0610 g_0^4}{1 - 0.7332 g_0^2} \tag{6.16}$$

and found to be in reasonable if not excellent agreement.

Throughout this chapter, axial and vector currents have been renormalised using the constants Z_A, Z_V as given by the ALPHA collaboration.

6.7 The h_{A_1} form factor

h_{A_1} is the most precisely determined form factor for this decay mode. For all the kinematic channels that have been used in the extraction of h_{A_1} $(0, 1, 2, 3, 4)$, both the front and the back side of the lattice have been examined. The signal on the back side of the lattice was found to be much cleaner than on the front

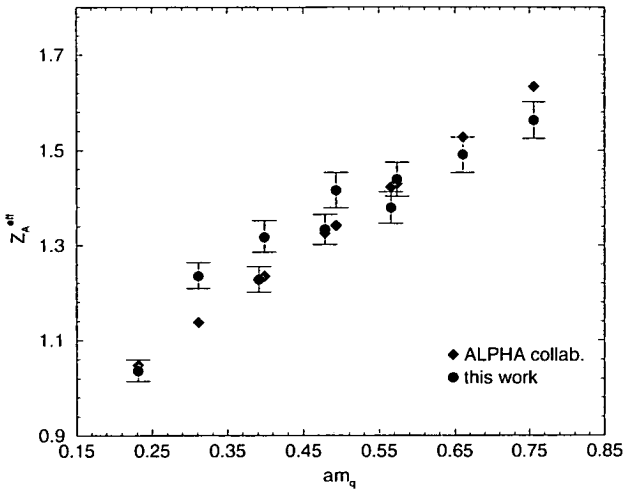

Figure 6.2: Axial current renormalisation $Z_A^{\rm eff}$, at $\beta = 6.0$, with $\kappa_{\rm P} = 0.13344$.

side. In several cases, the fits on the two sides of the lattice gave statistically incompatible answers.

The most interesting feature of the h_{A_1} form factor is that it can be used to extract the Isgur-Wise function. In fact, as long as power corrections can be neglected, the following equation can be used to extract the Isgur-Wise function:

$$\xi(\omega) \simeq \frac{h_{A_1}(\omega)}{1 + \beta_{A_1}(\omega)} \tag{6.17}$$

The radiative corrections have been calculated using the equations in [50]. Now, previous estimates of the power correction γ_{A_1}, both in lattice QCD [79] and sum rules [51], suggest that γ_{A_1} can be neglected in the range:

$$1.0 \leq \omega \leq 1.2 \tag{6.18}$$

At $\beta = 6.0$, the axial three-point functions for the heavy-light to heavy-light transition turned out to be very noisy, especially on the front side of the lattice and at non-zero recoil. On the back side of the lattice, data were less noisy, but did not allow for stable fits. In particular, no clear plateaus were identified. As a result, the spread of values of h_{A_1} was too large with respect to the width of the

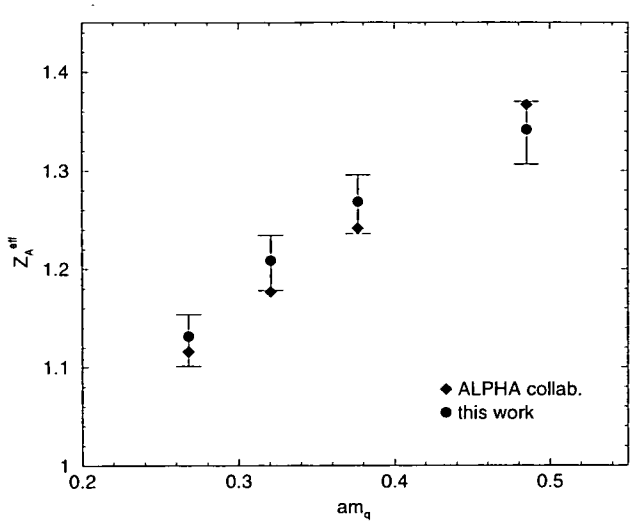

Figure 6.3: Axial current renormalisation Z_A^{eff}, at $\beta = 6.2$, with $\kappa_{\text{P}} = 0.1460$.

available range in ω to justify fits of the Isgur-Wise function. This could be due to large discretisation errors.

Nonetheless, the axial matrix elements could be fitted quite reasonably at zero recoil, providing estimates of Z_A^{eff} and $\xi(1)$.

At $\beta = 6.2$, the data were much cleaner, and the best fit ranges were found to be:

- 12-16 on the front side;
- 33-37 on the back side.

Figure (6.4) shows the values of the radiatively corrected h_{A_1} as extracted from fits on the front and the back side of the lattice, at $\beta = 6.2$, with $\kappa_P = 0.13460$.

Figures (6.5, 6.6) show the radiatively corrected $h_{A_1}(\omega)$ as extracted from fits on the front and the back side of the lattice, for each of the kinematic channels.

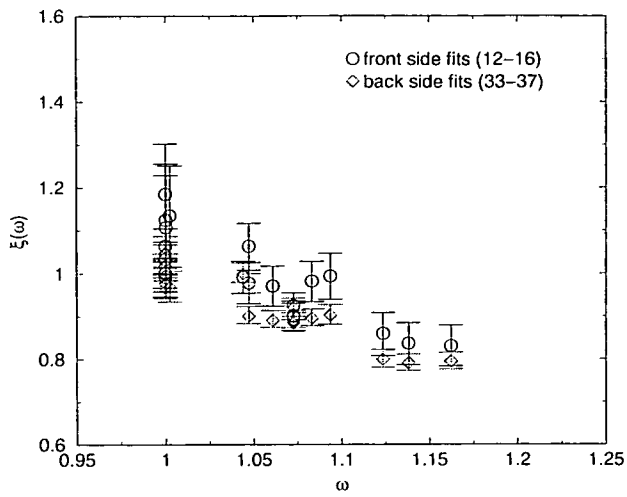

Figure 6.4: The radiatively corrected h_{A_1} form factor, equal to $\xi(\omega)$ up to power corrections, at $\beta = 6.2$, for $\kappa_P = 0.13460$, from fits on the back and the front side of the lattice

6.8 Light quark dependence of h_{A_1}

As already mentioned, in the dataset that was used for this work, only two values of the light passive quark were available. Therefore, extrapolations of the form factors to the chiral limit or to the strange quark mass were not possible. Nonetheless, the form factors using the two different values of κ_P were compared. At $\beta = 6.2$ the difference in the result was smaller than the statistical error on the form factors for all the channels, suggesting that the form factors can be regarded as independent of the passive quark mass.

At $\beta = 6.0$, the situation was similar, but the agreement was poor for channels 3 and 4. Figure (6.7) compares the values of the form factor h_{A_1} calculated at the two different available light quark masses, using fits on the back side of the lattice.

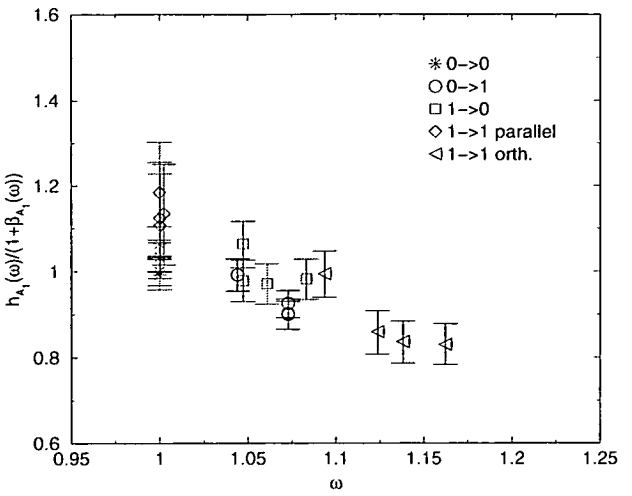

Figure 6.5: The radiatively corrected h_{A_1} form factor, at $\beta = 6.2$, for $\kappa_P = 0.13460$, from fits on the front side of the lattice. Different channels are shown.

6.9 The h_{A_2} and h_{A_3} form factors

The h_{A_2} and h_{A_3} form factors can be extracted using all the available non-zero recoil kinematic channels. At zero recoil, in fact, these form factors do not contribute to the matrix elements.

At $\beta = 6.0$, no satisfactory extraction of h_{A_2} and h_{A_3} was possible. In fact, these form factors were determined with errors that were very large (up to 100%).

Even at $\beta = 6.2$, the fitting procedure has produced values for the h_{A_2} and h_{A_3} form factors that were affected by very large statistical errors, on both sides of the lattice. Furthermore, it was not possible to extract these form factors using channel 3.

In particular, the results were consistent with:

$$h_{A_2}(\omega) = 0 \tag{6.19}$$

The results for $h_{A_3}(\omega)$ were somewhat better. In particular, if one assumed the power correction γ_{A_3} to be negligible, the data were consistent with the constraint $\xi(1) = 1$, as one can see in Figure (6.8).

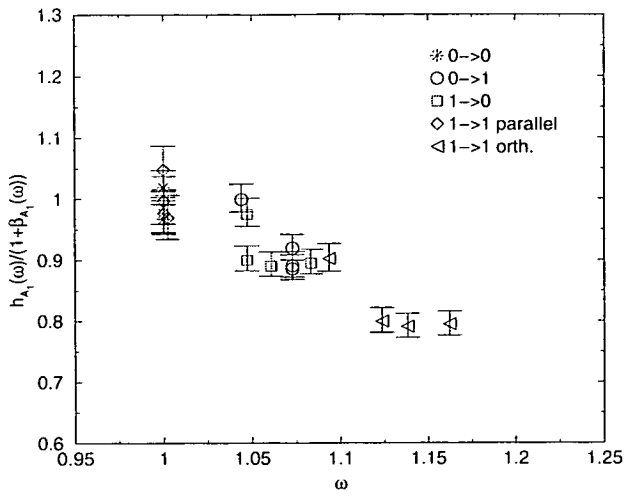

Figure 6.6: The radiatively corrected h_{A_1} form factor, at $\beta = 6.2$, for $\kappa_P = 0.13460$, from fits on the back side of the lattice. Different channels are shown.

Because of the extremely poor determination of h_{A_2} and h_{A_3}, it was not possible to use the approximation $\gamma_{A_1} \simeq 0$ to extract the power corrections γ_{A_2} and γ_{A_3}.

An attempt was also made to extract the ratio:

$$R_2(\omega) = \frac{h_{A_3}(\omega) + \frac{M_V}{M_{PS}} h_{A_2}(\omega)}{h_{A_1}(\omega)} \tag{6.20}$$

In the heavy quark limit, $R_2(\omega) = 1$, since $h_{A_2} = 0$ and $h_{A_1} = h_{A_3}$. Figure (6.9) shows $R_2(\omega)$, at $\beta = 6.2$.

No clean signal was found. Furthermore, the results from kinematic channel 2 seem to be systematically inconsistent with the other data points. However, the data seem to be consistent with the estimate given by the CLEO collaboration [80]:

$$R_2 = 0.71(23) \tag{6.21}$$

Neubert [81], quotes the HQET result:

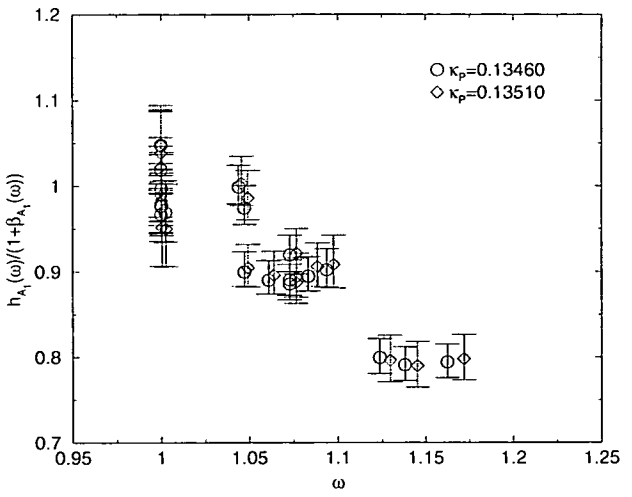

Figure 6.7: The h_{A_1} form factor, at $\beta = 6.2$, for $\kappa_P = 0.13460$ and $\kappa_P = 0.13510$

$$R_2 \simeq 0.8(2) \tag{6.22}$$

6.10 The h_V form factor

The h_V form factor can be extracted using the kinematic channels $(1, 2, 3, 4)$. Channel 0 is not useful since, for $\vec{p} = \vec{k} = \vec{0}$, equation (6.6) shows that $V^{\mu\nu} = 0$. This form factor is not protected by power corrections. As a matter of fact, calculations based on QCD sum rules [51] suggest that the $\mathcal{O}(1/m_Q)$ corrections to h_V are large. The power correction γ_V can be estimated by evaluating the following ratio:

$$R_1(\omega) = \frac{h_V(\omega)}{h_{A_1}(\omega)} \tag{6.23}$$

Figure (6.10) shows the radiatively corrected ratio R_1. This result is in good agreement with its determination by the CLEO collaboration [80]:

$$R_1 = 1.18(32) \tag{6.24}$$

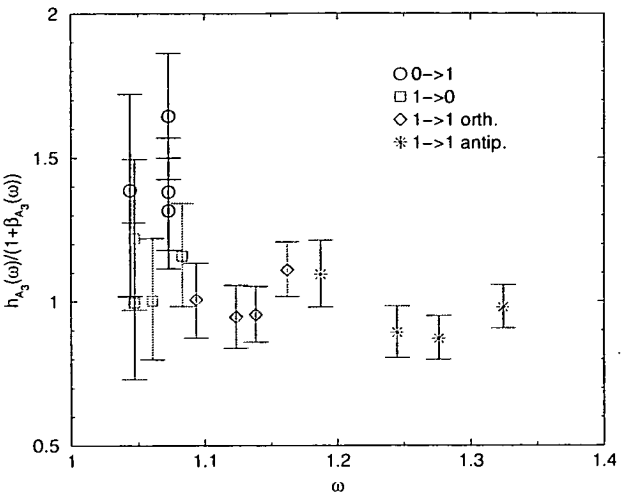

Figure 6.8: The h_{A_3} form factor, at $\beta = 6.2$, for $\kappa_P = 0.13460$

Neubert's HQET estimate [81] is:

$$R_2 \simeq 1.3(1) \tag{6.25}$$

Considering only values of ω in the range $1.0 \leq \omega \leq 1.2$, one can assume $\gamma_{A_1} \simeq 0$, and get the $\mathcal{O}(1/m_Q)$ power correction to the h_V form factor:

$$\gamma_V(\omega) \simeq R_1(\omega)[1 + \beta_{A_1}(\omega)] - [1 + \beta_V(\omega)] \tag{6.26}$$

The extraction of $h_V(\omega)$ has been performed at both values of β. In both cases, statistical precision dropped as ω increased.

The data for h_V, calculated with different values of the light quark mass, were statistically consistent. Figure (6.11) shows the results of the extraction of γ_V for three kinematic channels with ω in the desired range, at $\beta = 6.2$. The plot shows that the power correction γ_V varies between 10% and 30%.

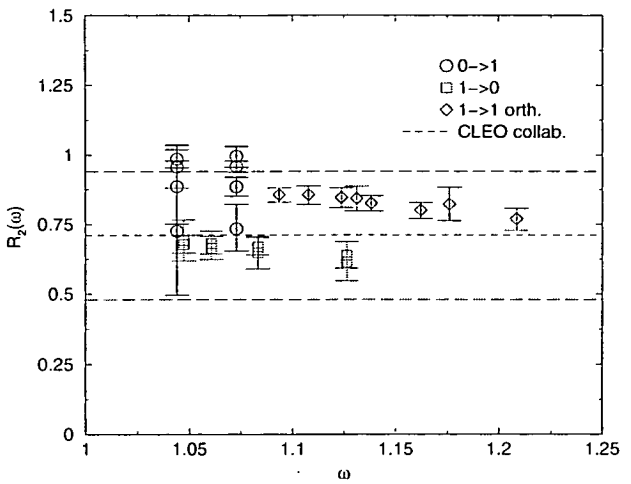

Figure 6.9: The $R_2(\omega)$ ratio, at $\beta = 6.2$, for $\kappa_P = 0.13460$

6.11 The Isgur-Wise function

For the reasons specified above, a study of the Isgur-Wise function was attempted at $\beta = 6.2$ only.

The Isgur-Wise function has been fitted to the model:

$$\xi(\omega) = 1 - \rho^2(\omega - 1) \tag{6.27}$$

Unconstrained fits were also attempted, as a consistency check:

$$\xi(\omega) = \xi(1) - \rho^2(\omega - 1) \tag{6.28}$$

At $\beta = 6.2$, using values of h_{A_1} extracted from fits on the front side of the lattice, the results were (Figure 6.12):

Fit	ρ^2	$\xi(1)$	$\chi^2/d.o.f.$
constrained	0.9(4)	$\equiv 1$	21.47/19
unconstrained	1.30^{+24}_{-27}	1.03(4)	16.2/18

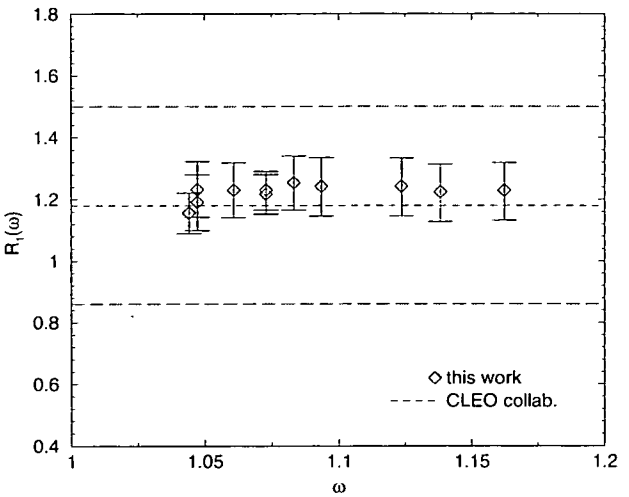

Figure 6.10: The R_1 ratio, at $\beta = 6.2$, for $\kappa_P = 0.13460$

Using the values of h_{A_1} that were extracted in fits on the back side of the lattice gave the following results (Figure 6.13):

Fit	ρ^2	$\xi(1)$	$\chi^2/d.o.f.$
constrained	1.38^{+16}_{-20}	$\equiv 1$	31.69/19
unconstrained	1.32^{+14}_{-13}	0.99(2)	31.68/18

In all the different cases, unconstrained fits were in excellent agreement with the $\xi(1) = 1$ condition.

6.11.1 Alternative models

The data for the Isgur-Wise function have also been fitted to the different possible models (see Chapter 4), giving results that were consistent with the fit to the linear model. This was not a surprise, since the different models agree up to $\mathcal{O}((\omega - 1)^2)$ terms and fits were done in a range in which

$$0 \leq (\omega - 1)^2 \leq 0.04 \qquad (6.29)$$

The differences between the different models turn out to be smaller than the

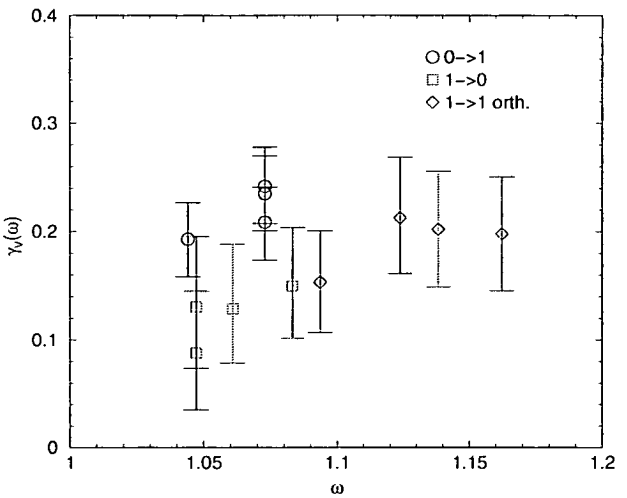

Figure 6.11: Power correction γ_V at $\beta = 6.2$, for $\kappa_P = 0.13460$

statistical errors on the data, showing that using different models for $\xi(\omega)$ has only a small effect on the extraction on ρ^2 from the dataset that was used, on the available fit range.

6.11.2 Quark mass dependence of the Isgur-Wise function

One of the most important features of the Isgur-Wise function, that derives from Heavy Quark Symmetry, is its universality. In other words, the Isgur-Wise function does not depend on the heavy quark masses. This property has been tested for the lattice determination of the Isgur-Wise function. In Figure (6.14), for three kinematic channels, the values of $\xi(\omega)$ at $\beta = 6.2$ at the same ω are plotted against average bare heavy quark mass. Dependence upon heavy quark mass is acceptably small, except at $am_q = 0.5$ due to probable discretisation effects.

6.12 Systematic error analysis

The central values for the final results are defined by:

- $\beta = 6.2$;

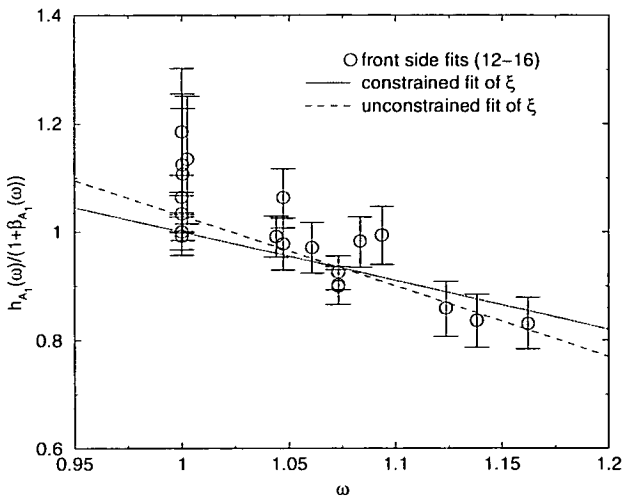

Figure 6.12: $\xi(\omega)$ from fits on the front side of the lattice, at $\beta = 6.2$, for $\kappa_P = 0.13460$

- $\kappa_P = 0.13460$;
- lattice spacing determined with r_0;
- form factor fits on the back side of the lattice.

The following sources of systematic uncertainty have been investigated:

- different values of κ_P;
- choice of the scale fixing quantity;
- momentum dependent systematic errors;
- different models for $\xi(\omega)$;
- different determinations of c_A.

As has been mentioned, the differences between the values of the form factors when calculated with the two different available light quark masses are negligible. However, the fits of the Isgur-Wise function are slightly different. In particular, the variations are:

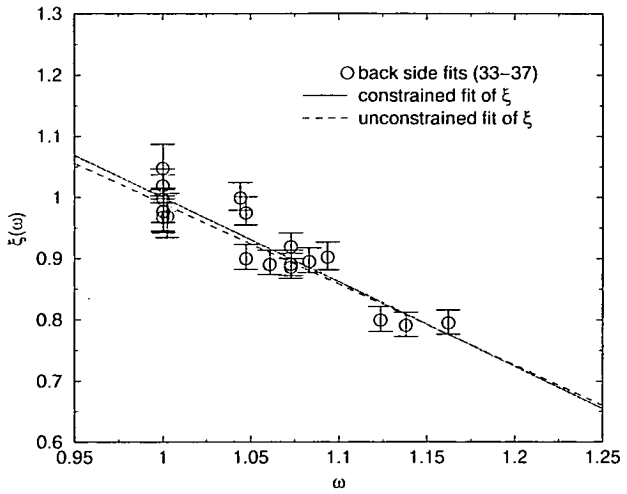

Figure 6.13: $\xi(\omega)$ from fits on the back side of the lattice, at $\beta = 6.2$, for $\kappa_P = 0.13460$

- constrained fit: $\delta\rho^2 \simeq 7\%$;
- unconstrained fit: $\delta\xi(1) \simeq 2\%$, $\delta\rho^2 \simeq 1.5\%$

Since the radiative corrections were calculated as functions of quark masses, the effect of the choice of the scale fixing quantity was investigated. Two different determinations of the lattice spacing have been employed, at $\beta = 6.2$:

- $a^{-1} = 2.913$ GeV from r_0 ;
- $a^{-1} = 2.544$ GeV from m_ρ .

The systematic uncertainty thus introduced was of the order of 3%.

Operators corresponding to different momenta have different systematic errors, whose effects on the extraction of the slope of the Isgur-Wise function have to be estimated. This estimate was performed in the following way: for each single kinematic channel with two or more values of ω, the data for the Isgur-Wise function were fitted to all the theoretical models. Variation in the central value was within 10%.

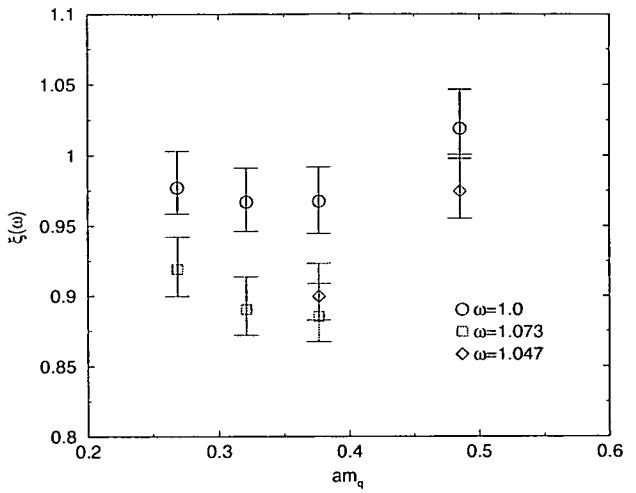

Figure 6.14: Heavy quark mass dependence of $\xi(\omega)$ at $\beta = 6.2$, for $\kappa_P = 0.13460$

As already mentioned, fits to the different models of the Isgur-Wise functions gave similar answers. The systematic uncertainty has been estimated to be around 7%.

An extraction of the axial form factors has been performed putting:

$$c_A = 0 \tag{6.30}$$

i.e. switching the axial current improvement off. No sizable difference has been observed to the case in which c_A was non-zero. This suggests that the statistical accuracy of the three-point functions is not high enough to resolve the contribution of the axial current improvement to the matrix elements of the $B \to D^* l\nu_l$ decay.

6.13 Extraction of $|V_{cb}|$

The differential decay rate for $B \to D^* l\nu_l$ can be written as:

$$\frac{d\Gamma}{d\omega} = \mathcal{G}(\omega)|V_{cb}|^2\mathcal{F}^2(\omega) \; . \tag{6.31}$$

The function $\mathcal{G}(\omega)$ is defined by:

$$\mathcal{G}(\omega) = \frac{G_F^2}{48\pi^3} m_{D^*}^3 (m_B - m_{D^*})^2 \sqrt{\omega^2 - 1} \times \tag{6.32}$$

$$\times \left[4\omega(\omega+1) \frac{1 - 2r\omega + r^2}{(1-r)^2} + (\omega+1)^2 \right]$$

where $r = m_{D^*}/m_B$. The $\mathcal{F}(\omega)$ function is, around $\omega = 1$:

$$\mathcal{F}(\omega) = \mathcal{F}(1) \left[1 - a^2(\omega^2 - 1) + b(\omega - 1)^2 \right] \tag{6.33}$$

where

$$\mathcal{F}(1) = \eta_A \xi(1) + \mathcal{O}\left(\frac{\Lambda_{QCD}^2}{m_Q^2} \right) \tag{6.34}$$

and η_A is a radiative correction equal to 0.986(6). Experimental data for the decay rate are fitted using this formula, to get three parameters:

$$\theta_0 = |V_{cb}| \mathcal{F}(1), \theta_1 = a^2, \theta_2 = b \; . \tag{6.35}$$

The CLEO collaboration quotes [82] :

$$\begin{aligned} \theta_0 &= (35.1 \pm 1.9 \pm 1.9) \times 10^{-3} \\ \theta_1 &= 0.84 \pm 0.13 \pm 0.08 \\ \theta_2 &= 0.0 \; . \end{aligned} \tag{6.36}$$

The simplest way to estimate $|V_{cb}|$ is to take the ratio:

$$|V_{cb}| = \frac{\theta_0}{\eta_A \xi_{\text{lat}}(1)} \tag{6.37}$$

Now,

$$\xi_{\rm lat}(1) = \frac{h^{\rm lat}_{A_1}(1)}{1+\beta_{A_1}(1)} + \mathcal{O}(1/m_Q^2) \ . \tag{6.38}$$

At zero recoil, the values of $\xi_{\rm lat}(1)$ are spread around one. From each of these values, an estimate of $|V_{cb}|$ can be extracted. The average of these quantities was chosen to be the central value, while the error bars have been estimated in a conservative way, mainly because there were only four different values. The error on $|V_{cb}|$ was taken to be half the interval between the highest and the lowest possible determinations of $|V_{cb}|$. Therefore, this work's estimate of V_{cb} is:

$$|V_{cb}| = 0.036(2)(1) \tag{6.39}$$

The quoted errors are statistical and systematic respectively. Systematic errors have been added in quadrature.

This value is in good agreement with the currently accepted determinations. The Particle Data Group quotes the following range:

$$0.037 - 0.043$$

A consistency check has been done in the following way: the value of $\xi_{\rm lat}(1)$ was taken from the unconstrained fits of the Isgur-Wise function over the whole range of ω. The estimates of $|V_{cb}|$ thus obtained were in excellent agreement with the estimates of the former method.

The estimates of $h_{A_1}(1)$ at $\beta = 6.0$ produced an estimate of $|V_{cb}|$ that was in statistical agreement with the $\beta = 6.2$ result.

6.14 Conclusions

As stated above, no satisfactory fits of the Isgur-Wise function were possible at $\beta = 6.0$. At $\beta = 6.2$, a discrepancy has been found between the fits on the front

and on the back side of the lattice. However the following facts have been noted:

- data on the back side were much cleaner than data on the front side;
- when different from the front side, back side signals were more stable.

For these reasons, the results at $\beta = 6.2$, with fits on the back side of the lattice have been chosen as preferred numbers and as final results for this work.

The slope of the Isgur-Wise function is estimated to be:

$$\rho^2 = 1.4(2)(2) \tag{6.40}$$

At the present time, several estimates of the slope parameter ρ^2 are available, covering the range:

$$0.6 \leq \rho^2 \leq 1.5$$

The result presented in this work is broadly consistent with the other determinations of ρ^2. Some of them are listed in the following table:

Authors	ρ^2	method
Bagan [83]	0.8(2)	sum rules
Blok [84]	0.70(25)	sum rules
Burdman [85]	1.08(10)	HQS
Close [86]	1.4	HQET
Hogaasen [87]	0.98	quark models
Morenas [88]	1.0	quark models
Neubert [89]	0.66(5)	sum rules
Voloshin [57]	1.4(3)	sum rules

This work's estimate is also in agreement with a previous lattice determination, performed on the same dataset, by G. Douglas [90] for the $B \rightarrow D$ decay. At $\beta = 6.2$, the author quotes $\rho^2_s = 1.2(1)$ and $\rho^2_{u,d} = 1.1(2)$.

It is clear that the calculations presented in this work could be improved in a significant manner by increasing the number of gauge configurations. In particular, one would hope to be able to extract the h_{A_2} and h_{A_3} form factors with good statistics: the knowledge of these functions permits a better study of the differential decay rate for $B \rightarrow D^* l \bar{\nu}_l$ and a cleaner extraction of $|V_{cb}|$. More simulated active and passive quark masses are also highly desirable, as they would permit solid investigations of the quark mass dependencies of the matrix elements.

Appendix A

Meson Spectrum and Decay Constants

The following tables show the values of the masses and the decay constants for pseudoscalar and vector mesons, at both values of β.

For the extrapolated values of the masses and decay constants, the following parameters were used:

	$\beta = 6.2$	$\beta = 6.0$
$\kappa_{\rm crit}$	0.13581^{+2}_{-1}	0.13525^{+2}_{-1}
$\kappa_{\rm n}$	0.13578^{+2}_{-1}	0.13520^{+2}_{-1}
$\kappa_{\rm s}$	0.13495^{+2}_{-2}	0.13476^{+3}_{-5}

Table A.1: Heavy-light pseudoscalar and vector masses in lattice units at $\beta = 6.2$ and $\beta = 6.0$. Fit ranges are $12 - 22$ at $\beta = 6.2$ and $10 - 22$ (P), $10 - 21$ (V) at $\beta = 6.0$.

$\beta = 6.2$			
κ_H	κ_L	aM_P	aM_V
0.1200	0.1346	0.841^{+1}_{-1}	0.871^{+2}_{-2}
	0.1351	0.823^{+2}_{-1}	0.856^{+2}_{-2}
	0.1353	0.817^{+2}_{-1}	0.848^{+3}_{-2}
0.1233	0.1346	0.739^{+1}_{-1}	0.775^{+2}_{-2}
	0.1351	0.721^{+2}_{-1}	0.759^{+2}_{-2}
	0.1353	0.714^{+2}_{-1}	0.752^{+3}_{-2}
0.1266	0.1346	0.628^{+1}_{-1}	0.673^{+2}_{-2}
	0.1351	0.609^{+1}_{-1}	0.656^{+2}_{-2}
	0.1353	0.602^{+2}_{-1}	0.650^{+3}_{-2}
0.1299	0.1346	0.505^{+1}_{-1}	0.563^{+2}_{-2}
	0.1351	0.484^{+1}_{-1}	0.546^{+2}_{-2}
	0.1353	0.476^{+1}_{-1}	0.540^{+2}_{-2}

$\beta = 6.0$			
κ_H	κ_L	aM_P	aM_V
0.1123	0.13344	1.145^{+2}_{-1}	1.188^{+2}_{-2}
	0.13417	1.121^{+2}_{-2}	1.166^{+3}_{-3}
	0.13455	1.110^{+3}_{-2}	1.158^{+4}_{-4}
0.1173	0.13344	1.006^{+2}_{-1}	1.056^{+2}_{-2}
	0.13417	0.981^{+2}_{-2}	1.034^{+3}_{-2}
	0.13455	0.969^{+2}_{-2}	1.026^{+4}_{-4}
0.1223	0.13344	0.851^{+1}_{-1}	0.915^{+2}_{-2}
	0.13417	0.825^{+2}_{-1}	0.892^{+3}_{-2}
	0.13455	0.811^{+2}_{-2}	0.883^{+4}_{-3}
0.1273	0.13344	0.675^{+1}_{-1}	0.759^{+2}_{-2}
	0.13417	0.646^{+2}_{-1}	0.736^{+3}_{-2}
	0.13455	0.631^{+2}_{-1}	0.727^{+4}_{-3}

Table A.2: Pseudoscalar and vector decay constants in lattice units at $\beta = 6.0$. Fit ranges are $14 - 21$ (P) and $16 - 23$ (V).

κ_H	κ_L	af_P	$f_V(c_V\text{BPT})$	$f_V(c_V\text{NP})$
	0.13344	0.111^{+1}_{-1}	7.9^{+1}_{-1}	12.7^{+2}_{-1}
0.1123	0.13417	0.106^{+1}_{-1}	8.0^{+1}_{-1}	12.7^{+2}_{-2}
	0.13455	0.104^{+1}_{-1}	8.0^{+2}_{-1}	12.5^{+3}_{-2}
	0.13344	0.1091^{+8}_{-9}	7.11^{+8}_{-7}	10.3^{+1}_{-1}
0.1173	0.13417	0.104^{+1}_{-1}	7.2^{+1}_{-1}	10.3^{+1}_{-1}
	0.13455	0.103^{+1}_{-1}	7.2^{+1}_{-1}	10.2^{+2}_{-2}
	0.13344	0.1056^{+7}_{-8}	6.26^{+7}_{-6}	8.34^{+9}_{-8}
0.1223	0.13417	0.1010^{+8}_{-9}	6.31^{+8}_{-8}	8.3^{+1}_{-1}
	0.13455	0.099^{+1}_{-1}	6.3^{+1}_{-1}	8.2^{+1}_{-1}
	0.13344	0.1000^{+6}_{-8}	5.30^{+6}_{-5}	6.54^{+7}_{-7}
0.1273	0.13417	0.0956^{+6}_{-9}	5.29^{+7}_{-6}	6.45^{+8}_{-8}
	0.13455	0.094^{+1}_{-1}	5.22^{+8}_{-7}	6.3^{+1}_{-1}

Table A.3: Pseudoscalar and vector decay constants in lattice units at $\beta = 6.2$. Fit ranges are $14 - 21$ (P) and $15 - 23$ (V).

κ_H	κ_L	af_P	$f_V(c_V\text{BPT})$	$f_V(c_V\text{NP})$
	0.1346	0.0889^{+8}_{-8}	8.53^{+9}_{-9}	10.2^{+1}_{-1}
0.1200	0.1351	0.0844^{+8}_{-9}	8.8^{+1}_{-1}	10.4^{+1}_{-1}
	0.1353	0.0828^{+9}_{-9}	8.9^{+1}_{-1}	10.5^{+2}_{-1}
	0.1346	0.0867^{+7}_{-7}	7.61^{+7}_{-7}	8.81^{+9}_{-8}
0.1233	0.1351	0.0823^{+7}_{-8}	7.79^{+9}_{-9}	9.0^{+1}_{-1}
	0.1353	0.0808^{+8}_{-9}	7.9^{+1}_{-1}	9.0^{+1}_{-1}
	0.1346	0.0839^{+6}_{-7}	6.62^{+6}_{-6}	7.46^{+7}_{-7}
0.1266	0.1351	0.0797^{+7}_{-8}	6.73^{+7}_{-7}	7.56^{+8}_{-8}
	0.1353	0.0782^{+7}_{-9}	6.76^{+9}_{-7}	7.6^{+1}_{-1}
	0.1346	0.0792^{+6}_{-7}	5.57^{+5}_{-5}	6.11^{+6}_{-5}
0.1299	0.1351	0.0754^{+6}_{-8}	5.60^{+6}_{-5}	6.12^{+6}_{-5}
	0.1353	0.0740^{+6}_{-9}	5.61^{+7}_{-5}	6.12^{+7}_{-6}

Table A.4: Masses and decay constants at physical light quark masses. $\beta = 6.0$.

κ_H	κ_L	aM_P	af_P	aM_V	f_V
0.1123	κ_n	1.087 ± 4	0.099 ± 2	1.138 ± 5	8.0 ± 2
	κ_s	1.125 ± 2	0.106 ± 1	1.171 ± 3	7.9 ± 1
0.1173	κ_n	0.945 ± 3	0.098 ± 1	1.005 ± 5	7.2 ± 2
	κ_s	0.985 ± 2	0.105 ± 1	1.039 ± 3	7.1 ± 1
0.1223	κ_n	0.786 ± 3	0.095 ± 1	0.862 ± 5	6.3 ± 1
	κ_s	0.829 ± 2	0.1019 ± 9	0.897 ± 3	6.22 ± 8
0.1273	κ_n	0.603 ± 2	0.090 ± 1	0.704 ± 5	5.2 ± 1
	κ_s	0.651 ± 2	0.0965 ± 8	0.740 ± 3	5.23 ± 7

Table A.5: Masses and decay constants at physical light quark masses. $\beta = 6.2$.

κ_H	κ_L	aM_P	af_P	aM_V	f_V
0.1200	κ_n	0.800 ± 2	0.078 ± 1	0.832 ± 4	9.0 ± 1
	κ_s	0.828 ± 2	0.0858 ± 8	0.860 ± 2	8.6 ± 1
0.1233	κ_n	0.696 ± 2	0.077 ± 1	0.736 ± 3	8.0 ± 1
	κ_s	0.726 ± 1	0.0837 ± 8	0.764 ± 2	7.68 ± 9
0.1266	κ_n	0.583 ± 2	0.074 ± 1	0.634 ± 3	6.8 ± 1
	κ_s	0.615 ± 1	0.0810 ± 8	0.661 ± 2	6.66 ± 7
0.1299	κ_n	0.455 ± 2	0.070 ± 1	0.523 ± 3	5.6 ± 1
	κ_s	0.491 ± 1	0.0766 ± 8	0.551 ± 1	5.57 ± 6

Appendix B

The h_{A_1} form factor

The following tables show the values of the renormalised (not radiatively corrected) form factor $h_{A_1}(\omega)$, at $\beta = 6.2$.

The h_{A_1} form factor has been extracted from fits on the back side of the lattice $(33 - 37)$.

Table B.1: $k_A = 0.12000$, $\vec{0} \to \vec{0}$ channel

κ_E	κ_P	ω	h_{A_1}	$\chi^2/(dof)$
0.12000	0.13460	1.0	0.95^{+2}_{-3}	2.01
0.12000	0.13510	1.0	0.98^{+4}_{-3}	2.78
0.12330	0.13460	1.0	0.94^{+2}_{-2}	2.56
0.12330	0.13510	1.0	0.97^{+3}_{-2}	1.16
0.12660	0.13460	1.0	0.93^{+2}_{-2}	2.82
0.12660	0.13510	1.0	0.98^{+4}_{-3}	1.46
0.12990	0.13460	1.0	0.93^{+2}_{-2}	3.34
0.12990	0.13510	1.0	0.98^{+3}_{-2}	0.80

Table B.2: $k_A = 0.12660$, $\vec{0} \to \vec{0}$ channel

κ_E	κ_P	ω	h_{A_1}	$\chi^2/(dof)$
0.12000	0.13460	1.0	0.93^{+2}_{-2}	2.01
0.12000	0.13510	1.0	0.94^{+4}_{-2}	2.78
0.12330	0.13460	1.0	0.92^{+2}_{-2}	2.56
0.12330	0.13510	1.0	0.94^{+4}_{-2}	1.16
0.12660	0.13460	1.0	0.89^{+2}_{-2}	2.82
0.12660	0.13510	1.0	0.94^{+4}_{-2}	1.46
0.12990	0.13460	1.0	0.88^{+2}_{-2}	3.34
0.12990	0.13510	1.0	0.93^{+3}_{-2}	0.80

Table B.3: $k_A = 0.12000$, $\vec{0} \to \vec{1}$ channel

κ_E	κ_P	ω	h_{A_1}	$\chi^2/(dof)$
0.12000	0.13460	1.044	0.92^{+2}_{-3}	1.99
0.12000	0.13510	1.046	0.93^{+3}_{-2}	1.18
0.12330	0.13460	1.044	0.93^{+2}_{-2}	0.92
0.12330	0.13510	1.046	0.93^{+3}_{-2}	0.75
0.12660	0.13460	1.044	0.93^{+2}_{-2}	0.46
0.12660	0.13510	1.046	0.94^{+3}_{-2}	0.34
0.12990	0.13460	1.044	0.95^{+2}_{-2}	2.04
0.12990	0.13510	1.046	0.96^{+3}_{-2}	0.84

Table B.4: $k_A = 0.12660$, $\vec{0} \to \vec{1}$ channel

κ_E	κ_P	ω	h_{A_1}	$\chi^2/(dof)$
0.12000	0.13460	1.073	0.84^{+2}_{-2}	1.99
0.12000	0.13510	1.077	0.84^{+3}_{-2}	1.18
0.12330	0.13460	1.073	0.83^{+2}_{-2}	0.92
0.12330	0.13510	1.077	0.84^{+3}_{-2}	0.75
0.12660	0.13460	1.073	0.83^{+2}_{-2}	0.46
0.12660	0.13510	1.077	0.84^{+3}_{-2}	0.34
0.12990	0.13460	1.073	0.84^{+2}_{-2}	2.04
0.12990	0.13510	1.077	0.85^{+3}_{-2}	0.84

Table B.5: $k_A = 0.12000$, $\vec{1} \to \vec{0}$ channel

κ_E	κ_P	ω	h_{A_1}	$\chi^2/(dof)$
0.12000	0.13460	1.047	0.90^{+2}_{-2}	0.35
0.12000	0.13510	1.049	0.91^{+3}_{-2}	0.27
0.12330	0.13460	1.062	0.89^{+2}_{-2}	0.22
0.12330	0.13510	1.064	0.89^{+3}_{-2}	0.19
0.12660	0.13460	1.083	0.87^{+2}_{-2}	0.10
0.12660	0.13510	1.088	0.88^{+3}_{-2}	0.11
0.12990	0.13460	1.126	0.84^{+2}_{-2}	0.07
0.12990	0.13510	1.137	0.85^{+3}_{-2}	0.07

Table B.6: $k_A = 0.12660$, $\vec{1} \to \vec{0}$ channel

κ_E	κ_P	ω	h_{A_1}	$\chi^2/(dof)$
0.12000	0.13460	1.047	0.86^{+2}_{-2}	0.47
0.12000	0.13510	1.049	0.86^{+3}_{-2}	0.41
0.12330	0.13460	1.061	0.84^{+2}_{-2}	0.39
0.12330	0.13510	1.064	0.84^{+3}_{-2}	0.33
0.12660	0.13460	1.083	0.81^{+2}_{-2}	0.26
0.12660	0.13510	1.088	0.82^{+2}_{-2}	0.22
0.12990	0.13460	1.126	0.78^{+2}_{-2}	0.18
0.12990	0.13510	1.137	0.79^{+2}_{-2}	0.16

Table B.7: $k_A = 0.12000$, $\vec{1} \to \vec{1}$ (parallel) channel

κ_E	κ_P	ω	h_{A_1}	$\chi^2/(dof)$
0.12000	0.13460	1.000	0.98^{+4}_{-3}	4.46
0.12000	0.13510	1.000	0.97^{+5}_{-4}	1.72
0.12330	0.13460	1.001	0.97^{+4}_{-3}	4.27
0.12330	0.13510	1.001	0.96^{+5}_{-4}	1.59
0.12660	0.13460	1.006	0.97^{+4}_{-3}	3.80
0.12660	0.13510	1.006	0.96^{+5}_{-4}	1.48
0.12990	0.13460	1.020	0.97^{+4}_{-4}	2.76
0.12990	0.13510	1.023	0.96^{+5}_{-5}	1.05

Table B.8: $k_A = 0.12660$, $\vec{1} \to \vec{1}$ (parallel) channel

κ_E	κ_P	ω	h_{A_1}	$\chi^2/(dof)$
0.12000	0.13460	1.003	0.92^{+4}_{-3}	8.21
0.12000	0.13510	1.003	0.91^{+4}_{-4}	3.73
0.12330	0.13460	1.000	0.92^{+2}_{-2}	8.39
0.12330	0.13510	1.001	0.90^{+5}_{-4}	3.60
0.12660	0.13460	1.000	0.91^{+3}_{-4}	7.04
0.12660	0.13510	1.000	0.90^{+5}_{-4}	3.19
0.12990	0.13460	1.007	0.91^{+4}_{-3}	5.72
0.12990	0.13510	1.008	0.89^{+5}_{-5}	2.19

Table B.9: $k_A = 0.12000$, $\vec{1} \to \vec{1}$ (orthogonal) channel

κ_E	κ_P	ω	h_{A_1}	$\chi^2/(dof)$
0.12000	0.13460	1.094	0.82^{+2}_{-2}	9.07
0.12000	0.13510	1.098	0.83^{+3}_{-2}	4.18
0.12330	0.13460	1.108	0.82^{+2}_{-2}	9.25
0.12330	0.13510	1.113	0.82^{+3}_{-2}	3.94
0.12660	0.13460	1.131	0.80^{+2}_{-2}	9.31
0.12660	0.13510	1.139	0.80^{+2}_{-2}	4.19
0.12990	0.13460	1.176	0.77^{+2}_{-2}	10.09
0.12990	0.13510	1.189	0.78^{+3}_{-2}	4.84

Table B.10: $k_A = 0.12660$, $\vec{1} \to \vec{1}$ (orthogonal) channel

κ_E	κ_P	ω	h_{A_1}	$\chi^2/(dof)$
0.12000	0.13460	1.124	0.75^{+2}_{-2}	13.30
0.12000	0.13510	1.130	0.75^{+3}_{-2}	7.47
0.12330	0.13460	1.138	0.74^{+2}_{-2}	14.10
0.12330	0.13510	1.145	0.73^{+3}_{-2}	6.83
0.12660	0.13460	1.162	0.73^{+2}_{-2}	12.07
0.12660	0.13510	1.172	0.71^{+2}_{-2}	5.88
0.12990	0.13460	1.208	0.69^{+2}_{-2}	10.72
0.12990	0.13510	1.224	0.69^{+2}_{-2}	5.15

Appendix C

The h_V form factor

The following tables show the values of the renormalised (not radiatively corrected) form factor $h_V(\omega)$, at both values of β.

The h_V form factor has been extracted from fits on the front side of the lattice $(12-16)$.

Table C.1: $k_A = 0.11230$, $\vec{0} \to \vec{1}$ channel

κ_E	κ_P	ω	h_V	$\chi^2/(dof)$
0.11230	0.13344	1.053	1.17^{+18}_{-18}	0.72
0.11230	0.13417	1.055	1.11^{+32}_{-32}	0.19
0.11730	0.13344	1.053	1.19^{+17}_{-17}	0.65
0.11730	0.13417	1.055	1.14^{+30}_{-29}	0.19
0.12230	0.13344	1.053	1.22^{+15}_{-15}	0.60
0.12230	0.13417	1.055	1.16^{+26}_{-26}	0.31
0.12730	0.13344	1.053	1.29^{+15}_{-15}	0.74
0.12730	0.13417	1.055	1.22^{+25}_{-22}	0.89

Table C.2: $k_A = 0.11730$, $\vec{0} \to \vec{1}$ channel

κ_E	κ_P	ω	h_V	$\chi^2/(dof)$
0.11230	0.13344	1.067	1.22^{+18}_{-17}	0.61
0.11230	0.13417	1.070	1.18^{+31}_{-31}	0.13
0.11730	0.13344	1.067	1.23^{+16}_{-16}	0.55
0.11730	0.13417	1.070	1.19^{+29}_{-28}	0.12
0.12230	0.13344	1.067	1.23^{+15}_{-15}	0.53
0.12230	0.13417	1.070	1.20^{+24}_{-25}	0.21
0.12730	0.13344	1.067	1.29^{+13}_{-14}	0.66
0.12730	0.13417	1.070	1.24^{+23}_{-22}	0.66

Table C.3: $k_A = 0.12230$, $\vec{0} \to \vec{1}$ channel

κ_E	κ_P	ω	h_V	$\chi^2/(dof)$
0.11230	0.13344	1.088	1.26^{+18}_{-17}	0.47
0.11230	0.13417	1.093	1.23^{+31}_{-29}	0.08
0.11730	0.13344	1.088	1.25^{+16}_{-15}	0.43
0.11730	0.13417	1.093	1.22^{+29}_{-27}	0.07
0.12230	0.13344	1.088	1.23^{+14}_{-14}	0.43
0.12230	0.13417	1.093	1.21^{+24}_{-24}	0.11
0.12730	0.13344	1.088	1.26^{+13}_{-13}	0.50
0.12730	0.13417	1.093	1.24^{+22}_{-21}	0.38

Table C.4: $k_A = 0.12730$, $\vec{0} \to \vec{1}$ channel

κ_E	κ_P	ω	h_V	$\chi^2/(dof)$
0.11230	0.13344	1.126	1.24^{+20}_{-19}	0.47
0.11230	0.13417	1.133	1.18^{+34}_{-32}	0.18
0.11730	0.13344	1.126	1.21^{+17}_{-17}	0.40
0.11730	0.13417	1.133	1.17^{+29}_{-31}	0.14
0.12230	0.13344	1.126	1.17^{+15}_{-15}	0.36
0.12230	0.13417	1.133	1.15^{+24}_{-25}	0.10
0.12730	0.13344	1.126	1.19^{+13}_{-13}	0.36
0.12730	0.13417	1.133	1.18^{+23}_{-20}	0.13

Table C.5: $k_A = 0.11230$, $\vec{1} \to \vec{0}$ channel

κ_E	κ_P	ω	h_V	$\chi^2/(dof)$
0.11230	0.13344	1.057	0.94^{+29}_{-27}	0.13
0.11230	0.13417	1.060	0.91^{+53}_{-50}	0.34
0.11730	0.13344	1.073	1.01^{+27}_{-26}	0.07
0.11730	0.13417	1.077	1.01^{+49}_{-47}	0.25
0.12230	0.13344	1.101	1.04^{+27}_{-25}	0.22
0.12230	0.13417	1.108	1.09^{+47}_{-44}	0.45
0.12730	0.13344	1.157	1.08^{+29}_{-28}	0.81
0.12730	0.13417	1.170	1.17^{+48}_{-45}	1.15

Table C.6: $k_A = 0.11730$, $\vec{1} \to \vec{0}$ channel

κ_E	κ_P	ω	h_V	$\chi^2/(dof)$
0.11230	0.13344	1.057	0.96^{+28}_{-26}	0.22
0.11230	0.13417	1.060	0.91^{+52}_{-47}	0.58
0.11730	0.13344	1.073	1.01^{+25}_{-25}	0.07
0.11730	0.13417	1.077	1.00^{+46}_{-44}	0.45
0.12230	0.13344	1.101	1.04^{+25}_{-23}	0.16
0.12230	0.13417	1.108	1.06^{+42}_{-41}	0.60
0.12730	0.13344	1.157	1.05^{+28}_{-25}	0.66
0.12730	0.13417	1.170	1.10^{+43}_{-41}	1.25

Table C.7: $k_A = 0.12230$, $\vec{1} \to \vec{0}$ channel

κ_E	κ_P	ω	h_V	$\chi^2/(dof)$
0.11230	0.13344	1.057	0.97^{+28}_{-27}	0.40
0.11230	0.13417	1.060	0.91^{+50}_{-47}	0.79
0.11730	0.13344	1.073	1.02^{+26}_{-25}	0.12
0.11730	0.13417	1.077	0.99^{+46}_{-42}	0.56
0.12230	0.13344	1.101	1.02^{+25}_{-23}	0.06
0.12230	0.13417	1.108	1.03^{+41}_{-40}	0.57
0.12730	0.13344	1.157	0.99^{+26}_{-24}	0.37
0.12730	0.13417	1.170	1.02^{+40}_{-38}	1.08

Table C.8: $k_A = 0.12730$, $\vec{1} \to \vec{0}$ channel

κ_E	κ_P	ω	h_V	$\chi^2/(dof)$
0.11230	0.13344	1.057	0.99^{+34}_{-31}	0.69
0.11230	0.13417	1.060	0.91^{+56}_{-52}	0.95
0.11730	0.13344	1.073	1.02^{+29}_{-29}	0.31
0.11730	0.13417	1.077	0.97^{+50}_{-47}	0.62
0.12230	0.13344	1.101	0.97^{+27}_{-26}	0.10
0.12230	0.13417	1.108	0.97^{+43}_{-41}	0.44
0.12730	0.13344	1.157	0.89^{+27}_{-25}	0.14
0.12730	0.13417	1.170	0.89^{+39}_{-37}	0.60

Table C.9: $k_A = 0.11230$, $\vec{1} \to \vec{1}$ (orthogonal) channel

κ_E	κ_P	ω	h_V	$\chi^2/(dof)$
0.11230	0.13344	1.113	0.99^{+36}_{-37}	0.97
0.11230	0.13417	1.118	0.72^{+64}_{-64}	0.91
0.11730	0.13344	1.131	0.98^{+35}_{-36}	0.96
0.11730	0.13417	1.137	0.76^{+63}_{-62}	0.96
0.12230	0.13344	1.160	0.95^{+35}_{-33}	0.93
0.12230	0.13417	1.169	0.79^{+62}_{-59}	1.04
0.12730	0.13344	1.218	0.95^{+40}_{-35}	0.91
0.12730	0.13417	1.235	0.82^{+66}_{-60}	1.20

Table C.10: $k_A = 0.11730$, $\vec{1} \to \vec{1}$ (orthogonal) channel

κ_E	κ_P	ω	h_V	$\chi^2/(dof)$
0.11230	0.13344	1.128	1.07^{+34}_{-36}	0.90
0.11230	0.13417	1.133	0.86^{+61}_{-62}	0.84
0.11730	0.13344	1.145	1.06^{+34}_{-34}	0.87
0.11730	0.13417	1.152	0.90^{+58}_{-60}	0.88
0.12230	0.13344	1.175	1.01^{+33}_{-32}	0.82
0.12230	0.13417	1.185	0.91^{+57}_{-55}	0.94
0.12730	0.13344	1.234	0.99^{+36}_{-34}	0.79
0.12730	0.13417	1.252	0.91^{+63}_{-54}	1.09

Table C.11: $k_A = 0.12230$, $\vec{1} \to \vec{1}$ (orthogonal) channel

κ_E	κ_P	ω	h_V	$\chi^2/(dof)$
0.11230	0.13344	1.150	1.18^{+35}_{-34}	0.75
0.11230	0.13417	1.158	1.01^{+59}_{-64}	0.69
0.11730	0.13344	1.168	1.16^{+33}_{-34}	0.69
0.11730	0.13417	1.177	1.06^{+56}_{-60}	0.69
0.12230	0.13344	1.198	1.10^{+32}_{-31}	0.63
0.12230	0.13417	1.210	1.06^{+52}_{-54}	0.72
0.12730	0.13344	1.259	1.06^{+35}_{-33}	0.61
0.12730	0.13417	1.279	1.06^{+57}_{-51}	0.86

Table C.12: $k_A = 0.12730$, $\vec{1} \to \vec{1}$ (orthogonal) channel

κ_E	κ_P	ω	h_V	$\chi^2/(dof)$
0.11230	0.13344	1.190	1.27^{+39}_{-39}	0.54
0.11230	0.13417	1.201	1.12^{+66}_{-67}	0.49
0.11730	0.13344	1.209	1.27^{+37}_{-38}	0.49
0.11730	0.13417	1.221	1.20^{+59}_{-63}	0.46
0.12230	0.13344	1.240	1.21^{+34}_{-35}	0.44
0.12230	0.13417	1.255	1.23^{+55}_{-56}	0.46
0.12730	0.13344	1.302	1.16^{+36}_{-36}	0.44
0.12730	0.13417	1.327	1.25^{+57}_{-57}	0.56

Table C.13: $k_A = 0.12000$, $\vec{0} \to \vec{1}$ channel

κ_E	κ_P	ω	h_V	$\chi^2/(dof)$
0.12000	0.13460	1.044	1.22^{+5}_{-5}	2.32
0.12000	0.13510	1.046	1.21^{+8}_{-8}	2.56
0.12330	0.13460	1.044	1.23^{+6}_{-6}	2.21
0.12330	0.13510	1.046	1.21^{+8}_{-8}	2.41
0.12660	0.13460	1.044	1.27^{+6}_{-6}	2.10
0.12660	0.13510	1.046	1.24^{+8}_{-8}	2.30
0.12990	0.13460	1.044	1.34^{+6}_{-6}	2.32
0.12990	0.13510	1.046	1.30^{+8}_{-8}	2.33

Table C.14: $k_A = 0.12660$, $\vec{0} \to \vec{1}$ channel

κ_E	κ_P	ω	h_V	$\chi^2/(dof)$
0.12000	0.13460	1.073	1.21^{+5}_{-5}	1.79
0.12000	0.13510	1.077	1.19^{+8}_{-7}	1.91
0.12330	0.13460	1.073	1.20^{+5}_{-5}	1.77
0.12330	0.13510	1.077	1.17^{+7}_{-7}	1.93
0.12660	0.13460	1.073	1.21^{+5}_{-5}	1.77
0.12660	0.13510	1.077	1.18^{+7}_{-7}	1.67
0.12990	0.13460	1.073	1.23^{+5}_{-5}	2.49
0.12990	0.13510	1.077	1.19^{+7}_{-7}	2.69

Table C.15: $k_A = 0.12000$, $\vec{1} \to \vec{0}$ channel

κ_E	κ_P	ω	h_V	$\chi^2/(dof)$
0.12000	0.13460	1.047	1.22^{+8}_{-8}	0.92
0.12000	0.13510	1.049	1.15^{+13}_{-13}	1.01
0.12330	0.13460	1.061	1.21^{+8}_{-8}	1.14
0.12330	0.13510	1.064	1.13^{+12}_{-12}	1.31
0.12660	0.13460	1.083	1.21^{+8}_{-7}	1.33
0.12660	0.13510	1.088	1.15^{+11}_{-11}	1.55
0.12990	0.13460	1.126	1.23^{+8}_{-8}	1.89
0.12990	0.13510	1.137	1.18^{+11}_{-12}	1.69

Table C.16: $k_A = 0.12660$, $\vec{1} \to \vec{0}$ channel

κ_E	κ_P	ω	h_V	$\chi^2/(dof)$
0.12000	0.13460	1.047	1.25^{+9}_{-8}	1.04
0.12000	0.13510	1.049	1.18^{+13}_{-12}	1.10
0.12330	0.13460	1.061	1.22^{+8}_{-8}	1.35
0.12330	0.13510	1.064	1.15^{+12}_{-11}	1.58
0.12660	0.13460	1.083	1.20^{+8}_{-7}	1.69
0.12660	0.13510	1.088	1.14^{+11}_{-10}	1.92
0.12990	0.13460	1.126	1.18^{+7}_{-7}	1.88
0.12990	0.13510	1.137	1.13^{+11}_{-10}	1.69

Table C.17: $k_A = 0.12000$, $\vec{1} \to \vec{1}$ (orthogonal) channel

κ_E	κ_P	ω	h_V	$\chi^2/(dof)$
0.12000	0.13460	1.094	1.17^{+8}_{-8}	3.81
0.12000	0.13510	1.097	1.14^{+13}_{-13}	2.42
0.12330	0.13460	1.108	1.14^{+8}_{-8}	4.19
0.12330	0.13510	1.113	1.13^{+12}_{-13}	2.73
0.12660	0.13460	1.131	1.12^{+8}_{-8}	4.68
0.12660	0.13510	1.138	1.11^{+12}_{-12}	2.86
0.12990	0.13460	1.176	1.11^{+8}_{-8}	4.81
0.12990	0.13510	1.189	1.10^{+11}_{-11}	2.71

Table C.18: $k_A = 0.12660$, $\vec{1} \to \vec{1}$ (orthogonal) channel

κ_E	κ_P	ω	h_V	$\chi^2/(dof)$
0.12000	0.13460	1.124	1.10^{+8}_{-8}	4.02
0.12000	0.13510	1.130	1.08^{+12}_{-12}	2.74
0.12330	0.13460	1.138	1.06^{+8}_{-8}	4.46
0.12330	0.13510	1.145	1.04^{+11}_{-12}	2.91
0.12660	0.13460	1.162	1.03^{+8}_{-8}	5.11
0.12660	0.13510	1.172	1.00^{+10}_{-11}	3.07
0.12990	0.13460	1.208	0.97^{+7}_{-8}	4.98
0.12990	0.13510	1.224	0.95^{+10}_{-11}	2.87

Bibliography

[1] J. Donoghue, E. Golowich, and B. Holstein, *Dynamics of the Standard Model* (Cambridge University Press, Cambridge, 1992).

[2] N. Cabibbo, Phys. Lett. **10**, 431 (1963).

[3] M. Kobayashi and K. Maskawa, **49**, 652 (1973).

[4] B. Brau, B decays to final states including $D_s^{(*)}$ andD^*, `hep-ex/0012027`, 2000.

[5] F. D. Lodovico, First Physics Results at BABAR, `hep-ex/0012005`, 2000.

[6] A. G. Cohen, Phys. Rev. Lett. **78**, 2300 (1997).

[7] A. Satpathy, Particle Identification with BELLE, `hep-ex/9903045`, 1999.

[8] K. Zuber, Phys. Rept. **305**, 295 (1998).

[9] V. Barger *et al.*, Phys. Rev. Lett. **82**, 2640 (1999).

[10] L. Wolfenstein, Phys. Rev. Lett. **51**, 1945 (1983).

[11] H. Wittig, Int. J. Mod. Phys. A **12**, 4477 (1997).

[12] C. T. Sachrajda, Flavour Physics, `hep-ph/9801343`, 1998.

[13] A. V. Manohar and M. B. Wise, *Heavy Quark Physics* (Cambridge University Press, Cambridge, 2000).

[14] I. Montvay and G. Münster, *Quantum Fields on a Lattice* (Cambridge University Press, Cambridge, 1994).

[15] H. J. Rothe, *Lattice Gauge Theories* (World Scientific, Singapore, 1992).

[16] K. G. Wilson, Phys. Rev. D **10**, 2445 (1974).

[17] H. B. Nielsen and M. Ninomiya, Nucl. Phys. B **185**, 20 (1981).

[18] R. Kenway, in *Confinement, Duality, and Non-perturbative Aspects of QCD*, edited by P. van Baal (Plenum Press, New York, 1997).

[19] M. Lüscher, Advanced Lattice QCD, `hep-lat/9802029`, 1998.

[20] P. Weisz, in *Confinement, Duality, and Non-perturbative Aspects of QCD*, edited by P. van Baal (Plenum Press, New York, 1997).

[21] G. Lepage, in *Confinement, Duality, and Non-perturbative Aspects of QCD*, edited by P. van Baal (Plenum Press, New York, 1997).

[22] B. Sheikholeslami and R. Wohlert, Nucl. Phys. B **259**, 572 (1985).

[23] M. Lüscher, S. Sint, R. Sommer, P. Weisz, H. Wittig and U. Wolff, Nucl. Phys. B (Proc. Suppl.) **53**, 905 (1997).

[24] M. Lüscher, S. Sint, R. Sommer, and H. Wittig, Nucl. Phys. B **491**, 344 (1997).

[25] G. P. Lepage and P. B. Mackenzie, Phys. Rev. D **48**, 2250 (1993).

[26] G. Veneziano, Nuovo Cimento **57A**, 190 (1968).

[27] H. Hamber and G. Parisi, Phys. Rev. Lett. **47**, 1792 (1981).

[28] E. Marinari, G. Parisi, and C. Rebbi, Phys. Rev. Lett. **47**, 1795 (1981).

[29] D. Weingarten, Phys. Lett. B **109**, 57 (1982).

[30] N. Metropolis *et al.*, J. Chem. Phys. **21**, 1087 (1953).

[31] M. E. Peskin and D. V. Schroeder, *An introduction to Quantum Field Theory* (Addison-Wesley, USA, 1996).

[32] P. Lacock *et al.*, Phys. Rev. D **51**, 5403 (1995).

[33] S. J. Perantonis, A. Huntley, and C. Michael, Nucl. Phys. B **326**, 544 (1989).

[34] N. Cabibbo and E. Marinari, Phys. Lett. B **119**, 387 (1982).

[35] P. Boyle, A novel gauge invariant multi-state smearing technique, `hep-lat/9903033`, 1999.

[36] M. Neubert, Heavy Quark Symmetry, `SLAC-PUB-6263`, 1993.

[37] N. Isgur and M. Wise, Phys. Lett. B **232**, 113 (1989).

[38] N. Isgur and M. Wise, Phys. Lett. B **237**, 527 (1990).

[39] E. Eichten and F. Feinberg, Phys. Rev. D **23**, 2724 (1981).

[40] W. E. Caswell and G. P. Lepage, Phys. Lett. B **167**, 437 (1986).

[41] E. Eichten and B. Hill, Phys. Lett. B **234**, 511 (1990).

[42] E. Eichten and B. Hill, Phys. Lett. B **243**, 427 (1990).

[43] H. Georgi, Phys. Lett. B **240**, 447 (1990).

[44] B. Grinstein, Nucl. Phys. B **339**, 253 (1990).

[45] H. D. Politzer and M. B. Wise, Phys. Lett. B **206**, 681 (1988).

[46] H. D. Politzer and M. B. Wise, Phys. Lett. B **208**, 504 (1988).

[47] A. F. Falk, H. Georgi, B. Grinstein, and M. B. Wise, Nucl. Phys. B **343**, 1 (1990).

[48] A. F. Falk, B. Grinstein, and M. E. Luke, Nucl. Phys. B **357**, 185 (1991).

[49] T. Mannel, W. Roberts, and Z. Ryzak, Nucl. Phys. B **368**, 204 (1992).

[50] M. Neubert, Phys. Rev. D **46**, 2212 (1992).

[51] M. Neubert, Phys. Rev. D **46**, 3914 (1992).

[52] M. E. Luke, Phys. Lett. B **252**, 447 (1990).

[53] M. Neubert and V. Rieckert, Nucl. Phys. B **382**, 97 (1992).

[54] N. Isgur, D. Scora, B. Grinstein, and M. Wise, Phys. Rev. D **39**, 799 (1989).

[55] J. D. Bjorken, Gauge Bosons and Heavy Quarks, Proceedings of the 18th SLAC Summer Institute on Particle Physics, Stanford, California, edited by J. F .Hawthorne, 1990.

[56] J. D. Bjorken, Results and Perspectives in Particle Physics, Proceedings of the 4th Rencontres de Physique de la vallé d'Aoste, La Thuile, Italy, edited by M. Greco (Editions Frontieres Gif-sur-Yvette), 1990.

[57] M. B. Voloshin, Phys. Rev. D **46**, 3062 (1992).

[58] M. Neubert and B. Stech, Heavy Flavours II, Vol. 15 of Advanced Series on High Energy Physics, edited by A. J. Buras and M. Lindner (World Scientific, Singapore), Chap.4, pp. 294-344, 1998.

[59] M. Ciuchini, R. Contino, E. Franco, and G. Martinelli, epjc **9**, 43 (1999).

[60] R. Sommer, Nucl. Phys. B **411**, 839 (1994).

[61] M. Guagnelli and R. Sommer, Nucl. Phys. B **535**, 389 (1998).

[62] G. D. Divitiis and R. Petronzio, Phys. Lett. B **491**, 311 (1998).

[63] S. Sint and P. Weisz, Nucl. Phys. B **502**, 251 (1997).

[64] T. Bhattacharya *et al.*, Phys. Lett. B **461**, 79 (1999).

[65] T. Bhattacharya and R. Gupta and W. Lee and S. Sharpe, Nucl. Phys. B (Proc. Suppl.) **63 A-C**, 886 (1998).

[66] J. Garden, Ph.D. thesis, University of Edinburgh, 2000.

[67] M. Neubert, Phys. Rev. D **45**, 2451 (1992).

[68] S. Bethke, Nucl. Phys. B (Proc. Suppl.) **54A**, 314 (1997).

[69] M. Neubert, Phys. Rev. D **46**, 1076 (1992).

[70] A. X. El-Khadra, A. S. Kronfeld, and P. B. Mackenzie, Phys. Rev. D **55**, 587 (1997).

[71] D. Becirevic *et al.*, Phys. Rev. D **60**, 074501 (1990).

[72] UKQCD Collaboration and D. G. Richards, Nucl. Phys. B (Proc. Suppl.) **73**, 381 (1999).

[73] UKQCD Collaboration and V. I. Lesk, Nucl. Phys. B (Proc. Suppl.) **83-84**, 313 (2000).

[74] S. Hashimoto, Nucl. Phys. B (Proc. Suppl.) **83-84**, 1 (2000).

[75] T. Draper, Nucl. Phys. B (Proc. Suppl.) **73**, 43 (1999).

[76] C. Bernard *et al.*, Phys. Rev. Lett. **81**, 4812 (1998).

[77] CP-PACS Collaboration and A. Ali Khan and others, Nucl. Phys. B (Proc. Suppl.) **83-84**, 331 (2000).

[78] T. Bhattacharya, R. Gupta, W. Lee, and S. Sharpe, Order a improved renormalization constants, `hep-lat/0009038`, 2000.

[79] H. Hoeber, Ph.D. thesis, University of Edinburgh, 1994.

[80] J. E. Duboscq, Phys. Rev. Lett. **76**, 3898 (1996).

[81] M. Neubert, Int. J. Mod. Phys. A **11**, 4173 (1996).

[82] B. Barish *et al.*, Phys. Rev. D **51**, 1014 (1995).

[83] E. Bagan *et al.*, Phys. Lett. B **301**, 249 (1993).

[84] B. Blok and M. Shifman, Phys. Rev. D **47**, 2949 (1993).

[85] G. Burdman, Phys. Lett. B **284**, 133 (1992).

[86] F. Close and A. Wambach, Phys. Lett. B **348**, 207 (1995).

[87] H. Hogaasen and M. Sadzikowski, Z. Phys. C. **64**, 427 (1994).

[88] V. Morenas *et al.*, Phys. Lett. B **408**, 357 (1997).

[89] M. Neubert, Phys. Rept. **245**, 259 (1994).

[90] G. Douglas, Ph.D. thesis, University of Edinburgh, 1999.